

Accelerated Zero-stress Hydrothermal Aging of Dry Glass, Basalt, and Carbon Fibers and
Service Life Prediction Using Arrhenius Model

by

John Sunny

A thesis submitted in partial fulfillment of the requirements for the degree of

Master of Science

Department of Mechanical Engineering

University of Alberta

© John Sunny, 2023

Abstract

The utilization of fiber-reinforced polymer composites (FRPC) has rapidly increased over the past few decades because of their attractive mechanical properties, comparatively low volumetric mass density, and excellent corrosion resistance compared to traditional engineering materials like steel and aluminum. Exposure to moist and humid environments can accelerate the aging process of composite materials and negatively impact mechanical properties, thus shortening their service life. Environmental aging coupled with elevated temperature constitutes a severe case of accelerated aging. Notably, different composite constituents are impacted by environmental aging in different ways. As a result, it is crucial to comprehend for each constituent the kinetics and mechanisms of environmental aging to ensure the composite's environmental durability. Data for service time assessments must currently be obtained via expensive and time-consuming test procedures.

In recent years, thermoplastic matrix-based composites have been gaining popularity over their thermoset counterparts due to a practically infinite shelf life of raw materials, the ability to recycle thermoplastic polymers, and possible reductions in manufacturing cost that can be achieved using rapid and continuous fabrication processes. While thermosetting matrices typically offer excellent resistance to water, moisture exposure may significantly affect fibers embedded in thermoplastic polymers. Additionally, some structural applications use fibers devoid of any matrix ('dry' fibers), in which water exposure must be avoided. In both cases, moisture may significantly impact the reinforcing elements and the degradation rate. Comprehending the degradation of reinforcements is crucial for service applications involving dry and wet conditions, especially when prolonged contact with water above room temperature is present. Knowing and forecasting the extent of the material property deterioration in water is of great interest to designers and users of FRP structures. Environmental durability becomes a limiting factor in using composites for structural applications since the uncertainty of the material interaction with the environment compromises the superior material properties. The present work focused on the effects of hydrothermal aging on the mechanical durability of long glass, carbon, and basalt fibers by immersion in water at 60°C, 71°C, and

82°C. Unidirectional thermoplastic composite tapes were also exposed to water at elevated temperatures to extend the study to composites. The main application of interest in the context of this research is thermoplastic composite piping where dry reinforcements or thermoplastic composite tapes are used as the load-carrying components. A service life forecast model was created for the fibers utilizing the Arrhenius technique. Using this modeling approach, it is possible to approximate the time it will take to attain a given degradation level over a specified range of temperatures. Scanning electron microscopy was used to evaluate morphology changes of fiber surfaces due to hydrothermal exposure. Fourier transforms infrared spectroscopy and mass dissolution studies were used to elucidate the mechanism of the strength loss.

Preface

This thesis is an original work by John Sunny. One journal paper and two conference proceedings related to this thesis have been published and are listed below. As such, the paper-based thesis guideline is followed in presenting the work.

1. J. Sunny, H. Nazariipoor, J. Palacios Moreno, P. Mertiny, “Accelerated zero-stress hydrothermal aging of dry E-glass fibers and service life prediction using Arrhenius model”, *Fibers*, vol. 11, p. 70-1-17, 2023.
2. J. Sunny, J. Palacios Moreno, H. Nazariipoor, P. Mertiny, “Accelerated zero-stress aging of glass, carbon, and basalt fibers- strength reduction explained by chemical and morphological analysis,” *Proceedings of the Canadian Society for Mechanical Engineering International Congress*, Quebec, 2023.
3. J. Sunny, J. Palacios Moreno, H. Nazariipoor, P. Mertiny, “Hydrothermal Aging of Glass Fiber Reinforced Thermoplastic Composites,” *Proceedings of the American Society for Composites - 38th Technical Conference*, Boston, 2023.

Acknowledgments

I would like to take this opportunity to express my heartfelt gratitude to my thesis supervisor, Dr. Pierre Mertiny, for his invaluable guidance, support, and encouragement throughout my thesis journey. I am grateful for the time and effort he has invested in helping me to grow as a researcher and scholar. His unwavering support has been a source of inspiration and motivation for me, and I am honored to have had the privilege of working under his guidance. His supervision helped me to develop and grow into the person and researcher I am today. Although it was a difficult process, I persisted and was compelled to overcome challenges by considering potential solutions from various angles.

Thank you to Composite Production Systems (CPS), Shawcor Ltd, for providing financial support for the project. The so-called AOP project enriched my experience by involving me in an exciting product development project but also introduced me to a team of well-informed and passionate people. I would also like to express my appreciation to all the team members of the AOP group, especially Drs. Ahmed Hammami and Hadi Nazariipoor, for their continued support throughout all phases of the project. The project's success would not have been possible without you.

Thank you to the members of the Mechanical Engineering machine shop and Nanofab (University of Alberta). I appreciate all the help and technical support you provided me. Thank you to Jorge Palacios Moreno, who worked closely with us throughout different phases of the project.

Finally, thank you to my family and colleagues. I believe our experiences shape who we are, and I would not be who I am today without your support.

Table of Contents

Chapter 1 : Introduction	1
1.1. Background and Motivation	1
1.2. Relevance of Thesis to Industrial Partner	2
1.3. Hypothesis and Thesis Objectives	3
1.4. Structure of the Thesis	4
1.5. References.....	4
Chapter 2 : Composites and Environmental Durability	6
2.1. Durability of Composites.....	6
2.2. Reinforcements and Environmental Durability	8
2.3. Environmental Aging of Sizing Rich Composite Interphases	9
2.4. Durability Prediction Models.....	11
2.4.1. Arrhenius Model	11
2.4.2. Time-temperature Superposition Approach.....	11
2.5. Determination of Fiber Strength.....	12
2.5.1. Fibers Used in Composite Materials.....	12
2.5.2. Fiber Tensile Testing	13
2.5.3. Critical Parameters in Fiber Strength Measurements	17
2.6. References.....	18
Chapter 3 : Aging Studies on Dry E-glass Fibers and Service Life Prediction Using Arrhenius Model.....	23
3.1. Introduction.....	23
3.2. Arrhenius Model and Time-Temperature Superposition Approach	27
3.3. Material and Specimen Preparation	28
3.4. Experimental Methods.....	29
3.4.1. Test Setup for Fiber Breaking Force Measurement	29
3.4.2. Mass Dissolution Experiments	30

3.4.3. Fourier Transform Infrared Spectroscopy	30
3.4.4. Scanning Electron Microscopy	31
3.5. Results and Discussion	31
3.5.1. Variations in Fiber Strength.....	31
3.5.2. Prediction of Long-term Behavior and Service Life of Glass Fibers.....	33
3.5.3. Elements Released During Degradation and Corresponding Chemical Reactions.....	36
3.5.4. FTIR Results.....	37
3.5.5. Morphological Analysis.....	38
3.6. Conclusions.....	40
3.7. References.....	41
Chapter 4 : Hydrothermal and Humidity Aging of Carbon and Basalt Fibers.....	45
4.1. Introduction.....	45
4.2. Materials and Methods	48
4.2.1. Dry Fiber Bundles.....	48
4.3. Sample Preparation and Conditioning	48
4.3.1. Hydrothermal Aging.....	48
4.3.2. Exposure to Humidity.....	49
4.3.3. Assessment of Damage Caused by Sample Preparation.....	50
4.4. Tensile Testing.....	50
4.4.1. Capstan Grips.....	51
4.4.2. Tapping Method.....	51
4.5. Mass Spectroscopy	52
4.6. Fourier Transform Infrared Spectroscopy	53
4.7. Scanning Electron Microscopy.....	53
4.8. Result and Discussion.....	53
4.8.1. Variations in Fiber Strength.....	53
4.9. Prediction of Tensile Strength	58

4.9.1. Basalt Fibers	58
4.9.2. Carbon Fibers.....	61
4.9.3. Variation in Tensile Strength After Exposure to Humidity	63
4.10. Leaching of Ions	64
4.10.1. Basalt Fibers	64
4.10.2. Carbon Fibers.....	64
4.11. FTIR Results.....	65
4.12. Morphological Changes.....	67
4.13. Conclusions.....	70
4.14. References.....	71
Chapter 5 : Hydrothermal Aging of Glass Fiber Reinforced Thermoplastic Composites.....	74
5.1. Introduction.....	74
5.2. Materials and Methods	76
5.2.1. Unidirectional Composite Tapes	76
5.2.2. Sample Conditioning	76
5.2.3. Water absorption testing	77
5.2.4. Mass Dissolution Testing.....	77
5.2.5. Tensile Testing.....	78
5.2.6. Fourier Transform Infrared Spectroscopy	78
5.2.7. Scanning Electron Microscopy	78
5.3. Results and Discussion	78
5.3.1. Water absorption results	78
5.3.2. Strength Changes After Aging.....	80
5.3.3. Concentration of Elements Released During Aging	82
5.3.4. FTIR Results.....	83
5.3.5. Changes in Surface Morphology	85
5.4. Conclusions.....	86

5.5. References.....	86
Chapter 6 : Conclusions and Future Work.....	89
6.1. Conclusions.....	89
6.2. Scope for Future Work.	91
Bibliography.....	93
Appendices.....	99
Appendix A: Humidity Aging Results for Glass Fibers	99
Appendix B: Investigation of strength variation of glass fibers across different batches.....	100

List of Tables

Table 1. Regression coefficients according to Eq. (3) for fitted curves in Figure 12, based on test data from fibers tested ‘dry’, and Ea/R values relating to the Arrhenius plot slopes in Figure 13.	34
Table 2. Mass of elements released from glass fiber samples aged in water at 60°C and 82°C for 168 hours (1 week).....	37
Table 3. Regression coefficients for strength retention curves for BF	59
Table 4. Regression coefficients for strength retention curves for CF	61
Table 5. Mass of elements released from basalt fiber samples aged in water at 60°C and 82°C for 7 days.	64
Table 6. Mass of elements released from carbons fiber samples aged in water at 60°C and 82°C for 168 hours (1 week).....	64
Table 7. Concentration of elements leached into solution for GF-PP.	82
Table 8. Concentration of elements leached into solution for GF-HDPE.	82

List of Figures

Figure 1. Layout of a FRPC Pipe [based on the image in [14].....	2
Figure 2. Representation of sizing rich composite interphase [1]	10
Figure 3. Roving's of commonly used Fibers. (A) Glass, (B) Carbon, (C) Basalt.....	13
Figure 4. Mechanical testing using Capstan grips, A, B (Carbon fibers: pretest, post failure)	14
Figure 5. Load vs displacement plot for tensile testing using capstan grips for carbon fiber sample ...	15
Figure 6. Mechanical testing of Glass fibers using paper tabs. A (Sample preparation), B, C (pretest, post-failure).....	16
Figure 7. Load vs displacement plot for tensile testing using paper tabs for glass fiber sample.....	17
Figure 8. Aging of fiber samples inside oven.....	29
Figure 9. Mechanical testing of glass fibers using Capstan grips: (A) Before testing and (B) post failure.	30
Figure 10. Load versus displacement plot from a tensile test of a GF sample.	32
Figure 11. Strength retentions after exposure at 60°C, 71°C, and 82°C: (A) samples tested 'wet', and (B) samples tested 'dry'.	33
Figure 12. Tensile strength retention versus aging duration for fibers tested dry. Solid lines are fitted curves according to Eq. (3) and regression coefficients in Table 1.	34
Figure 13. Arrhenius plots of calculated hydrothermal lives for different strength retention levels.	35
Figure 14. (A) TTS master curve at 60°C for glass fibers, (B) Arrhenius plot of shift factors.	36
Figure 15. (A) FTIR spectrum for pristine and aged glass fibers, and (B) intensity variations of Si O Si peaks at wavenumber 900 cm ⁻¹	38
Figure 16. SEM images showing glass fiber surfaces before and after aging. Baseline of pristine fiber (top row); aged at 60°C, 71°C and 82°C for 1 week (middle row); and for 5 weeks at 60°C and 71°C and 4 weeks at 82°C (bottom row).....	40
Figure 17. Aging of samples inside the oven.....	49
Figure 18. (a) Basalt fibers mounted on frames, (b) Carbon fibers inside the humidity chamber.....	50
Figure 19. Mechanical testing using capstan grips for Carbon fibers, (a, b) (pretest, post-failure).....	51
Figure 20. Mechanical testing of basalt fibers using paper tabs (a, b) (pretest, post-failure).....	52
Figure 21. (a) Samples inside plastic tubes, (b) Jars used for conditioning fibers.....	53
Figure 22. Variations in tensile strength for BF aged at (a) 60°C, (b) 71°C, (c) 82°C.....	55
Figure 23. Variations in tensile strength for CF aged at (a) 60°C, (b) 71°C, (c) 82°C.....	57
Figure 24. Plot for strength retention with fitted curves for BF.	59
Figure 25. Arrhenius plot with different retention levels for BF.....	60
Figure 26. Corrected Arrhenius plot with different retention levels for BF.	60

Figure 27. Plot for strength retention with fitted curves for CF.	62
Figure 28. Arrhenius plot with different retention levels for CF.	62
Figure 29. Variations in tensile strength for fibers exposed to 90°C and 90% humidity.	63
Figure 30. FTIR spectrum of aged and unaged fibers.	66
Figure 31. Variation in Transmittance values for aged and unaged fibers.	67
Figure 32. SEM images showing basalt fiber surfaces before and after aging. Baseline of pristine fiber (top row); aged at 60°C and 82°C for 7 days (middle row); and for 56 days (8 weeks) at 60°C and 28 days (4 weeks) at 82°C (bottom row).	68
Figure 33. SEM images showing carbon fiber surfaces before and after aging. Baseline of pristine fiber (top row); aged at 60°C and 82°C for 7 days (middle row); and for 70 days (10 weeks) at 60°C and 35 days (5 weeks) at 82°C (bottom row).	69
Figure 34. (A) Slitting of tapes, and (B) samples inside jars placed inside aging cell.	77
Figure 35. Weight gain vs time plot for GF-HDPE composites.	79
Figure 36. Weight gain vs time plot for GF-PP composites.	79
Figure 37. Variation in tensile strength at 95°C.	81
Figure 38. Variation in tensile strength at 60°C.	81
Figure 39. FTIR spectra of GF-PP samples before and after aging.	84
Figure 40. FTIR spectra of GF-HDPE samples before and after aging.	84
Figure 41. SEM images of fracture surfaces. GF-PP unaged (a) and after aging for 28 days at 95°C (b), and GF-HDPE unaged (c) and after aging for 28 days at 95°C (d).	85
Figure 42. Variations in tensile strength for fibers exposed to 90°C and 90% humidity.	99
Figure 43. Breaking load variation across the bobbins for Batch 1	100
Figure 44. Breaking load variation across the bobbins for Batch 2.....	101

List of Symbols

k : reaction rate constant or degradation rate constant

A : constant related to the material and aging environment

E_a : Activation energy

\bar{R} : universal gas constant

T : Absolute temperature

List of Abbreviations

FRPC: Fiber reinforced polymer composites

GF-HDPE: Glass fiber-reinforced high-density polyethylene

GF-PP: Glass fiber reinforced polypropylene

PBT: Polybutylene terephthalate.

GF: Glass fiber

BF: Basalt fiber

CF: Carbon fiber

TTS: Time temperature superposition

Chapter 1 : Introduction

Aspects of the material discussed in this chapter have been published in the proceedings of the Canadian Society for Mechanical Engineering (CSME) International Congress, Sherbrooke, Quebec, Canada, May 28 - 31, 2023.

1.1. Background and Motivation

For several decades, fiber-reinforced polymer composites (FRPC) have grown in use and popularity due to their superior mechanical qualities, such as high strength and modulus, while being relatively lightweight and corrosion-resistant compared to more conventional structural materials [1, 2]. An FRPC comprises three essential components: a polymer matrix, a fibrous reinforcement, and typically a multi-component coating on the surface of the fibers—the sizing. When making FRPC, the sizing causes the matrix polymer and the reinforcing fibers to produce a sizing-rich composite interphase, which chemically and/or physically bonds the fibers and the polymer [3].

High-performance filaments are widely used to reinforce composite materials, including basalt, glass, and carbon fibers. It is well known that the fibers in composites reinforce the matrix with its relatively low strength and rigidity. In composite structures, the fibers chiefly carry the applied loads while the matrix distributes stresses to and between the filaments and shields them from damaging external forces and environmental factors [4,5]. FRPC is commonly made with a thermoset polymer matrix. However, in recent years, thermoplastic matrix materials have been increasingly employed as an effective substitute. Some key benefits of thermoplastic matrix materials over their thermoset counterparts are practically infinite shelf life, the ability to recycle thermoplastic polymers, and possible reductions in manufacturing cost that can be achieved using rapid and continuous fabrication processes [6,7].

Commonly, FRPC are used in structural applications where humid air and water environments can be present, such as in offshore, wind energy, and oil and gas applications [2,8]. FRPC deteriorate over time in wet and humid conditions as hydrolytic degradation and environmental aging can reduce their mechanical qualities [8-11]. Degradation effects typically accelerate with exposure to elevated temperature conditions [12]. Additionally, environmental aging may impact the various elements of a composite material system by different mechanisms [13]. Therefore, a thorough understanding of the mechanisms and dynamics of environmental aging of the individual constituents is crucial to ensure the environmental durability of composites. A lack of understanding poses significant risks when employing composites in conditions that subject them to prolonged exposure to a mix of elevated temperatures, forms of water, and other fluids such as hydrocarbons. Expensive and time-consuming testing campaigns usually narrow such knowledge gaps. Although there have been several attempts to evaluate the performance of composite materials exposed to

various environmental conditions, the studies focusing on fiber reinforcements are limited. The same applies to fibers embedded in a thermoplastic matrix compared to their thermosetting counterparts. Thermoplastic composites, particularly glass fiber-reinforced high-density polyethylene (GF-HDPE) and glass fiber-reinforced polypropylene (GF-PP) material are attractive for aerospace, automotive, and oil and gas applications. Yet, data on their long-term durability is limited when compared with FRPC with thermoset matrices. The current situation demonstrates the need for more practical tools for accurately predicting changes in the characteristics of composite materials and their constituents due to environmental aging and the incomplete understanding of the processes involved, i.e., the degradation processes taking place at the micro-constituent level and their respective mechanisms. Also, very few attempts have been made to forecast the service life of ‘dry’ fibers and an effort to transfer these results into the composite level.

1.2. Relevance of Thesis to Industrial Partner

Combining the advantages of composite materials and those offered by thermoplastic composites, thermoplastic composite pipes are emerging as a viable alternative to traditional metal pipes [14]. This project is driven primarily by the high demand for recyclable and environmentally friendly spoolable composite piping ("linepipe") for oil, gas, and water applications. Figure 1 illustrates the structure of a thermoplastic polymer pipe, typically made up of an inner thermoplastic liner, a continuous reinforcing phase that is helically wrapped, and an outer thermoplastic jacket. The thermoplastic polymer pipe's primary load-bearing phase is the reinforcement phase, which can be either dry fiber reinforcement or a polymer composite bonded or unbonded to the inner and outer thermoplastic layers. Commonly used reinforcements are glass, carbon, and basalt fibers. The jacket serves as a protective covering for the reinforcements from external damage and environmental conditions.

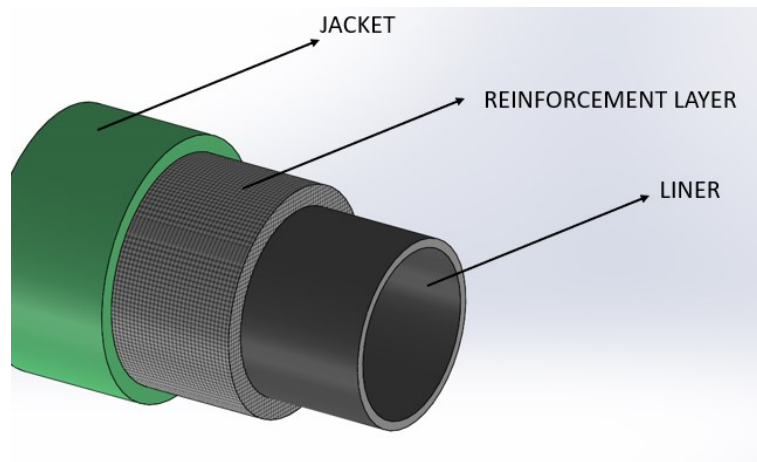


Figure 1. Typical structure of a FRPC pipe (adopted from [14]).

The ultimate goal of this partnership with the industrial partner is to identify an application envelope for lightweight thermoplastic composite pipes reinforced with glass, carbon, and basalt fibers based on their durability and thermomechanical performance under various environmental aging circumstances. One typical scenario under investigation is groundwater seeping in through vent holes or damage (cracks) in the pipe jacket, which can be in direct contact with the load-carrying reinforcements. So, understanding the possible reductions in strength due to these exposures could be an important design factor for the durability of thermoplastic composite pipes. Also, criteria developed from the research could be used to select reinforcements for elevated-temperature applications. This endeavor starts by understanding the performance of glass, carbon, and basalt fibers in hydrothermal aging conditions, which can be used to simulate the abovementioned situations. As a result of the collaboration, the industrial partner will be able to make selections for their future products based on the hydrothermal resistance data and may develop additional coatings or sizing to improve the performance of the selected fiber.

1.3. Hypothesis and Thesis Objectives

The thesis work is part of a more extensive collaboration with the industrial partner. The Advanced Composites Materials Engineering Group at the University of Alberta took on the task of evaluating the performance of carbon, glass, and basalt fibers exposed to water at different temperatures. The data provided through this research will be used as input for the company to create a comprehensive multiscale framework for evaluating the performance of composites when exposed to hydrothermal aging conditions. The industrial partner uses the findings provided by this research as input to guide future developments for the design and fabrication of polymer-based piping.

The underlying research hypothesis for this thesis project is that the damage occurring to the fibers and the fiber matrix interphase is the key factor for the reduction in the performance of composites exposed to hydrothermal conditions. When it comes to ‘dry’ fibers, the loss of sizing and water attack on the fiber itself leads to property loss. Also, it is postulated that an Arrhenius modeling approach can be used to forecast the lifetime of the reinforcement materials, and that short-term data can be used to predict the service life of actual composite structures.

The key objectives considered in this work are:

- Develop a strategy to condition fiber reinforcements for hydrothermal aging.
- Develop and establish a testing methodology for tensile testing of fibers.
- Investigate how the influencing environment, in this case, water, interacts with the fibers. The mechanical and chemical/physico-chemical aspects of the processes involved are explored to better understand the underlying mechanisms causing the change in properties.

- Develop an analytical approach based on environmental aging tests to forecast changes in the characteristics of the fibers due to exposure to such settings. In the current situation, the developed tools will help to replace demanding physical, time-consuming, and expensive testing methods.
- Extend the same methods to thermoplastic composites and understand the underlying mechanisms leading to the change in properties and establish a correlation with the previous studies.
- Provide input data for the reinforcement component to develop a multiscale model for predicting the service life of composites.

1.4. Structure of the Thesis

The thesis is divided into six chapters. The first chapter provides an overview of the project, highlighting the thesis objectives. The second chapter gives a comprehensive insight into earlier works and explains the utilized life prediction models in detail. Note that Chapters 3, 4, and 5 of this thesis are either already published or are to be submitted for publication. Chapter 3 focuses on establishing the conditioning and testing methodology on glass fibers and service life prediction using the Arrhenius model. Chapter 4 expands the subject matter of Chapter 3 to additional fiber materials (i.e., carbon and basalt) while also including extended conditioning durations and evaluating the performance of fibers exposed to humidity. Chapter 5 explores the aging mechanisms happening in a composite by comparing the performance of GF-HDPE and HG-PP composite tapes, demonstrating how the results of Chapters 3 and 4 translate into actual composite aging. Finally, Chapter 6 summarizes the study's findings and provides the scope for future work.

1.5. References

- [1] A. E. Krauklis, "Modular Paradigm for Composites: Modeling Hydrothermal Degradation of Glass Fibers," *Fibers*, vol. 9, no. 12, p. 83, 2021.
- [2] A.E. Krauklis, *Environmental Aging of Constituent Materials in Fiber-Reinforced Polymer Composites*, Trondheim: NTNU, 2019.
- [3] S. Feih, J. Wei, P. Kingshott and B. Sørensen, "The influence of fiber sizing on the strength and fracture toughness of glass fiber composites," *Composites Part A: Applied Science and Manufacturing*, vol. 36, no. 2, pp. 245-255, 2005.
- [4] B. Wei, H. Cao and S. Song, "Tensile behavior contrast of basalt and glass fibers after chemical treatment," *Materials & Design*, vol. 31, no. 9, pp. 4244-4250, 2010.
- [5] J. Sim and C. Park, "Characteristics of basalt fiber as a strengthening material for concrete structures," *Composites Part B: Engineering*, vol. 36, no. 6-7, pp. 504-512, 2005.

- [6] A. E. Krauklis, C. Karl, A. Gagani and J. Jørgensen, "Composite material recycling technology— State-of-the-art and sustainable development for the 2020s," *Journal of Composites Science*, vol. 5, no. 1, p. 28, 2021.
- [7] A. Kasper, "Recycling composites: FAQs," *Reinforced Plastics*, vol. 52, no. 2, p. 39, 2008.
- [8] I. Grabovac and D. Whittaker, "Application of bonded composites in the repair of ships structures— A 15-year service experience.," *Composites Part A: Applied Science and Manufacturing*, vol. 40, no. 9, pp. 1381-1398, 2009.
- [9] M. Robert, R. Roy and B. Benmokrane, "Environmental effects on glass fiber reinforced polypropylene thermoplastic composite laminate for structural applications.," *Polymer composites*, vol. 31, no. 4, pp. 604-611, 2010.
- [10] E. Kuram, "Thermal and water ageing effect on mechanical, rheological and morphological properties of glass-fiber-reinforced poly (oxymethylene) composite.," *Journal of Process Mechanical Engineering*, vol. 233, no. 2, pp. 211-224, 2019.
- [11] A. Messina, A. Airale, A. Ferraris, L. Sisca and M. Carello, "Correlation between thermo-mechanical properties and chemical composition of aged thermoplastic and thermosetting fiber reinforced plastic materials:," *Materialwissenschaft und Werkstofftechnik*, vol. 48, no. 5, pp. 447-455, 2017.
- [12] M. Silva, B. Fonseca and H. Biscaia, "On estimates of durability of FRP based on accelerated tests.," *Composite Structures*, vol. 116, pp. 377-387, 2014.
- [13] A.E. Krauklis, A. Gagani and A. Echtermeyer, "Long-term hydrolytic degradation of the sizing-rich composite interphase," *Coatings*, vol. 9, no. 4, p. 263, 2019.
- [14] J. De Kanter, L. C.G and A. Tubulars, "Thermoplastic composite pipe: analysis and testing of a novel pipe system for oil & gas.," *Proceedings of the 17th ICCM*, pp. 1-10, 2009.

Chapter 2 : Composites and Environmental Durability

2.1. Durability of Composites.

The application of continuous fiber-reinforced polymer (FRP) composites in structural applications has significantly increased over the last decade. This increased usage can be attributed to the superior performance of FRPs because of their unique qualities, which include low cost, high specific stiffness and strength, an almost infinite shelf life for raw materials, and exceptional corrosion resistance compared with conventional structural materials like steel and aluminum [1]. Three main components make up an FRP composite: the polymer matrix, reinforcements, and the sizing. The latter is a coating on the surface of the fibers. The constructive interaction between these components results in the superior mechanical performance of FRP composites. Traditional FRP composites comprise thermoset polymers, while thermoplastic (TP) matrix materials are emerging as an effective substitute in recent years. Due to their less hazardous chemical compositions, enhanced recyclability, non-necessity for a curing stage, and capacity for rapid mass manufacturing compared to conventional thermosetting resins, thermoplastics have drawn much attention as polymer matrices [2]. The aerospace, military, automotive, and chemical industries are now widely employing thermoplastic-based composites because of the added benefits that a thermoplastic matrix offers to a composite [3].

FRPs used in structural applications are often exposed to water and humid environments, and these exposures deteriorate their mechanical properties. These situations become more severe at higher temperatures, where the degradation phenomenon will be accelerated [4]. The individual components in the composite behave differently under these exposures and contribute to the overall reduction in mechanical properties. It is important to comprehend the strength reduction under these conditions as it is a vital input to any design based on durability. Understanding the degradation mechanisms of individual components involves time-consuming and costly testing processes. There have been several attempts to investigate the effect of environmental conditions on composites. Most of these studies have been focused on thermoset matrix-based composites. For example, Julio et al. [5] performed a durability study on glass fiber-reinforced polymer (GFRP) bars exposed to tap water. They stated that the degradation of the fiber/matrix interphase was the primary reason for reduced GFRP bar performance. The authors also emphasized that fiber corrosion due to prolonged exposure may dominate the degrading process. In a similar study by Idrisi et al. [6] the resilience of an E-glass/epoxy composite was tested in a salt-water environment. The leading causes for a loss in tensile strength were the breakdown of chemical bonds between fiber and resin caused by chemical corrosion and poor interlocking between fibers and resin caused by resin swelling owing to water absorption, particularly at 90°C immersion. Later, Noamen et al. [7]

conducted hydrothermal aging studies of glass-epoxy and carbon-epoxy laminated composites exposed to temperatures 24, 70, and 90°C. The water absorption was found to obey Fickian behavior in all the tested laminates. Moreover, GF-epoxy composites were reported to have a higher diffusion coefficient due to their polarity and hydrophilicity. Matrix plasticization brought on by moisture and temperature resulted in the loss of mechanical characteristics.

There is an increased emphasis on expanding the knowledgebase for durability studies on thermoplastic-based composites due to the inherent advantages they offer over thermoset matrix composites. Thermoplastic-based composites have been studied by comparatively very few researchers and aimed toward aerospace and military applications [3]. In [8], the variation in flexural properties of glass fiber-reinforced polypropylene composite laminates was studied by exposing them to tap water, salt solution, and freeze-thaw cycles at 23°C, 50°C, and 70°C. The results indicated that salt solution had a more detrimental effect on the flexure properties than tap water. Strength reductions were attributed to degradation effects occurring at the fiber matrix interphase. Later, Emel et al. [9] investigated the aging behavior of glass fiber reinforced poly(oxymethylene) composite exposed to air or water at room temperature and in an oven at 100°C. A decrease in tensile and flexural strength was observed for every aging environment, with samples aged in water experiencing the greatest strength loss. All aged samples were found to have melt flow index values higher than those of the unaged samples. Variations in melt flow index may thus be an indicator of degradation. In another study, Borges et al. [10] showed that mechanical qualities were more sensitive to temperature than humidity level, as the former promoted water uptake in short glass fiber-reinforced polybutylene terephthalate (PBT). Even though stiffness and tensile strength decreased due to humidity, a definite dependence on water uptake was not seen. It was determined that the decrease in mechanical properties was brought about by water intrusion induced polymer chain relaxing. When samples were examined using Fourier-transform infrared spectroscopy (FTIR) after aging, the PBT laminates above 80°C showed signs of chemical alteration. Fang et al. [11] investigated the performance of carbon fiber-reinforced polycarbonate (CF/PC) composites exposed to deionized water at 80°C and measured the changes in storage modulus and erosion angle. The maximum erosion angle of composites was observed to deviate due to hydrothermal aging, showing that the composites underwent a transition from ductile to brittle behavior. Furthermore, using scanning electron microscopy, cracks and cavities caused by water absorption were visible, suggesting that hydrothermal aging causes CF/PC composites to plasticize and degrade, which lowers their corrosion resistance.

Research on FRP composites demonstrates hydrolytic deterioration in long-term exposure is mainly brought on by degradation occurring in the matrix fiber interphase and via fiber dissolution processes [12-14]. Although thermoplastic-based FRPCs are known for being lightweight and corrosion-resistant, their

durability in wet environments and at elevated temperatures raise concerns. Studies demonstrating the vulnerability of thermoplastic-based FRPC to water exposure and elevated temperatures have demonstrated how important the durability of the fiber and thermoplastic matrix is for the safe functioning of a structure [8-11]. The corrosion resistance of the resin is a major factor in the filament's corrosion resistance, and resin toughness also impacts how quickly corrosion cracks spread [15].

It should be mentioned here that further details and key findings on environmental aging of the thermoset and thermoplastic matrix-based composites, including mechanisms and deterioration of the mechanical properties, can be found in the introduction parts of Chapters 3, 4 and 5

2.2. Reinforcements and Environmental Durability

Glass, carbon, and basalt fibers are commonly used as reinforcements in composites for structural applications. Most of the time, these fibers are combined with a thermoset or thermoplastic matrix. However, some applications use 'dry' fibers as the load-carrying member [16]. 'Dry' fiber refers to the fibers without any matrix, with just the sizing or even without it. There are only few studies focusing on 'dry' fibers, and among those, most are limited to glass fibers exposed to aggressive chemical environments. Jones et al. [17] examined the corrosion rate of glass fibers (GFs) by comparing the residual strength of the fibers before and after exposure to sulphuric acid at various concentrations and temperatures ranging from 10°C to 50°C. They discovered that an increase in temperature accelerates corrosion, while the concentration of sulphuric acid did not significantly influence the corrosion rate. It was explained that precipitation, rather than complex ion formation, facilitates the removal of calcium from glass. In a similar study on E-glass fibers exposed to sulphuric acid, the authors found that the sulfuric acid treatment causes a decrease in the Si, Ca, Al, Mg, Fe, and Na content of the surface of GFs while increasing the oxygen concentration. In addition to the ion exchange reaction, the hydrolysis of Si-O-Si bonds was also considered a contributing factor in the corrosion of E-type GFs in sulfuric acid [18]. In another work, the impact of temperature and heating duration on the tensile strength and failure mechanisms of GFs was studied at temperatures up to 650° C and heating times as long as two hours. It was proven that the glass mirror constant, which reflects the network structure, does not change during heat treatment, and the strength degradation was caused by greater surface imperfections present after heat treatment [19]. Andrey et al. [20] developed a model utilizing zero-order kinetics to predict the mass dissolution of fibers exposed to water at 60°C. Elements released during degradation included Na, K, Ca, Mg, Fe, Al, Si, and Cl. Rate constants for the overall mass loss and each ion release were discovered. Si contributed the most to mass loss (56.1%) compared to other components. Bin et al. compared the performance of basalt and glass fibers treated with sodium hydroxide and hydrochloric acid solutions based the mass loss ratio and the strength retention ratio of the fibers. They observed that basalt fibers' acid resistance is far greater than their alkali

resistance. The acid resistance, however, is comparable to the alkali resistance for glass fibers. Overall, basalt fibers were more chemically stable than glass fibers, especially in an acidic environment [21].

It is understood that the eventual seepage of the corrosion fluid beyond the resin-rich liner and the fluid's attack on the glass itself are the primary causes of failure in fiber reinforced corrosion-resistant pipe and tanks. Considering the above-mentioned situation, Kliger et al. [22] performed a durability study on glass and carbon fibers exposed to strong acids and bases. They stated that carbon fiber exposed to strong acids or bases over a prolonged length of time (10 weeks) at high temperatures (150–180°F), did not show any evidence of strength or modulus degradation. Weight loss was found to be insignificant. Comparing carbon fiber to E and E-CR type glasses, carbon fiber exhibits significantly improved corrosion performance. This was shown for the case of sodium hydroxide and HF-containing acids, with a lesser extent for hydrochloric, nitric, and sulfuric acids. Recently, Andreas et al. [23] investigated the strength degradation of glass and carbon fibers exposed to water and toluene at 60°C and developed a model that connects the loss of strength of fibers in water to the Griffith flaw theory. A reduction in strength by 33% was observed for glass fibers after exposure to water at 60°C for 90 days. While carbon fibers are thought to be inert to both liquids, results revealed minor changes in strength for both ageing in water and toluene. Interestingly, a 10% increase in strength was observed for carbon fibers after 90 days of exposure to water. From the review of the technical literature, it can be concluded that most studies on environmental degradation of reinforcements are concerned with the direct deterioration of the mechanical characteristics, and the mechanistic basis and the kinetics of chemical degradation tend to be disregarded. Note that additional details and key findings for environmental aging of glass, carbon, and basalt fibers, including chemical analysis, can be found in Chapters 3 and 4.

2.3. Environmental Aging of Sizing Rich Composite Interphases

Nearly all synthetic fibers are manufactured with a thin surface layer called size, composed primarily of organic components. Sizing can be defined as a technique of covering fibers with a size. Nevertheless, the words sizing, and size can be used interchangeably. Even though fiber sizes are crucial to virtually every aspect of the processing and performance of fiber reinforced polymer (FRP) composites, size and sizing remain a "black box" technology in composites technology because fiber producers are very reluctant to divulge much information about the intricate formulations they employ. The right sizing provides effective wetting during composite manufacturing with a low void rate, protects the fibers throughout processing, reduces fuzz during handling, disperses well on the fibers providing a homogeneous result, and protects the fibers during handling. Consequently, the composition promotes high fiber matrix interaction for effective stress transfer at minimal cost [24]. The film former and the coupling agent are the main elements of a sizing [25, 26]. The film former is designed to protect and lubricate the fibers and hold them together before

composite processing, yet also to stimulate their separation when in contact with resin, assuring the wet-out of all the filaments. The coupling agent, generally an alkoxy silane molecule, is often said to principally link the fiber to the matrix resin. Sizes may also contain other lubricants, antistatic agents, and surfactants in addition to these two main ingredients [24,27]. Improvements in interphase strength and hydrothermal resistance of the composite interphase have been documented in many cases due to the presence of sizing [26]. A schematic representation of polymer interphase is depicted by Figure 2. A composite interphase is typically about a micrometer thick and is a gradient-type mixture of the sizing chemicals and the bulk matrix polymer [28-30]. The composite interface is crucial since the mechanical properties of a composite depend on an efficient load transfer from the matrix to the reinforcement phase [12]. Also, it is well known that the composite interphase is frequently the mechanical weak link and a possible starting point for faults in fiber-reinforced composite structures [1,28]. Water and humid environments significantly affect the mechanical characteristics of FRPs partially because of a loss of the interfacial bonding [26,28, 31]. Flaws in the interphase can be introduced due to the interaction with water uptake from the environment [32]. The removal of the sizing material can also lead to microcrack initiation at the surface of glass fibers, and various sizing components can dissolve by water, resulting in the loss of the material [33,34]. Understanding the kinetics and environmental aging mechanism of a sizing-rich composite interphase is crucial. To investigate the environmental aging of the composite interphase, there are no direct measurement techniques available. The interphase loss in the composite due to environmental exposure is yet to be quantified.

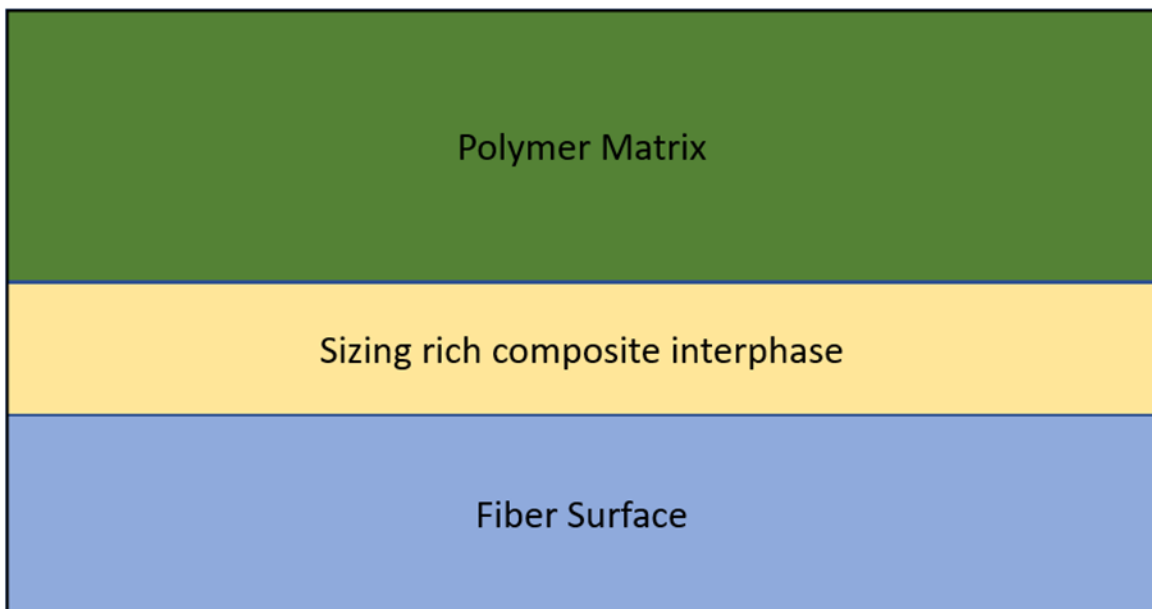


Figure 2. Representation of sizing rich composite interphase [1].

2.4. Durability Prediction Models

2.4.1. Arrhenius Model

When temperature is the main accelerating factor in aging for composites, the Arrhenius model is frequently employed to determine service life [4,14,35,36]. For materials below their glass transition temperatures, the Arrhenius model accurately predicts the effects of temperature in accelerated aging experiments. The underlying assumption is that there is a single dominating degradation mechanism that does not change throughout exposure and that the degradation rate accelerates as exposure temperature increases. The general form of the Arrhenius model is given as:

$$k = A \cdot \exp\left(-\frac{E_a}{RT}\right), \text{ or, } \ln k = -\frac{E_a}{RT} + \ln A \quad (1)$$

where k is the reaction rate constant or degradation rate constant, A is a constant related to the material and aging environment, E_a is the activation energy, \bar{R} is the universal gas constant, and T is the absolute temperature. Recognizing that the reaction rate constant is inversely related to time, k in the Arrhenius equation is frequently used for computing the time to attain a material's particular strength loss [37]. Using ultimate mechanical properties and their retention, such as tensile strength, interfacial shear strength, creep strength, and fatigue strength, the Arrhenius relationship has frequently been used to forecast the lifetime of polymers and composites [35]. The prediction procedure involves the following three main steps [37-39]:

- Step 1: Plotting the property values at a specific temperature against time and fitting a curve through the points that reflect the degradation pattern.
- Step 2: Determining the retention levels, also known as lifetime points, that represent the time required for a material to reach a given degree of property degradation. These are directly obtained from the fitted curve.
- Step 3: Plotting the logarithm retention time (hours) versus the inverse of temperature ($1/T$). The model is established via a linear fit with a regression coefficient (R^2) value of at least 0.8.

2.4.2. Time-temperature Superposition Approach

Another commonly used durability prediction methodology is the time temperature superposition (TTS) approach. It involves calculating a shift factor for two temperatures. The TTS theory states that a material's properties achieved after a brief exposure to a higher temperature are equal to those obtained after longer exposure to a lower temperature [37-40]. For two temperatures T_1 and T_2 where $T_1 < T_2$ is given by:

$$TSF = \frac{t_1}{t_2} = (A * \exp\left(-\frac{E_a}{RT_2}\right)) / (A * \exp\left(-\frac{E_a}{RT_1}\right)) \quad (2)$$

where T_{SF} is the time shift factor. The process involves selecting a reference temperature and calculating the shift factor for the other temperatures. Then, the natural logarithm of the shift factor is plotted against the inverse of temperature ($1/T$). The agreement with the Arrhenius model is established via a linear fit with a regression coefficient (R^2) value of at least 0.8 [38,39].

2.5. Determination of Fiber Strength

The strength of a material is defined as its ability to resist applied loads without failing. Usually, for fibers, load is applied monotonically until failure occurs. Materials fail at their weakest point, usually because of imperfections in the material. Studies of tensile failure data shed light on how fiber defects are distributed. Fiber strength is commonly represented in breaking tenacity, which is the breaking load divided by linear density. Also, it can be represented in terms of ultimate strength, which is breaking load divided by the original cross-section area.

2.5.1. Fibers Used in Composite Materials

Composite materials use a variety of fibers as reinforcements. Most reinforcing fibers are designed to have high strength, high stiffness, and low density. Based on length, fibers can be divided into three categories: continuous fibers, long fibers, and short fibers. Glass, carbon and basalt fibers are among the most commonly used reinforcements in composite materials. Due to an extraordinarily high performance-to-price ratio, more than 95% of the reinforcement used in the composite industry is made of glass fiber [26]. The primary component of glass fibers is silica (SiO_2) consisting of an irregular network of silicon atoms bonded together by Si-O-Si bonds [41]. The major application areas for GF in the global market are wind turbines, transportation, construction, consumer items, and industrial uses. Because of excellent qualities, including high specific tensile strength, high modulus, and outstanding wear resistance, carbon fibers (CFs) have been widely used to reinforce advanced composite materials in industries such as aerospace, transportation, and sporting goods [2]. As the name implies, carbon fibers mostly comprise carbon above 90%, and nitrogen, in concentrations ranging from 3% to 7% [42]. In recent years, basalt fibers have evolved as an innovative replacement for GFs. The absence of additives and a continuous manufacturing process gives basalt fibers added advantages in terms of cost. For these reasons, basalt fibers are applied to a variety of fields, including the chemical industry for corrosion-resistance materials, the automobile industry for wear and friction materials, the construction industry as reinforcing materials, and the automotive industry for high temperature insulation of catalysts. An iron oxide composition is one way that basalt fibers differ significantly from other metal oxide fibers, including glass or ceramic fibers. In contrast to the translucent and white glass and ceramic fibers, basalt fibers are dark colored due to the presence of iron oxides [43]. Although the above-mentioned fibers offer excellent properties, one key characteristic which separates these three fibers is the corrosion resistance, relative to the applications. For

most part of the thesis the focus will be on glass, carbon and basalt fibers (Figure 3), nevertheless the same concepts and theories could be applied to other fiber reinforcements as well.



Figure 3. Roving's of commonly used fibers. (A) glass, (B) carbon, (C) basalt.

2.5.2. Fiber Tensile Testing

Characterizing fibers is always challenging because of their small diameter, particularly for brittle fibers like glass. Because of their small cross-section, fibers are incredibly delicate to handle, making preparing and testing fiber specimens quite laborious. These difficulties significantly impact accuracy of prepared specimens and may result in incorrect assessments of fiber strength. Despite significant advancements in characterization methods, it is still quite challenging to collect reliable data on fiber strength. The strength of a fiber material and its distributions can be determined using various techniques, including fiber bundle tests, fiber fragmentation tests, single fiber tensile testing, loop tests, etc. Each technique, though, has its own drawbacks.

2.5.2.1. Capstan Grips

Testing of carbon fibers using capstan grips is shown in Figure 4. This technique involves wrapping the fibers around a capstan or drum and locking the fiber ends to prevent slipping. Then, the fibers are loaded until failure occurs. A typical load extension curve using the capstan method is shown in Figure 5, where l_0 represents the slack in the fiber creating a non-linearity in the load elongation curve. The capstan technique is frequently employed, such as when adhering to standards ASTM D2256M-10 and ASTM D2343-17 [44,45]. This method is the primary choice for testing high-strength fibers and prepregs. However, some limitations exist as follows:

- The capstan method can hardly be used to obtain accurate estimates of the modulus and the elongation at break, as the slack, as shown in Figure 5, interferes greatly determining values needed for calculating the modulus and elongation.
- Fine control of test gauge length is impossible with this method. Usually, the gauge length is specified within a range of lengths. As fiber strength is dependent on the gauge length, this could implicate variations in the strength values.
- The possibility of damaging the fibers during the mounting process is very high, and the required additional care needed during sample preparation makes it a time-consuming and laborious test process.
- If there is improper handling of fibers, twist can occur in the sample mounted for testing, which can cause large variations in the test results.
- If the fiber is having catenary issues, i.e., unequal filament or bundle lengths, then testing using this method can cause an unequal distribution of stresses on the fibers leading to premature failure of filaments.

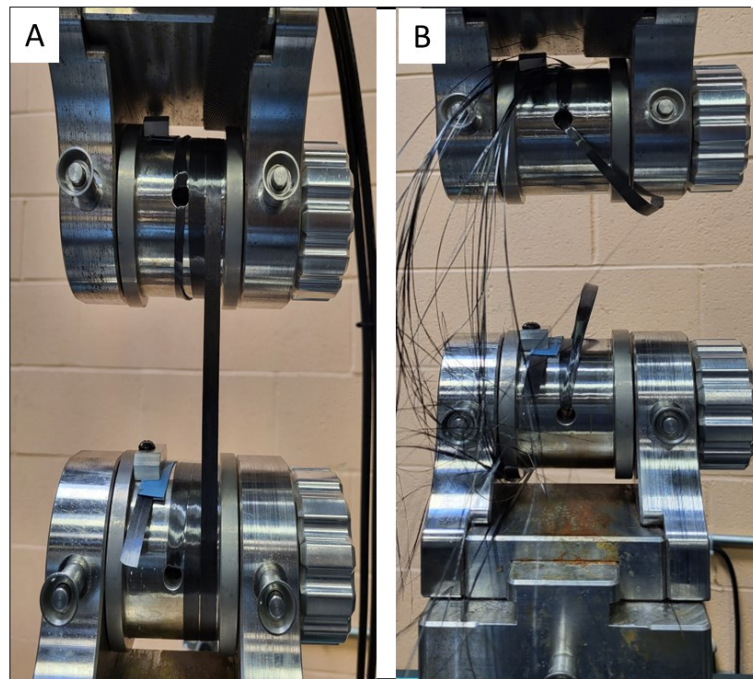


Figure 4. Mechanical testing using capstan grips: Carbon fibers pretest (A) and post failure (B).

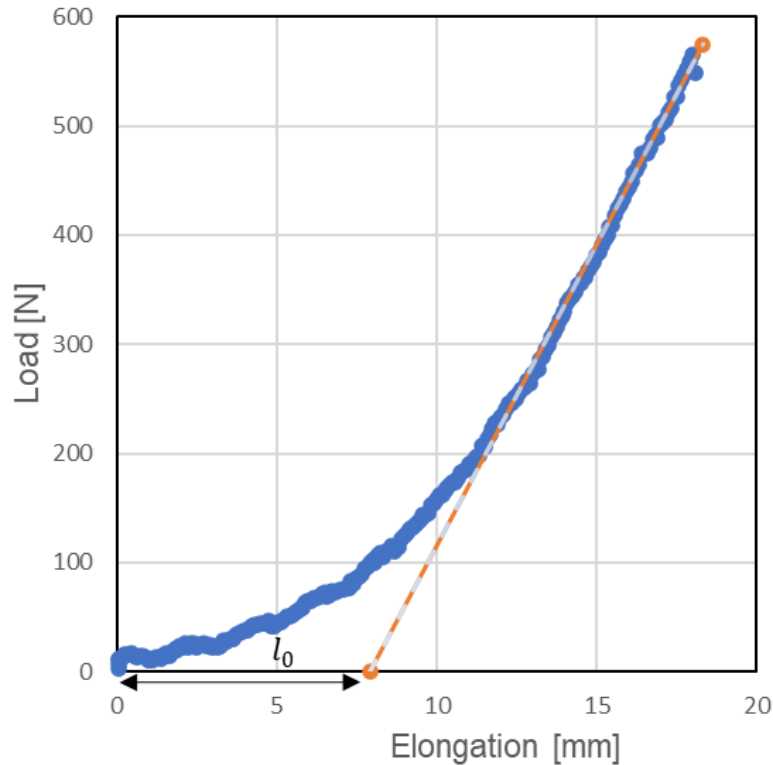


Figure 5. Load versus displacement plot for tensile testing using capstan grips for a carbon fiber sample.

2.5.2.2. Tabbing Method

The tabbing method is illustrated in Figure 6, where (A) represents the gluing of fiber ends using paper tabs, and B and C represent the pretest and post-failure images. The testing process involves removing a fiber from the fiber bundle and mounting them on a piece of paper with dimensions specified using a marker. Then the ends are carefully glued so that it matches the lines to keep them straight without any misalignment and twists. After that, the sample is mounted into the grips. The center paper portion is removed before commencing the test. This test is usually carried out at a very high stroke rate, adhering to standard ASTM C1557-20 and ISO 3341 [46, 47]. A load elongation curve for glass fibers tested using the tabbing method is shown in Figure 7. Compared to the capstan method, this method gives a more reliable estimation of the elongation at break, and the effect of slack and twist in the fibers is eliminated to a great extent. The lines drawn on the paper can control the gauge length and keep the fiber aligned in a straight line. Still, this testing method is still subject to limitations:

- It is challenging to test fibers or tapes with very high values of breaking load (typically above 1.5 kN), as fiber slippage from the grips frequently occurs.

- If improper gripping pressure is applied, there is a high chance of breakage of fibers in the gripping portion.
- It is crucial for the test to be carried out properly that the fibers are well aligned in the direction of the applied force, which depends on the precision of the paper tabs' size and form as well as how the fibers are mounted on top of these tabs. Since these procedures are typically performed manually, the operator skill has a significant impact on test accuracy.

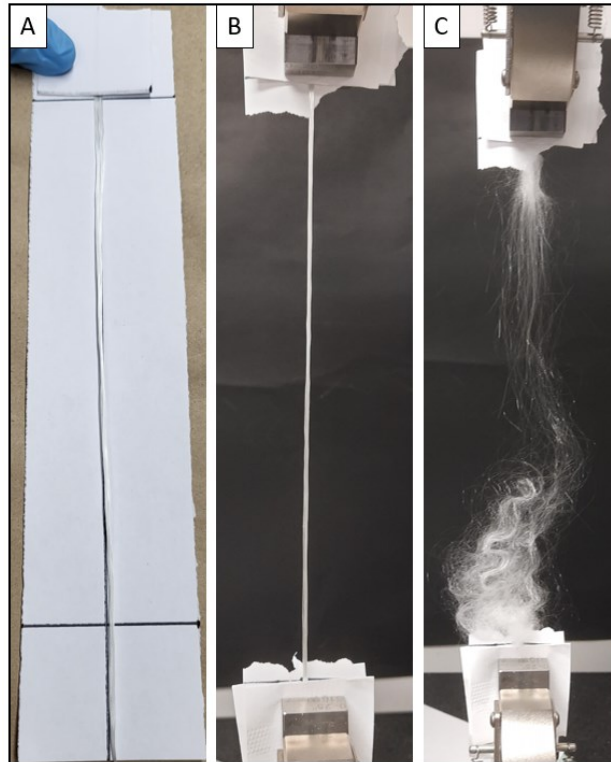


Figure 6. Mechanical testing of glass fibers using paper tabs: Sample preparation (A), and fiber pretest (B) and post-failure (C).

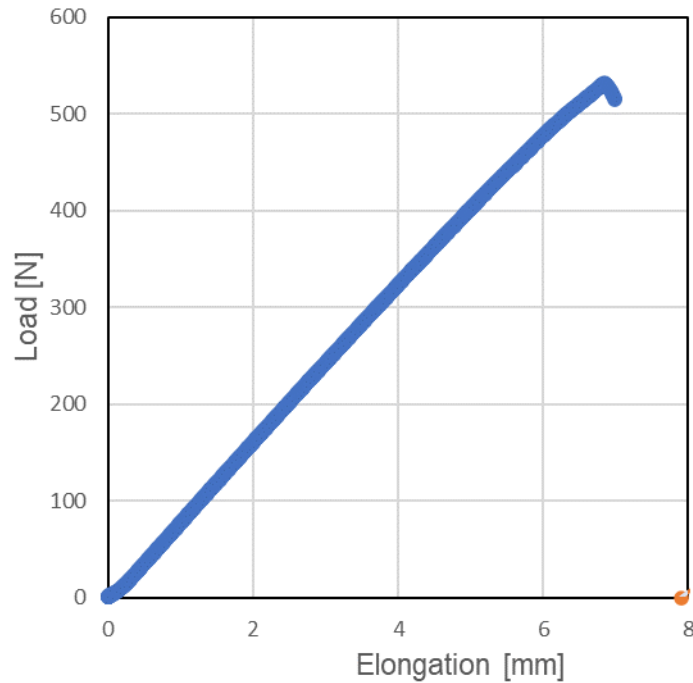


Figure 7. Load versus displacement plot for tensile testing of a glass fiber sample using the paper tabs method.

2.5.3. Critical Parameters in Fiber Strength Measurements

The following is a list of critical factors affecting single fiber testing and the determination of fiber strength distribution:

- **Gauge length:** Fiber strength is highly dependent on gauge lengths. Shorter fibers are more likely to be stronger since they are less likely to have flaws. So, variations in gauge lengths can affect the variations in the strength of fibers. So, it is crucial to select an appropriate gauge length. Moreover, it needs be held constants for all the tested specimens.
- **Alignment of fibers:** During a test, it is crucial to ensure the applied load is appropriately transferred to the fiber. A minimal amount of fiber misalignment could result in improper load transmission. This could lead to an inaccurate estimation of fiber strength and measurement of the failure load [48].
- **Variations within fibers:** Depending on the type of material and manufacturing procedure used to make the fibers, the diameter or width of certain fibers and tows, can in some circumstances vary significantly. So, attention should be paid to selecting the representative samples for testing.
- **Sample preparation:** The breaking load is very low for individual filaments due to their small diameters. Hence, during the fiber extraction process from a bobbin or bundle and specimen

preparation, multiple filaments can easily be broken, leading to lower fiber strength values. Therefore, attention must be given to carefully extracting samples from fiber bobbins and mounting them for testing.

- **Number of tests:** It is necessary to have sufficient data points for fiber strength to prevent misinterpreting the test data. Depending on the selected testing method, the appropriate number of experimental repeats should be chosen. If a large number of fiber strength data points are available for analysis, the precision of a statistical function that is used to characterize the fiber strength distribution could be significantly increased. The derived parameter values for the typical statistical distribution would be more trustworthy as a result.

2.6. References

- [1] A.E. Krauklis, A. Gagani and A. Echtermeyer, "Long-term hydrolytic degradation of the sizing-rich composite interphase," *Coatings*, vol. 9, no. 4, p. 263, 2019.
- [2] X. Gabrion, V. Placet, F. Trivaudey and L. Boubakar, "About the thermomechanical behaviour of a carbon fiber reinforced high-temperature thermoplastic composite," *Composites Part B: Engineering*, vol. 95, pp. 386-394, 2016.
- [3] S. Yao, F. Jin, K. Rhee, D. Hui and S. Park, "Recent advances in carbon-fiber-reinforced thermoplastic composites: A review," *Composites Part B: Engineering*, vol. 142, pp. 241-250, 2018.
- [4] M. A. Silva, B. da Fonseca and H. Biscaia, "On estimates of durability of FRP based on accelerated tests.," *Composite Structures*, vol. 116, pp. 377-387, 2014.
- [5] J. F. Davalos, Y. Chen and I. Ray, "Long-term durability prediction models for GFRP bars in concrete environment," *Journal of Composite materials*, vol. 46, no. 16, pp. 1899-1914, 2012.
- [6] A. Idrisi, A. Mourad, B. Abdel -Magid and B. Shivamurthy, "Investigation on the durability of E-Glass/Epoxy composite exposed to seawater at elevated temperature.," *Polymers*, vol. 13, no. 13, p. 2182, 2021.
- [7] N. Guermazi, A. Tarjem, I. Ksouri and H. Ayedi, "On the durability of FRP composites for aircraft structures in hygrothermal conditioning.," *Composites Part B: Engineering*, vol. 85, pp. 294-304, 2016.
- [8] M. Robert, R. Roy and B. Benmokrane, "Environmental effects on glass fiber reinforced polypropylene thermoplastic composite laminate for structural applications.," *Polymer composites*, vol. 31, no. 4, pp. 604-611, 2010.

- [9] E. Kuram, "Thermal and water ageing effect on mechanical, rheological and morphological properties of glass-fiber-reinforced poly (oxymethylene) composite," *Proceedings of the Institution of Mechanical Engineers, Part E: Journal of Process Mechanical Engineering*, vol. 233, no. 2, pp. 211-224, 2019.
- [10] C. Borges, A. Akhavan-Safar, E. Marques, R. Carbas, C. Ueffing, P. Weißgraeber and L. Silva, "Effect of water ingress on the mechanical and chemical properties of polybutylene terephthalate reinforced with glass fibers," *Materials*, vol. 14, no. 5, p. 1261, 2021.
- [11] M. Fang, N. Zhang, M. Huang, B. Lu, K. Laamnawar, C. Liu and C. Shen, "Effects of hydrothermal aging of carbon fiber reinforced polycarbonate composites on mechanical performance and sand erosion resistance.," *Polymers*, vol. 12, no. 11, p. 2453, 2020.
- [12] A.E. Krauklis, "Environmental Aging of Constituent Materials in Fiber-Reinforced Polymer Composites.," 2019.
- [13] A.E. Krauklis, A. Gagani, K. Vegere, I. Kalnina, M. Klavins and A. Echtermeyer, "Dissolution Kinetics of R-Glass Fibers: Influence of Water Acidity, Temperature, and Stress Corrosion.," *Fibers*, vol. 7, no. 3, p. 22, 2019.
- [14] J. Davalos, Y. Chen and I. Ray, "Long-term durability prediction models for GFRP bars in concrete environment.," *Journal of composite materials*, vol. 46, no. 16, pp. 1899-1914, 2012.
- [15] B. Wei, H. Cao and S. Song, "Tensile behavior contrast of basalt and glass fibers after chemical treatment.," *Materials & Design*, vol. 31, no. 9, pp. 4244-4250, 2010.
- [16] Shawcor, "Composite linepipe," [Online]. Available: <https://www.shawcor.com/composite-systems/composite-linepipe..> [Accessed 23 October 2022].
- [17] R. Jones and J. Stewart, "The kinetics of corrosion of e-glass fibers in sulphuric acid.," *Journal of non-crystalline solids*, vol. 356, no. 44-49, pp. 2433-2436, 2010.
- [18] A. Baharlou and K. Nasouri, "A new comprehensive evaluation of the corrosion mechanism of E-type glass fibers in sulfuric acid solutions," *Construction and Building Materials*, vol. 268, p. 121213, 2021.
- [19] S. Feih, K. Manatpon, Z. Mathys, A. Gibson and A. Mouritz, "Strength degradation of glass fibers at high temperatures," *Journal of materials science*, vol. 44, pp. 392-400, 2009.
- [20] A.E Krauklis and A. Echtermeyer, "Long-term dissolution of glass fibers in water described by dissolving cylinder zero-order kinetic model: Mass loss and radius reduction.," *Open Chemistry*, vol. 16, no. 1, pp. 1189-1199, 2018.

- [21] B. Wei, H. Cao and S. Song, "Tensile behavior contrast of basalt and glass fibers after chemical treatment.," *Materials & Design*, vol. 31, no. 9, pp. 4244-4250, 2010.
- [22] H. Kliger and E. Barker, " A comparative study of the corrosion resistance of carbon and glass fibers.," *Polymer-Plastics Technology and Engineering*, vol. 24, no. 1, pp. 85-108, 1985.
- [23] A. Echtermeyer, A. Krauklis, A. Gagani and E. Saeter, "Zero Stress Aging of Glass and Carbon Fibers in Water and Oil—Strength Reduction Explained by Dissolution Kinetics.," *Fibers*, vol. 7, no. 12, p. 107, 2019.
- [24] R. Gorowara, W. Kosik, S. Mcknight and R. Mccullough, "Molecular characterization of glass fiber surface coatings for thermosetting polymer matrix/glass fiber composites," *Composites Part A: Applied Science and Manufacturing*, vol. 32, no. 3-4, pp. 323-329, 2001.
- [25] J. Thomason, "Glass fiber sizing: A review of size formulation patents.," *Create Space Independent Publishing Platform.*, 2015.
- [26] J. Thomason , " Glass fiber sizing: A review.," *Composites Part A: Applied Science and Manufacturing*, vol. 127, p. 105619, 2019.
- [27] M. Bader, K. Kedward, Y. Sawada, A. Kelly and C. Zweben, *Comprehensive Composite Materials: Design Applications.*, Elsevier, 2000.
- [28] A. DiBenedetto, "Tailoring of interfaces in glass fiber reinforced polymer composites: a review.," *Materials Science and Engineering: A*, vol. 302, no. 1, pp. 74-82, 2001.
- [29] I. Rocha, S. Raijmaekers, R. Nijssen, F. Van der meer and L. Sluys, "Hygrothermal ageing behaviour of a glass/epoxy composite used in wind turbine blades.," *Composite Structures.*, vol. 174, pp. 110-122, 2017.
- [30] J. Kim, M. Sham and J. Wu, "Nanoscale characterisation of interphase in silane treated glass fiber composites.," *Composites Part A: applied science and manufacturing*, vol. 32, no. 5, pp. 607-618, 2001.
- [31] Y. Weitsman, "Coupled damage and moisture-transport in fiber-reinforced, polymeric composites.," *International Journal of Solids and Structures*, vol. 23, no. 7, pp. 1003-1025, 1987.
- [32] R. Plonka, E. Mader, S. Gao, C. Bellman, V. Dutschk and S. Zhandarov, "Adhesion of epoxy/glass fiber composites influenced by aging effects on sizings.," *Composites Part A: Applied science and manufacturing*, , vol. 35, no. 10, pp. 1207-1216, 2004.
- [33] L. Peters, " Influence of glass fiber sizing and storage conditions on composite properties.," *Durability of composites in a marine environment 2*, pp. 19-31, 2018.

- [34] D. Wang, F. Jones and P. Denison, "TOF SIMS and XPS study of the interaction of hydrolysed γ -aminopropyltriethoxysilane with E-glass surfaces.," *Journal of adhesion science and technology*, vol. 6, no. 1, pp. 79-98, 1992.
- [35] O. Starkova, A. Gagani, C. Karl, I. Rocha, J. Burlakovs and A. Krauklis, "Modelling of environmental ageing of polymers and polymer composites- durability prediction methods," *Polymers*, vol. 14, no. 5, p. 907, 2022.
- [36] J. Zhou, X. Chen and S. Chen, "Durability and service life prediction of GFRP bars embedded in concrete under acid environment.," *Nuclear Engineering and Design*, vol. 241, no. 10, pp. 4095-4102, 2011.
- [37] I. 11346, Rubber, vulcanized or thermoplastic-Estimation of life-time and maximum temperature of use., ISO, 2014.
- [38] L. Bank, T. Gentry, B. Thomson and J. Russel, " Model specification for composites for civil engineering structures," *Transportation research record*, vol. 1814, no. 1, pp. 227-236, 2002.
- [39] J. Zhu, Y. Deng, P. Chen, G. Wang, H. Min and W. Fang, " Prediction of long-term tensile properties of glass fiber reinforced composites under acid-base and salt environments.," *Polymers*, vol. 14, no. 15, p. 3031, 2022.
- [40] M. Hoque, A. Saha, H. Chung and P. Dolez, "Hydrothermal aging of fire-protective fabrics.," *Journal of Applied Polymer Science*, vol. 139, no. 30, p. e52666, 2022.
- [41] B. Mahltig and Y. Kyosev, *Inorganic and composite fibers: Production, properties, and applications*, Duxford, United Kingdom: Woodhead Publishing, 2018.
- [42] J. Pusch and B. Wohlmann, "Chapter 2 - Carbon fibers," in *Inorganic and Composite Fibers*, Woodhead Publishing, 2018, pp. 31-51.
- [43] B. Mahltig, "Chapter 9 -Basalt fibers," in *Inorganic and Composite Fibers*, Woodhead Publishing, 2018, pp. 195-217.
- [44] ASTM D2256M-10, 2015, Standard Test Method for Tensile Properties of Yarns by the Single-Strand Method, ASTM International: West Conshohocken, PA, USA.
- [45] ASTM D2343-17, 2009, Standard Test Method for Tensile Properties of Glass Fiber Strands, Yarns, and Rovings Used in Reinforced Plastics, ASTM International: West Conshohocken, PA, USA.
- [46] ASTM C1557-20-17, 2020, Standard Test Method for Tensile strength and Young's Modulus of fibers, ASTM International: West Conshohocken, PA, USA.

- [47] ISO 3341, Textile glass — Yarns — Determination of breaking force and breaking elongation, 2000.
- [48] A. Kelly and A. Tyson, "Tensile properties of fiber-reinforced metals: copper/tungsten and copper/molybdenum," *Journal of the Mechanics and Physics of Solids*, vol. 13, no. 6, pp. 329-350, 1965.

Chapter 3 : Aging Studies on Dry E-glass Fibers and Service Life Prediction Using Arrhenius Model

A version of this chapter has been published in: J. Sunny, H. Nazariipoor, J. Palacios Moreno, P. Mertiny, “Accelerated zero-stress hydrothermal aging of dry E-glass fibers and service life prediction using Arrhenius model”, *Fibers*, vol. 11, p. 70-1-17, 2023.

3.1. Introduction

Utilization of fiber-reinforced polymer composites (FRPC) has rapidly increased over the past few decades because of their attractive mechanical properties (strength, stiffness), comparatively low volumetric mass density, and excellent corrosion resistance compared to traditional engineering materials like steel and aluminum [1]. Due to an extraordinarily high performance-to-price ratio, more than 95% of the reinforcement used in the composite industry is made of glass fiber [2]. Different types of glass fibers (GFs) are commercially available. Most common are E, ECR, R, and S-glass, which are listed here in ascending order of mechanical strength [3]. Boron oxide and fluorides are added as a melting agent to ease the melting process in the E-glass formulation. Current environmental regulations in the United States and Europe prohibit the discharge of boron into the atmosphere. As per new regulations, the composition of E-glass containing low boron levels is SiO₂ (59-60 %), Al₂O₃ (12-13 %), CaO (22-23%), MgO (3- 4 %) ZrO₂ (0.5-1.5%), Na₂O (0.6 -0.9 %), K₂O (0-0.2 %), Fe₂O₃ (0.2%) and F (0.1 %) [4]. One crucial element that affects the performance of glass fibers is sizing, an organofunctional silane-containing coating on the fiber surface that promotes fiber adherence to the matrix [5]. Sizing has been shown to increase the interphase strength and strength retention of composites subjected to hydrothermal aging conditions [2,6]. Exposure to moist and humid circumstances can accelerates the aging process of composite materials, negatively impact mechanical properties, and thus shorten their service life. Environmental aging coupled with elevated temperature constitutes a severe case of accelerated aging [7-11]. Notably, different composite constituents are impacted by environmental aging in different ways. As a result, it is crucial to comprehend for each constituent the kinetics and mechanisms of environmental aging to ensure the composite’s environmental durability. A comprehensive understanding of aging effects is still missing when composites are utilized with prolonged exposure to elevated temperatures, water, and hydrocarbons. Data for service time assessments must currently be obtained via expensive and time-consuming test procedures [12].

Interest in environmental aging of FRPCs is significant, with many studies focusing on composites with E-glass as the reinforcement phase [7,9,10,11,13]. Julio et al. [7] performed a durability study on GF-reinforced polymer (GFRP) bars exposed to tap water. They stated that the degradation of the fiber/matrix interphase was the primary mechanism for reduced GFRP bar performance. The authors also emphasized

that fiber corrosion due to prolonged exposure may dominate the degrading process. In a similar study by Idrisi et al. [9], the resilience of E-glass/epoxy composite was tested in a salt-water environment. The leading causes for a loss in tensile strength were found to be the breakdown of chemical bonds between fiber and resin caused by chemical corrosion and poor interlocking between fibers and resin caused by resin swelling owing to water absorption, particularly at 90°C immersion. Later, Noamen et al. [10] conducted hydrothermal aging studies of GF-epoxy and carbon fiber-epoxy laminated composites exposed to temperatures 24, 70, and 90°C. The water absorption was found to obey Fickian behavior in all the tested laminates. Moreover, GF-epoxy composites were reported to have a higher diffusion coefficient due to their polarity and hydrophilicity. Matrix plasticization brought on by moisture and temperature resulted in the loss of mechanical characteristics. Bobbaa et al. [11] performed axial compression and internal pressure burst tests on E-glass and S-glass fiber-epoxy reinforced composite pipes created by filament winding after they were subjected to hydrothermal aging at 90°C. The burst pressure and compression behavior of the conditioned specimens were significantly reduced because of the environmental aging. As the aging duration increased, the degradation of the matrix and fiber/matrix connection increased as the moisture entered through the pipe outer surface into the resin matrix. The result was a reduced load-carrying capacity of the E-glass and S-glass fiber/epoxy composite pipes. Recently, Borges et al. [13] investigated the water uptake behavior for PBT-GF30 (polybutylene terephthalate with 30% short glass fibers) and fiber-free PBT in conjunction with the effect on the material's mechanical properties. They found that PBT absorbs more water than PBTGF30, albeit at a higher rate. The water diffusion was also shown to obey Fickian behavior. Polymeric chain relaxation was ascertained because of water ingress, resulting in mechanical properties loss. Chemical changes in the PBT were elucidated by the material's FTIR profile changing from 80°C to 85°C. In a recent work, Shao et al. [14] discovered that polyester matrix GFRP did not exhibit symptoms of water-absorption saturation after 260 days submerged in water at 23°C, despite a 17.5% reduction in tensile strength. The tensile strength of the GFRP declined by 56.3% at 70°C, and its water absorption increased and then reduced, even reaching negative values. However, the GFRP's Young's modulus was practically constant at the two temperatures. Similar results were reported by Grammatikos et al. [15], who concluded that because of the increase in temperature, there was an increase in moisture absorption and water diffusion and that the complete process of water diffusion does not reach saturation. In a recent study, Ghabezi et al. [16] investigated the changes in mechanical properties of glass/epoxy and carbon/epoxy composite specimens after immersion in an accelerated marine environment (artificial seawater, with 3.5% salinity at room temperature and 60°C). They observed a change in composite laminates' microstructure and mechanical properties (microcracks and debonding between matrix and fiber), indicating the degrading phenomenon. Additionally, the reductions in tensile and shear strengths of glass/epoxy samples were much higher than those of carbon/epoxy specimens. In contrast, carbon/epoxy composites exhibited a higher

reduction in flexural strength values than glass/epoxy samples. These findings showed that in composite materials, deterioration mechanisms persist even after reaching the saturation threshold. They concluded that the impact of chemical-based degradation (such as the reaction between water and epoxy or chain scission) on the loss of mechanical properties of composite samples is greater than the impact of mechanical-based damages, such as stress-induced by water absorption or the capillary and osmosis phenomenon. In a related study, Guo et al. [17] investigated the hygrothermal properties of pultruded carbon, glass, and carbon/glass hybrid fiber reinforced polymer (C/GFRP) composites by immersing them in deionized water for up to 135 days at 40°C, 60°C, and 80°C. They stated that the water uptake behavior of all three composite plates followed an initial Fickian diffusion behavior and a long-term degradation behavior. When submerged in deionized water, thermal and mechanical properties of C/GFRP were degraded by up to 29.5% for short beam shear strength (SBSS), 25.8% for three-point bending strength, and 43.1% for glass transition temperature, respectively. The diffusion of water molecules resulted in the reversible effect of resin plasticization and the irreversible effect of resin relaxation leading to property deterioration. Furthermore, the degradation of SBSS was accelerated by the irreversible fiber/resin interface debonding. Recently, Messana et al. [18] investigated the effect of hydrothermal aging on the chemical, mechanical, and thermal properties of woven carbon fiber and glass fiber with traditional epoxy resin and advanced thermoplastic polyphenylene sulfide (PPS). It was observed that the epoxy-based composites exhibited a property gain by an increase in cross-link density and a property loss due to matrix plasticization. In the PPS composites, the matrix was chemically stable, and the strength reduction occurred due to damage at the fiber matrix interphase. Fang et al. [19] investigated the performance of carbon fiber-reinforced polycarbonate (CF/PC) composites exposed to deionized water at 80°C and measured the changes in storage modulus and erosion angle. The maximum erosion angle of composites was observed to deviate due to hydrothermal aging, showing that the composites underwent a transition from ductile to brittle behavior. Furthermore, using scanning electron microscope, cracks and cavities caused by water absorption were visible, suggesting that hydrothermal aging causes CF/PC composites to plasticize and degrade, which lowers their corrosion resistance. Dong et al. [20] investigated the durability of glass fiber-reinforced polypropylene (GF/PP) unidirectional sheet material by exposing it to distilled water and a combination of seawater, sea sand, and concrete for up to 6 months at 25°C and 60°C and evaluated changes in mechanical properties. The results demonstrated the GF/PP sheet material to be highly susceptible to immersion in seawater at high temperatures, leading to an unusually elevated water uptake of 3.4% at 60°C. Following a 6-month immersion in seawater at 25°C and 60°C, the longitudinal tensile strength retention was 22.7% and 3.3%, respectively. The GF/PP sheet material showed significantly better property retention while submerged in water; for instance, at 60°C for 6 months, the longitudinal and transverse tensile strength retentions were 79.3% and 84.0%, respectively. The GF/PP sheet material absorbed 0.69% water at

saturation in water at 60°C. A poor glass fiber/polypropylene interface, the sheet's relatively low thickness, and a low resistance of glass fiber to seawater were stated as factors that led to decreased mechanical properties of the GF/PP sheet material. It should be noted that the preceding studies focused on the polymeric matrix and the fiber-matrix interphase yet changes to the fiber phase were not given in-depth attention.

Some research on GFRP shows that during long-term exposure, hydrolytic deterioration is primarily due to degradation occurring in the matrix-fiber interphase and fiber dissolution processes [1,3,7,11,21]. Further studies on the direct exposure of GFs to various aging solutions ensued because of these discoveries. Models based on mass dissolution have primarily been used to explain the strength loss of glass fibers exposed to adverse environmental conditions [1,21,22,23]. In their research, Krauklis et al. [21] created a model to estimate the mass dissolution of fibers exposed to water at 60°C using zero-order kinetics. Na, K, Ca, Mg, Fe, Al, Si, and Cl were among the elements released during degradation, and constant rates for the total mass loss and each ion release were found. Compared with other elements, Si was shown to have the highest contribution to mass loss (56.1%). Moreover, Jones and Stewart [24] examined the corrosion of E-glass fibers in sulphuric acid at various temperatures and concentrations. They found that the pace of corrosion does not depend primarily on the quantity of sulphuric acid since precipitation, not complex ion formation, made it easier to remove ions from the GF. Also, an increase in temperature accelerated the corrosion rate, which was described by Arrhenius-based activation energy models. In another study by Wei et al. [25], basalt and glass fibers exposed to sodium hydroxide and hydrochloric acid solutions showed a noticeable loss in strength. The attack of the hydroxyl ion on the SiO₂ framework, shared by glass and basalt, caused the loss in strength. In a thermal aging study performed by Feih et al. [26], the strength loss of two types of GF (E-glass and Advantex, an E-glass substitute free of boron) were investigated at temperatures up to 650°C and heating durations up to 2 hours. It was established that the glass's mirror constant, which reflected the network structure, remained constant during heat treatment and that the decrease in strength was caused by greater surface imperfections that remained after heat treatment.

In the case of composite pipes or tanks, one of the main reasons for failure is the permeation of corrosive fluids either internally through a liner or resin-rich liner, or externally through a cover or jacket, causing an attack on the reinforcement layer. Several studies on aging E-glass exposed to harmful chemicals and acids have been conducted, and most of the research has been concentrated on this mode of corrosive fluid penetration [21,22,23,24]. The eventual ingress of the corrosive fluid beyond a polymeric barrier and the fluid's attack on the GF itself can lead to failure in corrosion-resistant pipes and underground tanks. Motivated by these observations, the present work focused on two main aspects relating to GFs. First, several applications exist in which dry GFs (i.e., without being impregnated with a polymer matrix) are the

main load-bearing element [27], or GFs are imbedded in thermoplastic matrix, which, depending on the polymer materials, may be susceptible to water exposure. In such situations, possible significant fluctuations in fiber performance must be considered for design factors. Therefore, accounting for changes to a composite structure's physical and mechanical properties requires a thorough understanding of the strength degradation of dry GFs when subjected to hydrothermal conditions, as well as the mechanisms causing the strength loss. Second, this work also seeks to build a foundation for multiscale examination of FRPC degradation by focusing on understanding the change in fiber strength when exposed to water at different temperatures. Structures made of composite materials are typically overdesigned due to insufficient data for the individual components. By examining the performance of the fibers and matrix independently and then extrapolating pertinent attributes of the composite laminate from constituent behavior, a multiscale method may be derived that has the potential to alleviate the need for comprehensive testing campaigns. It is acknowledged that a complete set of attributes is required for a thorough design, nevertheless, exploring a multiscale approach is still attractive due to its benefits upon implementation. In summary, this study aims to pinpoint environmental factors that cause GFs to age prematurely, analyze the effects that aging has on mechanical properties, and anticipate changes in mechanical properties using an Arrhenius modeling approach.

3.2. Arrhenius Model and Time-Temperature Superposition Approach

When temperature is the main accelerating factor in aging of composites, the Arrhenius model has frequently been employed to determine service life [7,8,28,29]. For materials below their glass transition temperatures, the Arrhenius model was shown to rather accurately predict the effects of temperature in accelerated aging experiments. The underlying assumption is that there is a single dominating degradation mechanism that does not change throughout exposure and that the degradation rate accelerates as exposure temperature increases. The general form of the Arrhenius model is given as:

$$k = A \cdot \exp\left(-\frac{E_a}{RT}\right), \text{ or, } \ln k = -\frac{E_a}{RT} + \ln A \quad (1)$$

where k is the reaction rate constant or degradation rate constant, A is a constant related to the material and aging environment, E_a is the activation energy, \bar{R} is the universal gas constant, and T is the absolute temperature. Recognizing that the reaction rate constant is inversely related to time, k in the Arrhenius equation is frequently used for computing the time to attain a material's particular strength loss [30]. Using ultimate mechanical properties and their retention, such as tensile strength, interfacial shear strength, creep strength, and fatigue strength, the Arrhenius relationship is therefore frequently used to forecast the lifetime of polymers and composites [28]. The detailed prediction procedure is well explained in the literature as well as in Chapter 2 of this thesis [30,31,32].

A related and commonly used method for durability prediction is the time-temperature superposition (TTS) approach. It involves calculating shift factors for different temperatures. The TTS theory states that the qualities of a material achieved after a brief exposure to a higher temperature are equal to those obtained after longer exposure to a lower temperature [30,31,33]. For two temperatures T_1 and T_2 where $T_1 < T_2$ is given by:

$$TSF = \frac{t_1}{t_2} = (A * \exp\left(-\frac{E_a}{RT_2}\right)) / (A * \exp\left(-\frac{E_a}{RT_1}\right)) \quad (2)$$

where TSF is the time shift factor. The process involves selecting a reference temperature and calculating the shift factor for the other temperature. Then, the natural logarithm of the shift factor is plotted against the inverse of temperature ($1/T$). Thus, the agreement with the Arrhenius model is established via a linear fit with a regression coefficient (R^2) value of at least 0.8 [31,32].

3.3. Material and Specimen Preparation

An E-glass fiber material (E6DR-735-306B, Jushi, Zhejiang, China) was used in this study, which is commercially available and frequently used in the industry. The sizing on the GFs is silane-based. The sizing, which exact composition is proprietary, is compatible for thermoplastic composites and suitable for the fabrication of pipes and vessels using filament winding techniques. Each roving has a nominal filament diameter was 12 μ m with a linear density of 0.735 g/m [34].

For conditioning, GFs were exposed to tap water for a maximum duration of 840 hours (5 weeks) at 60°C and 71°C, and 672 hours (4 weeks) at 82°C. The pH of tap water assessed in this study was assumed to be within a narrow range, with an average of 7.9 for all aging tests. GFs of a fixed length of 2.5 m (100 inches) were selected and submerged in a beaker with volume of 4 liters, as shown in Figure 3.1. Only the gauge section length of the fibers was submerged in tap water to ensure that fiber breakage was restricted to the sample gauge length. Then the beaker was covered using aluminum foil and placed in the oven (see Figure 8). Calibrated thermocouples were used to measure the water temperature inside the beaker. Heated water was added periodically to compensate for evaporative losses.



Figure 8. Aging of fiber samples inside oven.

3.4. Experimental Methods

3.4.1. Test Setup for Fiber Breaking Force Measurement

Fiber tensile tests were conducted in air at room temperature (23°C) using a universal testing machine (type 810, MTS Systems, Eden Prairie, MN, USA) with special Capstan grips made for fiber testing (see Figure 9). All tests were performed with a displacement rate of 50 mm/min and a gauge length of approximately to 250 mm. At least ten specimens were tested for each aging duration for dry and wet test conditions. In wet testing, samples taken straight from the oven were tested without drying. In contrast, samples for dry testing were left to dry at room temperature for at least 24 hours before testing. A large reduction in testing load was considered indicative of specimen failure, and the maximum load from the load-displacement curve was taken as the breaking load. Figure 9(B) depicts fiber failure upon reaching the maximum load, i.e., the fiber strands became fuzzy resembling Mohair yarn after failure. Notably, some filaments remained in various states of tensioning even after specimen failure. All the tests were done adopting standards ASTM D 2256M-10 and ASTM D2343-17 [35,36].

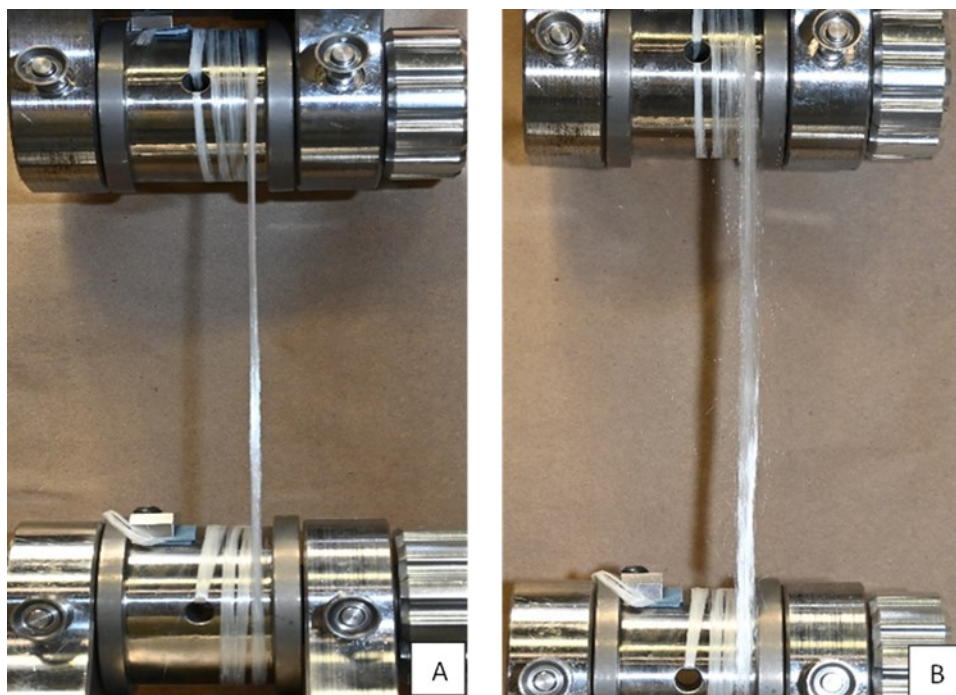


Figure 9. Mechanical testing of glass fibers using Capstan grips: (A) Before testing and (B) post failure.

3.4.2. Mass Dissolution Experiments

To understand which elements are released during the aging process, mass dissolution studies were performed on glass fibers aged for a duration of 168 hours (1 week) at 60°C and 82°C. Seven strands of fibers of 75 mm in length each and an average mass of 0.4 g were selected. These strand sections were immersed in plastic tubes filled with 50 ml deionized water. To capture any elements that may be released by the conditioning tubes, reference water samples without fibers were exposed simultaneous to the aging conditions that the fibers experienced. The concentration of dissolved ions in water was measured using a spectrometer of type iCAP6300 Duo / ICP-OES (Thermo Fisher Scientific, Waltham, MA, USA).

3.4.3. Fourier Transform Infrared Spectroscopy

Fourier transform infrared spectroscopy (FTIR) of the pristine and conditioned fibers was completed using a Nicolet Is50 FTIR spectrometer (Thermo Fisher Scientific). In this method, an infrared spectrum is created based on the absorption of electro-magnetic radiation at frequencies corresponding to the vibration of sets of chemical bonds within a molecule. The aged samples were dried at room temperature for 24 hours and stored in a controlled environment before performing the FTIR tests. Samples were examined in attenuated total reflectance (ATR) mode with a diamond detector, in the range of 400-4000 cm^{-1} with a resolution of 4 $\text{cm}^{-1}/\text{min}$.

3.4.4. Scanning Electron Microscopy

Scanning Electron Microscopy (SEM) was conducted with an S-4800 instrument (Hitachi, Tokyo, Japan) to examine the surface morphology of unaged and hydrothermally aged fibers. Before imaging, the samples were coated with a gold layer using gold sputter coating equipment (Desk II, Denton, Moorestown, NJ, USA). An acceleration voltage of 10 KV and an emission current of 10 μ A were applied. SEM images were captured at two different magnification levels.

3.5. Results and Discussion

3.5.1. Variations in Fiber Strength

The tensile strength of GFs varies statistically, and therefore, strength is often quantified in conjunction with Weibull statistics [37]. Obtaining relevant statistics requires bulk testing of fibers in the range of 40-100 separate fibers for each condition. The Weibull parameters of individual fibers can also be back-calculated, provided the load-displacement curves are correctly measured. This study examined the relative change in fiber strength following various exposure durations to water at 60°C, 71°C, and 82°C. Measuring the peak load of a single fiber bundle test is sufficient for examining the strength changes, presuming that Weibull and Young's moduli remain constant and that exposure to water solely affects the fibers' characteristic strength [38]. The variations in fiber strength can be expressed as breaking tenacity (N/Tex), which is the maximum load (in N) divided by the linear density (in Tex = g/1000 m) of glass fibers, or tensile strength, which is the breaking load divided by the fiber cross-sectional area. The load-displacement plot for a pristine GF sample tested at room temperature is depicted in Figure 10. The dashed line indicates the linear section of the load-displacement curve, which displays a Hookean region. Any slack in the fiber is denoted as l_0 , see Figure 10, and corresponding displacement does not accurately reflect the behavior of the fiber because strands typically slip and tighten on the grips when loaded. However, since the maximum load is the only property of relevance, as it serves as the basis for calculating fiber strength, the effect of fiber slack received little consideration. In this study, strength retention or reduction is used to compare the variation in the mechanical performance of fibers with different aging durations and temperatures. So, tenacity and tensile strength become equivalent data. It should be noted that the initial strength of GFs was slightly lower than that given in manufacturer data sheet [34]. The reason for these differences could be due to differences in test methods and conditions, such as fiber-to-fiber friction, misalignment or twist in the fibers during testing. However, since this paper mainly focuses on understanding the relative changes in strengths due to aging, a lower strength compared to manufacturer specifications is immaterial for the outcome of this study.

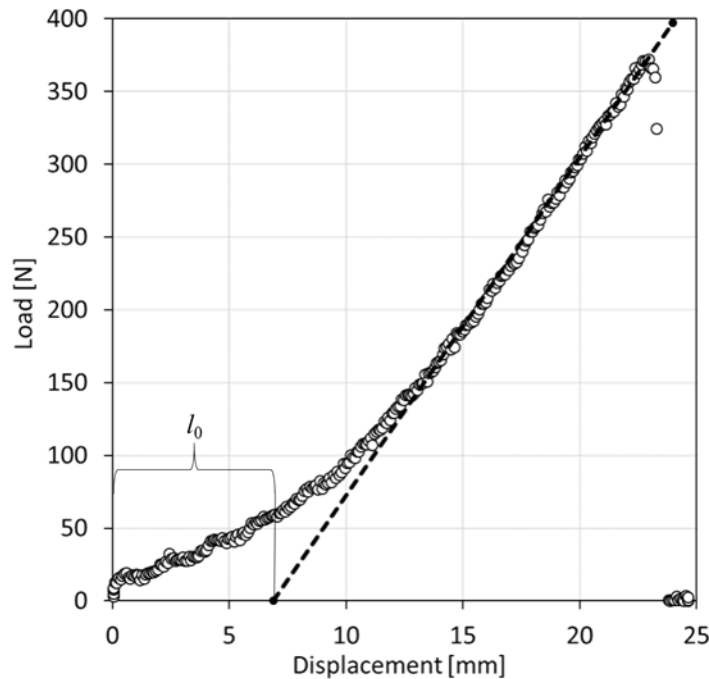


Figure 10. Load versus displacement plot from a tensile test of a GF sample.

A large difference in the strength values was ascertained between fibers tested wet and dry, see Figure 11 (A) and (B), respectively. Error bars in these graphs denote one standard deviation from the mean value. Data labeled ‘Baseline’ refers to samples that were tested as received from the manufacturer, that is, without aging. Wet samples exhibited significantly lower strengths than dry samples for all aging durations and temperatures. The lowest strength values were observed for fibers aged at 82°C for 672 hours (4 weeks), with an almost 77% reduction in strength for fibers tested in wet conditions and a 55% drop in strength for dried fibers. It is postulated that when fibers are tested in wet conditions, the water between the filaments acts like a lubricant which counteracts any load sharing from weak or broken to stronger filaments. Conversely, there is more friction in dry fibers, thus promoting load sharing mechanisms between filaments and thus greater fiber strength, which is similar to filaments being embedded in a polymer matrix, but to a much lesser extent. The strength values dropped by 62% and 55% (tested wet) and 45% and 32% (tested dry) for fibers aged at 71°C and 60°C for 840 hours (5 weeks). Similarly, when comparing the drop in strength values for fibers aged at 82 °C, 71°C, and 60 °C for 168 hours (1 week), the reductions are 49%, 41%, 33% (wet), and 32%, 23%, and 12% (dry), respectively. These data demonstrate the severity that hydrothermal attack can have on GFs, as fibers suffered significant reductions in strength even after just 1 week of exposure at elevated temperatures. Presumably, strength reductions are chiefly caused by the attack of water on the Si-O-Si framework, which serves as the backbone for GFs, which will be discussed in detail in later in this chapter.

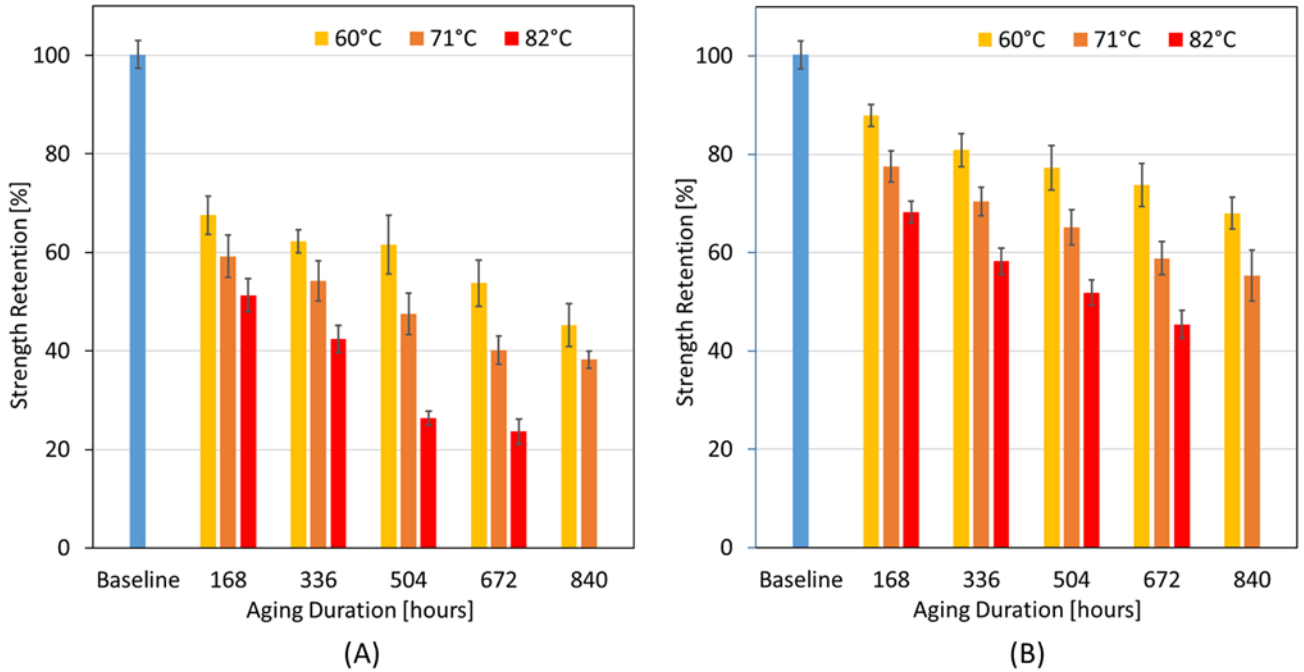


Figure 11. Strength retentions after exposure at 60°C, 71°C, and 82°C: (A) samples tested ‘wet’, and (B) samples tested ‘dry’.

3.5.2. Prediction of Long-term Behavior and Service Life of Glass Fibers

The basis of the herein adopted prediction methodology is the basic Arrhenius relation, and the time-temperature superposition approach. Corresponding analysis steps and references were already given in Section 3.2. The data for fibers tested in dry condition was used for the analysis. The Arrhenius method is sometimes also referred to as the predetermined life approach, where the first step involves the representation of the strength retention values by a fitted curve with a high R^2 value (>0.8). Equation (3) describes the relation in this model between performance retention, Y , and degradation time, t . This model is commonly used to represent the retention values at different temperatures for composite materials exposed to hydrothermal aging conditions [32].

$$Y = A_1 \exp^{-\left(\frac{t}{\tau}\right)} + Y_0 \quad (3)$$

where Y represents the retention in mechanical properties, t is the exposure time, and, A_1 and Y_0 are regression fitting parameters. The values for the regression coefficients are given in Table 1, and the tensile strength retention is shown in Figure 12 as a function of time for the different temperatures. Notably, the different regression curves exhibit R^2 values of at least 0.98, which corroborates the Arrhenius approach and its presumption that the material exhibits the same degradation mechanism for the different aging temperatures.

Table 1. Regression coefficients according to Eq. (3) for fitted curves in Figure 12, based on test data from fibers tested dry, and E_a/\bar{R} values relating to the Arrhenius plot slopes in Figure 13.

Aging Temperature [°C]	A_1 [N]	τ [hour]	Y_0 [N]	E_a/\bar{R} [K]
60	36.81	493.80	62.61	6802.0
71	45.65	311.52	53.48	6802.0
82	54.93	216.10	44.66	6802.0

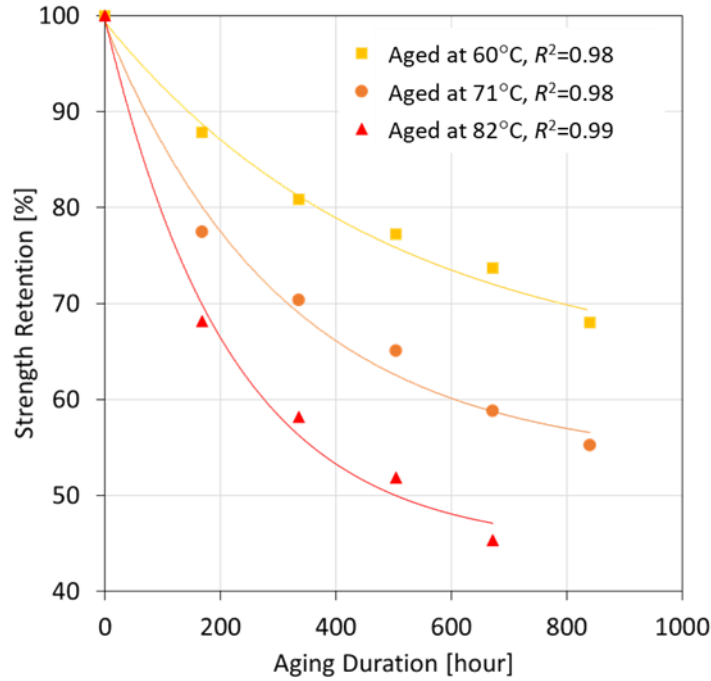


Figure 12. Tensile strength retention versus aging duration for fibers tested dry. Solid lines are fitted curves according to Eq. (3) and regression coefficients in Table 1.

The next step in the analysis involved plotting the logarithm of time to reach the retention values versus $1000/T$, where T is temperature given in units of Kelvin. Strength retention levels of 70%, 80% and 90% were selected for this study. In the technical literature, a retention value of 50 % has been proposed for composite materials [30,31]. However, for both, dry fibers and fibers inside a matrix, the present authors consider a loss in properties even by only 10 to 30% as significant; hence, this is justification for selecting the above-mentioned retention levels. The Arrhenius plots for different retention values are displayed in Figure 13. The fitted straight lines for the different retention levels are parallel and have R^2 values very close to unity, proving the validity of the accelerated deterioration test and the applicability of the model to forecast the loss of GF tensile strength. The activation energy for E-glass was reported to be in the range of 55 to 79 KJ/mol in alkaline solutions [3,23]. In the present study, an activation energy of 56.6 kJ/mol was calculated from the slope of the plots (for convenience E_a/\bar{R} data is given Table 1), which is within the

range found in the technical literature. As such, using the Arrhenius model for estimating the useful life of GFs under hydrothermal aging conditions proves effective. For example, if interpolating the curves to room temperature (23°C), the aging time to reach retention levels 70%, 80% and 90% is predicted as 372 days, 193 days, and 79 days, respectively.

Referring to Eq. (2), the shift factors were determined by inspection, adopting an approach similar to other work [33], taking the reference temperature as 60°C. Invoking the TTS principle in conjunction with Arrhenius’s theory, the effect of temperature on the tensile strength of GFs can thus be described. The exposure times were multiplied with their corresponding shift factors at each temperature and plotted as shown in Figure 14(A). Finally, a linear relationship was observed (with $R^2=0.99$) when the logarithm of the shift factors was plotted against the inverse of the absolute temperature as shown by Figure 14(B). These findings indicate that within the investigated temperature range, the Arrhenius model can adequately represent the effects that temperature has on hydrothermal aging and thus on the tensile strength of the studied GF material. The theory as employed herein is therefore shown to be effective for predicting the property loss at other aging temperatures of interest.

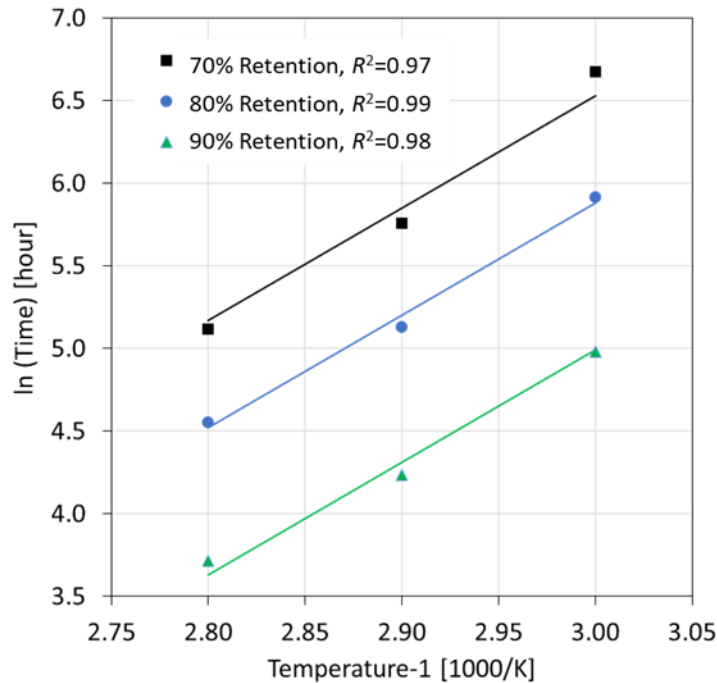


Figure 13. Arrhenius plots of calculated hydrothermal lives for different strength retention levels.

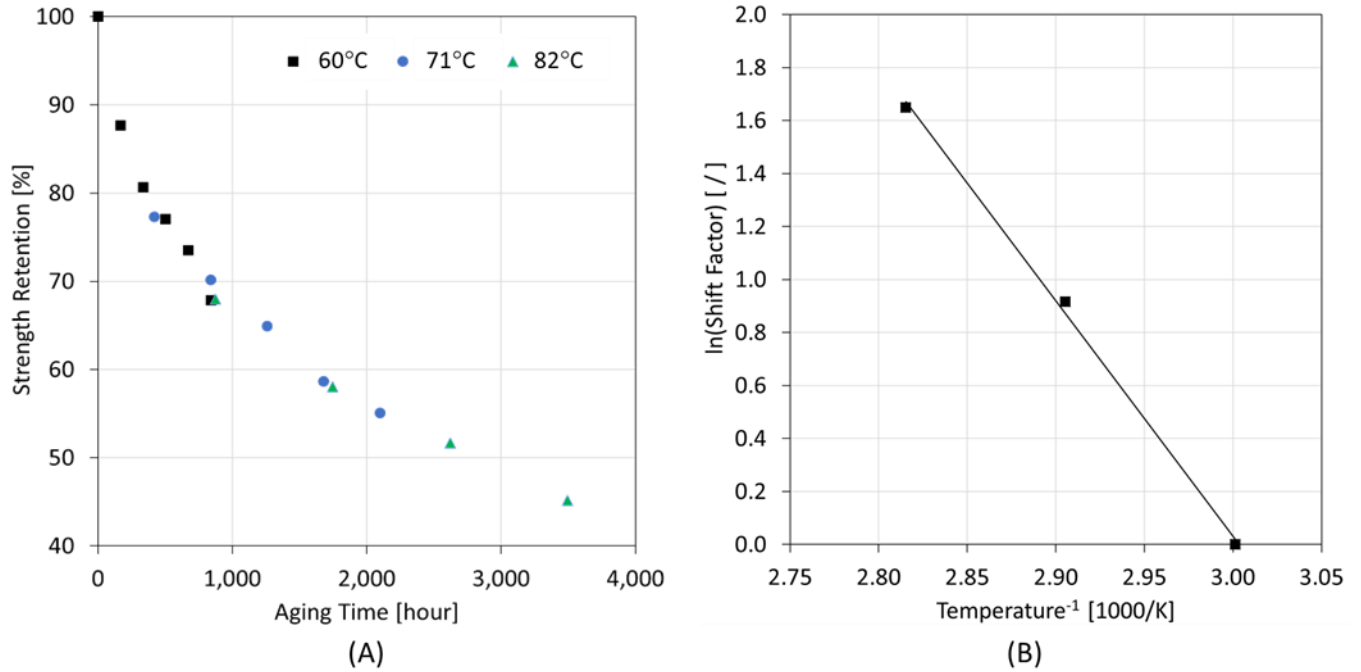


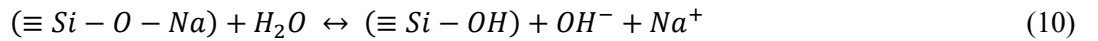
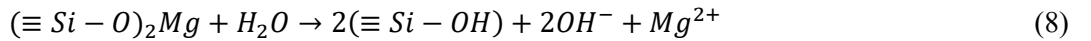
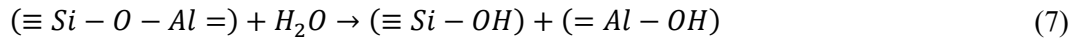
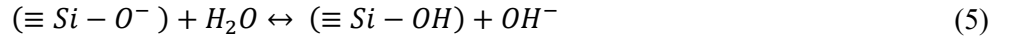
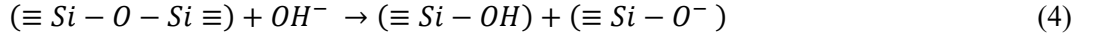
Figure 14. (A) TTS master curve at 60°C for glass fibers, (B) Arrhenius plot of shift factors.

3.5.3. Elements Released During Degradation and Corresponding Chemical Reactions

The mass dissolution experiments on GFs aged at 60°C and 82°C for a duration of 168 hours (1 week) indicated that the following elements were released, arranged in the order of decreasing concentration in the solution: Si, Ca, Al, Na, Mg, K, S, Fe. Corresponding data are shown in Table 2. All detected elements were present in the chemical composition of GF, except for sulfur, which origin is unclear. It is speculated that S originated from an external contamination or is a residue from the GF fabrication process. An increasing trend in concentration with temperature was ascertained for all the elements except for Fe and K, which approximately had had the same concentration values at 60°C and 82°C. Noticeably, the amount of Si released after aging the fibers for 168 hours at 82°C was almost 75% higher than that at 60°C for the same duration. The detected release of elements is in agreement with previous studies [21,23,39]. Corresponding chemical reactions are depicted in Eqs. (4) to (10). These observations support the hypothesis that due to hydrothermal aging the GFs incurred damage to the Si-O-Si framework which caused the significant release of Si ions and other elements.

Table 2. Mass of elements released from glass fiber samples aged in water at 60°C and 82°C for 168 hours (1 week).

Element	Si	Ca	Al	Na	Mg	K	S	Fe
Concentration at 60° C [mg/L]	9.43	6.507	1.938	0.284	0.219	0.14	0.056	0.002
Concentration at 82° C [mg/L]	16.551	9.056	3.128	0.42	0.341	0.133	0.078	0.002



3.5.4. FTIR Results

The transmittance spectrum obtained from the FTIR analysis is depicted in Figure 15 (A), where the broad peaks at wavenumbers of around 685 cm⁻¹ and 900 cm⁻¹ can be attributed to Si-O bending and Si-O-Si stretching vibrations, respectively [40,41]. According to the Beer Lambert law, peak intensity or peak height can be attributed to a species concentration within the specimen [42]. A chemical bond's vibration is influenced by its surroundings. A sample will absorb radiations from a range of IR wavenumbers as if chemically exposed to more varied wavenumbers. Because of the extremely short-range order in glass, broad bands are seen instead of sharp peaks at 685 cm⁻¹ and 900 cm⁻¹ for the tested GFs. As seen from the spectrum, no new bands originated between wavenumbers from 400 cm⁻¹ to 1800 cm⁻¹. Instead, there was a decrease in peak intensities of the baseline peaks compared with aged samples. There is a sharp decrease in intensity of peaks around 685 cm⁻¹ and 900 cm⁻¹, with the least intensity being for GF samples aged 672 hours (4 weeks) at 82°C, followed by samples aged 840 hours (5 weeks) at 71°C and 60°C, respectively.

Figure 15 (B) shows the variation in transmittance values corresponding to the Si-O-Si peaks occurring at around a wavenumber of 900 cm⁻¹. There is a steady increase in the transmittance values as temperature and aging duration increase, which implies a reduction in peak intensity and absorbance values. Samples aged for 672 hours (4 weeks) at 82°C have the highest increase in their transmittance values (20 %), i.e., the highest peak intensity reduction. Similarly, samples aged for 840 hours (5 weeks) at 71°C and 60°C showed an increase in their transmittance values by 18% and 14%, respectively, implicating a

corresponding reduction in intensity values. Here, the emphasis is given to the reduction across aging durations and within aging temperatures rather than pointing out the absolute values of variation, which may not be true in all cases. The observed intensity reductions confirm the hydrothermal attack on the Si-O-Si framework that forms the backbone of GFs, either weakening the bond or breaking the bonds leading to the release of ions by the reactions highlighted in the previous section. The FTIR analysis therefore provides further corroboration that rising tensile strength reductions in GFs caused by the prolonged and more severe hydrothermal aging are the result of progressive damage to the Si-O-Si framework in the GFs.

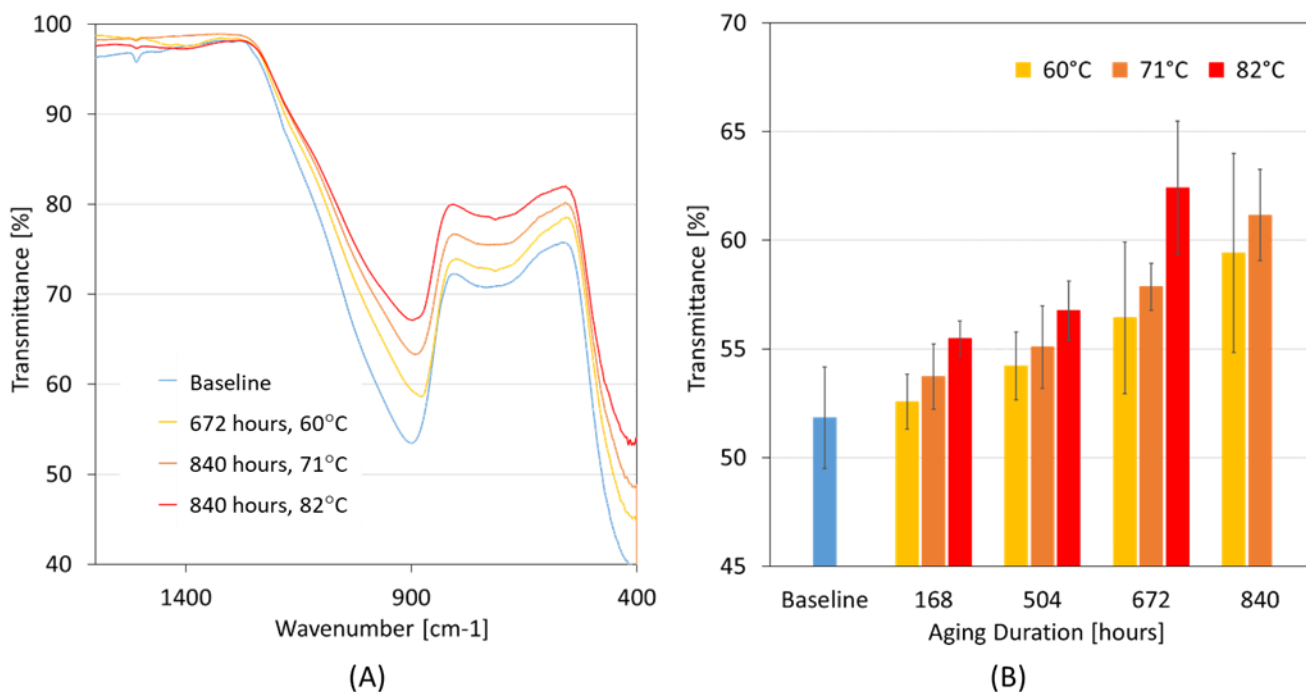


Figure 15. (A) FTIR spectrum for pristine and aged glass fibers, and (B) intensity variations of Si O Si peaks at wavenumber 900 cm⁻¹.

3.5.5. Morphological Analysis

SEM images of glass fibers are shown in Figure 16, which show in the top row the surface of a pristine fiber, in the middle row the surface of fibers aged at 60°C, 71°C and 82°C for 168 hours (1 week)), and in the bottom row the surfaces of samples aged for 840 hours (5 weeks) at 60°C and 71°C (left) and 672 hours (4 weeks) at 82°C (right). Notably, fibers aged for 4 weeks at 82°C exhibit significant surface deterioration compared with the pristine fibers, which have a smooth surface without noticeable imperfections. For fibers subjected to aging, in addition to surface roughening, certain deposits can be observed on the fiber surface. Presumably, these deposits originate from fiber sizing breaking down in the tap water, or from chemical reactions leading to mass loss, as discussed in Section 3.5.3, as released elements may have formed new chemical compound on the fiber surface. The effect of hydrothermal aging is less severe for fibers aged for

1 week at 60°C, 71°C, and 82°C when compared to the fiber aged for longer durations at the same temperatures. Also, the level of degradation is seen to increase with aging temperatures. The SEM images in Figure 9 provide an insight into the damage progression starting on the fiber surface and progressing deeper into the material with aging duration. Notably, some patches of fiber material appear to have flaked off. Similarities can be ascertained when comparing present SEM images with those reported in the technical literature for GFs exposed to alkaline solution [25]. Recalling the pronounced loss in mechanical properties after aging at 82°C as compared to fibers aged at 71°C and 60°C, it stands to reason that chemical degradation is more aggressive at 82°C and affects a greater portion of the GF material. The SEM images of aged fibers reveal structural damage occurring to the fiber surface, resulting not only in material degradation but also stress risers and friction points, with the latter two further contributing to premature filament failures under tensile loading.

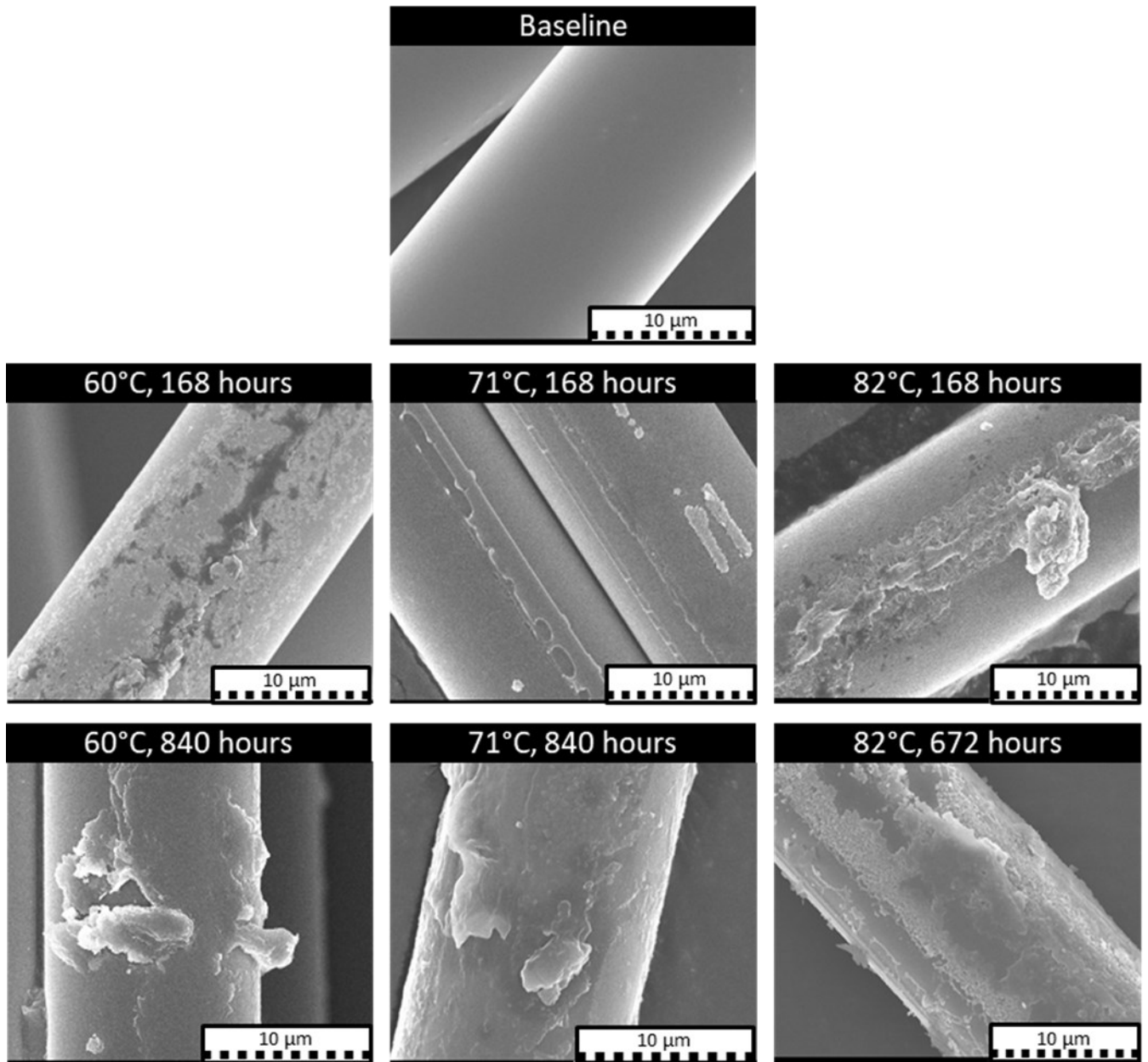


Figure 16. SEM images showing glass fiber surfaces before and after aging. Baseline of pristine fiber (top row); aged at 60°C, 71°C and 82°C for 1 week (middle row); and for 5 weeks at 60°C and 71°C and 4 weeks at 82°C (bottom row).

3.6. Conclusions

Mechanical testing of E-glass fiber samples was performed to study the effects of hydrothermal aging at three elevated temperatures. Fiber samples were tested either after drying or in a wet state. After aging in tap water, the fiber materials generally exhibited a loss in breaking strength, with fibers tested in wet conditions showing the most significant decline in strength. The residual tensile strength declined as immersion time and aging temperature increased, yet the rate of decline slowed down with time. Results

from mass dissolution and FTIR measurements indicate that hydrothermal exposure caused an attack on the Si-O-Si framework in the E-glass material, which coupled with the loss of sizing caused substantial reductions in tensile strength. This conclusion was further supported by the SEM imaging, which showed significant damage occurring to the fiber surface and a loss of material.

An analytical model based on the Arrhenius theory was adopted to predict the tensile strength retention of E-glass fibers upon aging. The Arrhenius model was validated using experimental data, proving its broad applicability. The activation energy calculated using the Arrhenius model was 56.6 KJ, which agrees with values found in the technical literature. Based on the developed model, the time to reach retention levels of 70%, 80%, and 90% at room temperature (23°C) were calculated as 372 days, 193 days, and 79 days, respectively. A master curve was created using a time-temperature superposition approach for a reference temperature of 60°C. The modeling approach proved to be consistent with experimental data and yield reasonable results. Still, additional research should be completed to explore the model's validity over extended periods of time and gain greater confidence in the model parameters.

Although only E-glass was the focus of present testing campaign and modeling effort, the general strategy is thought to hold for all types of glass fibers, and possibly similar materials like basalt fibers. These findings offer novel insights regarding the significant decline in the mechanical performance of E-glass fibers when subjected to a combination of water and temperature. Upon completing additional studies into the aging of technical fibers, the created tools may form a tool to forecast and track the long-term performance of fibers in engineering applications. Also, it is of interest to explore if findings from this study can form the foundation for a multiscale approach for predicting the performance of fiber reinforced polymer matrix composites, which may involve examining the performance of fibers, matrix and their interface condition independently and then extrapolating attributes of the composite material from the constituents' behavior

3.7. References

- [1] A. E. Krauklis, A. I. Gagani, and A. T. J. C. Echtermeyer, "Long-term hydrolytic degradation of the sizing-rich composite interphase", *Coatings*, vol. 9, no. 4, p. 263, 2019.
- [2] J. L. Thomason, "Glass fiber sizing: A review," *Composites Part A: Applied Science and Manufacturing*, vol. 127, p. 105619, 2019.
- [3] A. E. Krauklis, A. I. Gagani, K. Vegere, I. Kalnina, M. Klavins, and A. T. Echtermeyer, "Dissolution Kinetics of R-Glass Fibers: Influence of Water Acidity, Temperature, and Stress Corrosion," *Fibers*, vol. 7, no. 3, p. 22, 2019.
- [4] B. Mahltig and Y. Kyosev, "Inorganic and composite fibers: production, properties, and applications," 2018.

- [5] S. Feih, J. Wei, P. Kingshott, and B. F. Sørensen, "The influence of fiber sizing on the strength and fracture toughness of glass fiber composites," *Composites Part A-Applied. Science.*, vol. 36, no. 2, pp. 245-255, 2005.
- [6] Z. M. Ishak, A. Ariffin, and R. Senawi, "Effects of hygrothermal aging and a silane coupling agent on the tensile properties of injection molded short glass fiber reinforced poly (butylene terephthalate) composites," *European polymer journal*, vol. 37, no. 8, pp. 1635-1647, 2001.
- [7] J. F. Davalos, Y. Chen, and I. Ray, "Long-term durability prediction models for GFRP bars in concrete environment," *Journal of Composite Materials*, vol. 46, no. 16, pp. 1899-1914, 2012.
- [8] M. A. Silva, B. S. da Fonseca, and H. Biscaia, "On estimates of durability of FRP based on accelerated tests," *Composite structures*, vol. 116, pp. 377-387, 2014.
- [9] A. H. Idrisi, A.-H. I. Mourad, B. M. Abdel-Magid, and B. Shivamurty, "Investigation on the durability of E-Glass/Epoxy composite exposed to seawater at elevated temperature," *Polymers*, vol. 13, no. 13, p. 2182, 2021.
- [10] N. Guermazi, A. B. Tarjem, I. Ksouri, and H. F. Ayedi, "On the durability of FRP composites for aircraft structures in hygrothermal conditioning," *Composites Part B: Engineering*, vol. 85, pp. 294-304, 2016.
- [11] S. Bobbaa, Z. Lemana, E. Zainudina, and S. Sapuana, "The influence of hydrothermal aging on E-glass and S-glass fiber/epoxyreinforced composite pipes," *Journal of Materials and Environmental Science*, vol. 10, pp. 790-804, 2019.
- [12] A. T. Echtermeyer, A. E. Krauklis, A. I. Gagani, and E. Sæter, "Zero Stress Aging of Glass and Carbon Fibers in Water and Oil—Strength Reduction Explained by Dissolution Kinetics," *Fibers*, vol. 7, no. 12, p. 107, 2019.
- [13] C. S. Borges *et al.*, "Effect of water ingress on the mechanical and chemical properties of polybutylene terephthalate reinforced with glass fibers," *Materials*, vol. 14, no. 5, p. 1261, 2021.
- [14] Y. Shao and S. Kouadio, "Durability of fiberglass composite sheet piles in water.," *Journal of composites for construction*, vol. 6, no. 4, pp. 280-287, 2002.
- [15] S. A. Grammatikos, M. Evernden, J. Mitchels, B. Zafari, J. T. Mottram and G. C. Papanicolaou, "On the response to hygrothermal aging of pultruded FRPs used in the civil engineering sector," *Materials & Design*, vol. 96, pp. 283-295, 2016.
- [16] P. Ghabezi and N. M. Harrison, "Hygrothermal deterioration in carbon/epoxy and glass/epoxy composite laminates aged in marine-based environment (degradation mechanism, mechanical and physicochemical properties).," *Journal of Materials Science*, vol. 57, no. 6, pp. 4239-4254, 2022.

- [17] R. Guo, G. Xian, F. Li, C. Li and B. Hong, "Hygrothermal resistance of pultruded carbon, glass and carbon/glass hybrid fiber reinforced epoxy composites.," *Construction and Building Materials*, vol. 315, p. 125710, 2022.
- [18] A. Messana, A. Airale, A. Ferraris, L. Sisca and M. Carello, "Correlation between thermo-mechanical properties and chemical composition of aged thermoplastic and thermosetting fiber reinforced plastic materials.," *Materialwissenschaft und Werkstofftechnik*, vol. 48, no. 5, pp. 447-455, 2017.
- [19] M. Fang, N. Zhang, M. Huang, B. Lu, K. Lamnawar, C. Liu and C. Shen, "Effects of hydrothermal aging of carbon fiber reinforced polycarbonate composites on mechanical performance and sand erosion resistance.," *Polymers*, vol. 12, no. 11, p. 2453, 2020.
- [20] S. Dong, P. Zhou, R. Guo, C. Li and G. Xian, "Durability study of glass fiber reinforced polypropylene sheet under simulated seawater sea sand concrete environment.," *Journal of Materials Research and Technology*, vol. 20, pp. 1079-1092, 2022.
- [21] A. E. Krauklis and A. T. Echtermeyer, "Long-term dissolution of glass fibers in water described by dissolving cylinder zero-order kinetic model: Mass loss and radius reduction," *Open Chemistry*, vol. 16, no. 1, pp. 1189-1199, 2018.
- [22] S. Bashir, L. Yang, J. Liggat, and J. Thomason, "Kinetics of dissolution of glass fibre in hot alkaline solution," *Journal of Materials Science*, vol. 53, pp. 1710-1722, 2018.
- [23] L. Mišíková, M. Liška, and D. Galuskova, "Corrosion of E-glass fibers in distilled water," *Ceramics. Silik*, vol. 51, pp. 131-135, 2007.
- [24] R. Jones and J. Stewart, "The kinetics of corrosion of e-glass fibers in sulphuric acid," *Non-Crystalline Solids*, vol. 356, no. 44-49, pp. 2433-2436, 2010.
- [25] B. Wei, H. Cao, and S. Song, "Tensile behavior contrast of basalt and glass fibers after chemical treatment," *Material Design*, vol. 31, no. 9, pp. 4244-4250, 2010.
- [26] S. Feih, K. Manatpon, Z. Mathys, A. Gibson, and A. Mouritz, "Strength degradation of glass fibers at high temperatures," *Journal of Materials Science*, vol. 44, pp. 392-400, 2009.
- [27] Shawcor. "Composite Linepipe." <https://www.shawcor.com/composite-systems/composite-linepipe> (accessed jan 2022, 2022).
- [28] O. Starkova, A. I. Gagani, C. W. Karl, I. B. Rocha, J. Burlakovs, and A. E. Krauklis, "Modelling of environmental ageing of polymers and polymer composites—durability prediction methods," *Polymers*, vol. 14, no. 5, p. 907, 2022.
- [29] J. Zhou, X. Chen, and S. Chen, "Durability and service life prediction of GFRP bars embedded in concrete under acid environment," *Nuclear Engineering and Design*, vol. 241, no. 10, pp. 4095-4102, 2011.

- [30] ISO 11346, Rubber, vulcanized or thermoplastic — Estimation of life-time and maximum temperature of use, ISO, 2014.
- [31] L. C. Bank, T. R. Gentry, B. P. Thompson, and J. S. Russell, "Model specification for composites for civil engineering structures," *Transportation Research Record*, vol. 1814, no. 1, pp. 227-236, 2002.
- [32] J. Zhu, Y. Deng, P. Chen, G. Wang, H. Min, and W. Fang, "Prediction of long-term tensile properties of glass fiber reinforced composites under acid-base and salt environments," *Polymers*, vol. 14, no. 15, p. 3031, 2022.
- [33] M. S. Hoque, A. Saha, H. J. Chung, and P. I. Dolez, "Hydrothermal aging of fire-protective fabrics," *Journal of applied polymer science*, vol. 139, no. 30, p. e52666, 2022.
- [34] Jushi. "Fiberglass Products for Pipes." <https://www.jushi.com/en/product/product-introduction-151.html> (accessed Jan, 2022).
- [35] ASTM D2256M-10 Standard Test Method for Tensile Properties of Yarns by the Single-Strand Method, ASTM, 2015.
- [36] ASTM D2343-17 Standard Test Method for Tensile Properties of Glass Fiber Strands, Yarns, and Rovings Used in Reinforced Plastics, ASTM, 2009.
- [37] W. Weibull, "A statistical distribution function of wide applicability," *Journal of Applied Mechanics*, 1951.
- [38] E. Lara-Curzio, "Oxidation induced stress-rupture of fiber bundles," 1998.
- [39] B. Grambow and R. Müller, "First-order dissolution rate law and the role of surface layers in glass performance assessment," *Journal of Nuclear Materials*, vol. 298, no. 1-2, pp. 112-124, 2001.
- [40] M. Rani, P. Choudhary, V. Krishnan, and S. Zafar, "Development of sustainable microwave-based approach to recover glass fibers for wind turbine blades composite waste," *Resources, Conservation and Recycling*, vol. 179, p. 106107, 2022.
- [41] A. Ahmadi, B. Ramezanzadeh, and M. Mahdavian, "Hybrid silane coating reinforced with silanized graphene oxide nanosheets with improved corrosion protective performance," *Rsc Advances*, vol. 6, no. 59, pp. 54102-54112, 2016.
- [42] N. Abidi, FTIR microspectroscopy: Selected emerging applications. Cham, Switzerland: Springer, 2021.

Chapter 4 : Hydrothermal and Humidity Aging of Carbon and Basalt Fibers

Some aspects of the material discussed in this chapter have been published in the proceedings of the Canadian Society for Mechanical Engineering (CSME) International Congress, Sherbrooke, Quebec, Canada, May 28 - 31, 2023. This chapter is further prepared for publication in the Journal of Composite Science and Technology. While the present chapter is closely related to the previous one, the latter was concerned with the methodology development for the aging and testing of glass fibers, and the present chapter constitutes an expansion to hydrothermal aging of carbon and basalt fibers. Also, this chapter investigates the exposure of these fibers to humidity.

4.1. Introduction

For the past several decades, fiber-reinforced polymer composites (FRPCs) have grown in use and popularity due to their superior mechanical properties, such as high strength and modulus, while being relatively lightweight and corrosion-resistant compared to more conventional structural materials [1,2]. An FRPC comprises three basic components, a polymer matrix, a fibrous reinforcement, and a multi-component coating on the surface of the fibers - the sizing. When making FRPCs, the sizing causes the matrix polymer and the reinforcing fibers to produce a sizing-rich composite interphase, which chemically and physically bonds the fibers and the polymer [3]. High-performance filaments are widely used to reinforce composite materials, including basalt, glass, and carbon fibers [4]. It is well known that the fibers in composites considerably reinforce the matrix with its relatively low strength and rigidity. When a composite structure is used, the reinforcing filaments carry the most applied loads [5,6]. Commonly, FRPCs may be utilized in structural applications where humid air and water environments are present, such as in offshore, wind energy, and oil and gas applications [2, 7]. FRPCs deteriorate over time in wet and humid conditions as hydrolytic degradation and environmental aging reduce their mechanical qualities [7-11]. Degradation effects typically accelerate with exposure to elevated temperature conditions [12]. Additionally, environmental aging may impact the various elements of a composite material system by different mechanisms [13]. Therefore, to ensure environmental durability, a thorough understanding of the mechanisms and dynamics of environmental aging of the individual constituents is crucial. A lack of understanding poses significant risks when employing composites in conditions that subject them to prolonged exposure to a mix of elevated temperatures, forms of water, and/or other fluids such as hydrocarbons. Expensive and time-consuming testing campaigns usually narrow such knowledge gaps.

FRPCs commonly comprise of a thermoset polymer matrix. However, thermoplastic matrix materials have increasingly been employed as an effective substitute in recent years. Some key benefits of thermoplastic matrix materials over their thermoset counterparts are practically infinite shelf life, the ability to recycle thermoplastic polymers, and the reduction in manufacturing costs that may be achieved using

rapid and continuous fabrication processes [14,15]. While thermosetting matrices provide a high level of protection against water permeation, exposure to moisture may still be significant in certain thermoplastics [11].

There have been several efforts to recreate the environmental conditions to which thermoplastic matrix-based fiber composites are exposed, intending to understand how mechanical properties are affected over time. The variation in flexural properties of glass fiber-reinforced polypropylene composite laminates was studied by exposing them to tap water, salt solution, and freeze-thaw cycles at 23°C, 50°C, and 70°C [8]. The results indicated that salt solution had a higher detrimental effect on the flexure properties than tap water. Strength reductions were attributed to degradation effects occurring at the fiber matrix interphase. Later, Emel et al. [9] investigated the aging behavior of glass fiber-reinforced poly(oxyethylene) composite exposed to air or water at room temperature and in an oven at 100°C. A decrease in tensile and flexural strength was observed for all aging environments, with samples aged in water experiencing the most significant strength loss. All aged samples were found to have melt flow indices higher than those of the unaged samples. Variations in the melt flow index may thus be an indicator of degradation. In another study, Borges et al. [10] showed that mechanical properties were more sensitive to temperature than humidity level, as the former promoted water uptake in short glass fiber-reinforced polybutylene terephthalate (PBT). Even though stiffness and tensile strength decreased due to humidity, a definite dependence on water uptake was not seen. It was determined that the decrease in mechanical properties was brought about by water intrusion-induced polymer chain relaxing. After aging, samples were examined using Fourier-transform infrared spectroscopy (FTIR), and the PBT laminates aged above 80°C showed signs of chemical alteration. Recently, Messana et al. [11] investigated the effect of hydrothermal aging on the chemical, mechanical, and thermal properties of woven carbon fiber and glass fibers with traditional epoxy resin and advanced thermoplastic polyphenylene sulfide (PPS). It was observed that the epoxy-based composites can exhibit a property gain by an increase in crosslink density and a property loss due to matrix plasticization. In the PPS composites, the matrix was chemically stable, and strength reductions occurred due to damage occurring in the fiber matrix interphase. Fang et al. [16] investigated the performance of carbon fiber-reinforced polycarbonate (CF/PC) composites exposed to deionized water at 80°C and measured the changes in storage modulus and erosion angle. The maximum erosion angle of composites was observed to deviate due to hydrothermal aging, showing that the composites underwent a transition from ductile to brittle behavior. Furthermore, using a scanning electron microscope, cracks and cavities caused by water absorption were visible, suggesting that hydrothermal aging causes CF/PC composites to plasticize and degrade, which lowered their corrosion resistance. Recently, Shaoce et al. [17] investigated the durability of glass fiber reinforced polypropylene (GF/PP) unidirectional sheets by exposing them to distilled water and a combination of seawater, sea sand, and concrete for up to 6 months at 25°C and 60°C

and evaluated changes in mechanical properties. The results demonstrated that the GF/PP sheet material is strongly susceptible to immersion in seawater at high temperatures, leading to an unusually elevated water uptake of 3.4% at 60°C. Following a 6-month immersion in seawater at 25°C and 60 °C, the longitudinal tensile strength retention was 22.7% and 3.3%, respectively. The GF/PP sheet material showed significantly better property retention while submerged in water; for instance, at 60°C for 6 months, the longitudinal and transverse tensile strength retentions were 79.3% and 84.0%, respectively. The GF/PP sheet material absorbed 0.69% of the saturated water in water at 60°C. A poor glass fiber/polypropylene interface, a relatively thin sheet thickness, and a low resistance of glass fiber to seawater were the factors that led to decreased mechanical properties of the GF/PP sheet material.

Although thermoplastic based FRPC are known for being lightweight and corrosion-resistant, their durability in wet environments and at high temperatures raises some questions. Studies indicating a vulnerability of thermoplastic-based FRPC to water exposure and elevated temperatures have demonstrated how important the durability of the fiber and thermoplastic matrix is for the safe functioning of a structure [8-11,16, 17]. Research on FRPCs demonstrates hydrolytic deterioration in long-term exposure is mostly brought on by degradation occurring in the matrix fiber interphase and via fiber dissolution processes [2,18,19]. The corrosion resistance of the resin is a major factor affecting the filaments' corrosion resistance, and resin toughness also impacts how quickly corrosion cracks spread [5]. Additionally, when fibers embedded in a matrix are exposed to water at elevated temperatures, not only might the matrix and fibers degrade but also the fiber sizing, weakening the fiber-matrix interface and lowering a laminate's mechanical qualities as a result. The longevity of the FRPC constructions was shown to be significantly impacted by the degradation of the fiber sizing and fibers [3].

The research works cited herein indicate that the entry of water molecules into the matrix and fiber-matrix interface impacts the durability and performance of FRPCs. Less consideration has, however, been given to how hydrothermal aging affects the mechanical characteristics of the reinforcing element. Additionally, studies evaluating the impact of humidity on basalt and carbon fibers are limited. Moreover, by examining the performance of the fibers and matrix independently and then extrapolating pertinent attributes of the composite laminate from the constituents' behavior, a multiscale method has the potential to simplify and reduce experimental efforts [1,20]. The change in fiber strength, when exposed to water at elevated temperatures, is one such feature, which is the subject of the present research, serving as a foundation for a thorough multiscale examination of thermoplastic matrix-based composites. The current study looks at the impacts of hydrothermal aging on commercially available basalt and carbon fiber materials, by monitoring mechanical performance, chemical changes, and surface morphology. Fibers were exposed to elevated temperatures and high humidity conditions to understand the difference in performance

when compared with hydrothermal aging. Tensile tests were performed on aged fibers, whereas scanning electron microscopy (SEM) and FTIR was used to examine surface morphology and chemical changes. Mass dissolution tests were performed to understand the elements leached into the solution. The feasibility of using the Arrhenius technique to develop a service life prediction model for both fibers was explored.

4.2. Materials and Methods

4.2.1. Dry Fiber Bundles

Commercially available carbon fiber (CF, type HexTow® IM2A 12K-GP, HEXCEL, Stamford, CT, USA) and basalt fiber (BF, type DR500-17-06P-IA, Mafic, Shelby, NC, USA) were used in this study [21, 22]. These fibers have thermoplastic-compatible sizing on the filaments and are suitable for fabricating pipes using filament winding techniques. Samples from the same bobbins were used for all the experiments

4.3. Sample Preparation and Conditioning

4.3.1. Hydrothermal Aging

BFs were conditioned by exposing them to tap water for a maximum of 56 days at 60°C, 42 days at 71°C, and 28 days at 82°C. Similarly, the longest exposure durations for CFs were 70 days at 60°C, 35 at 71°C, and 35 days at 82°C. As a general approximation considering Arrhenius's theory, the reaction rate doubles for every 10°C increase, meaning that the material will lose strength in half the time compared to the corresponding lower temperature [19, 23]. This is the rationale for the choice of reduced duration of exposure at a higher temperature. Also, the temperatures used in this study are commonly used for conditioning composites. Even though it is known that tap water may change from place to place and over the course of the year, the pH of the tap water examined in this study was assumed to be within a narrow range, with an average of 7.9 for all aging conditions. Fibers with a set length of 2.5 m (100 inches) were obtained and placed in a 4 L beaker for conditioning, as illustrated in Figure 17. To promote fiber failure from occurring in the sample gauge length, only the gauge section length of the fibers was immersed in tap water. As seen in Figure 17, the beaker was covered with aluminum foil and placed in the oven. Calibrated thermocouples monitored the water temperature in the beakers. Hot water was added periodically to make up for evaporative losses.



Figure 17. Aging of samples inside the oven.

4.3.2. Exposure to Humidity

To explore damage occurring to the fibers by exposure to humidity, BFs and CFs were also exposed to 90% humidity at 90°C in an environmental chamber. This could be seen as a more realistic condition of elevated temperature exposure to moisture for composites used in real-life applications, as the water could be seen in a vapor state in elevated temperature applications. BFs were cut to the desired length and mounted onto stainless steel frames, as shown in Figure 18(a), and the frames were hung in the oven. Similarly, CFs were cut to the desired length and supported by rods at the top and bottom to prevent the effects of fatigue bending and abrasion due to airflow inside the oven. The fibers were taped together at their non-gauge length portion, as illustrated in Figure 18(b). This approach ensures that the fiber gauge length is well exposed and that any other possible contact points are well outside the gauge length.

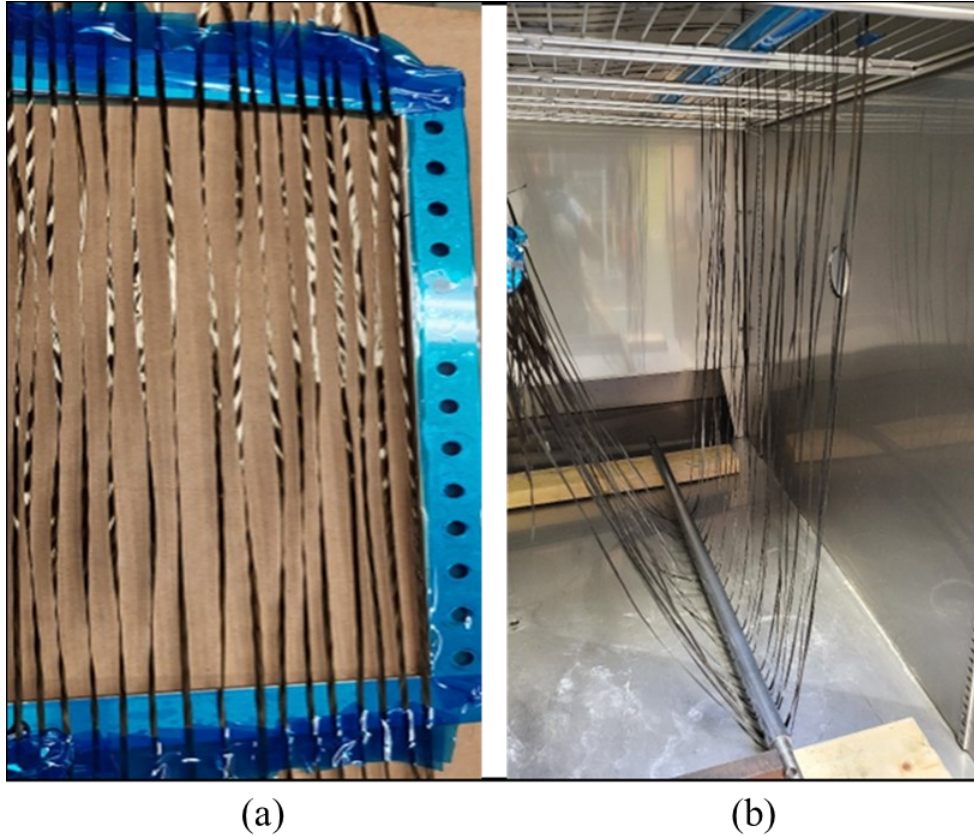


Figure 18. (a) Basalt fibers mounted on frames, (b) carbon fibers inside the humidity chamber.

4.3.3. Assessment of Damage Caused by Sample Preparation

In case of hydrothermal aging, there is a possibility of damaging fibers due to the bending of samples inside the glass beaker (Figure 17), as this may induce stresses to the fiber, causing a loss of strength. Also, due to air circulation inside the oven, fibers are agitated which may lead to fatigue and bending effects that could damage to the fibers. Therefore, considering these possible factors that may lead to strength reductions, parallel experiments simulating the conditioning of samples were performed by placing the samples inside the beaker at room temperature, and testing was therefore done for any possible effects causing reductions in properties.

4.4. Tensile Testing

All the tensile tests were conducted at room temperature (23°C) and for each aging condition. At least ten samples were tested in both ‘dry’ and ‘wet’ conditions. In the case of ‘wet’ testing, samples taken directly from their aging environment and tested. In contrast, samples for ‘dry’ testing were allowed to dry at ambient temperature for at least 24 hours before testing. For samples exposed to humidity conditions, testing was done immediately after removal from the chamber. After tensile testing, the maximum load

from the load-displacement curve was used as the breaking load since a significant reduction in the testing load is considered an indication of failure.

4.4.1. Capstan Grips

Figure 19 shows the capstan grips and how fibers failed using this test method. This method was employed for CFs. Note that a different approach, i.e., the tabbing method (see next subsection), was required for BFs, as they failed during the sample mounting step, due to becoming brittle after aging, leading to significant variations in their breaking load values. A gage length close to 250 mm and a stroke rate of 50.0 mm/min were set for testing. A universal testing machine (type 810, MTS Systems, Eden Prairie, MN, USA) equipped with a 100 kN load cell was used to conduct the experiments. Testing was done adhering to standards ASTM D2256M-10 [24].

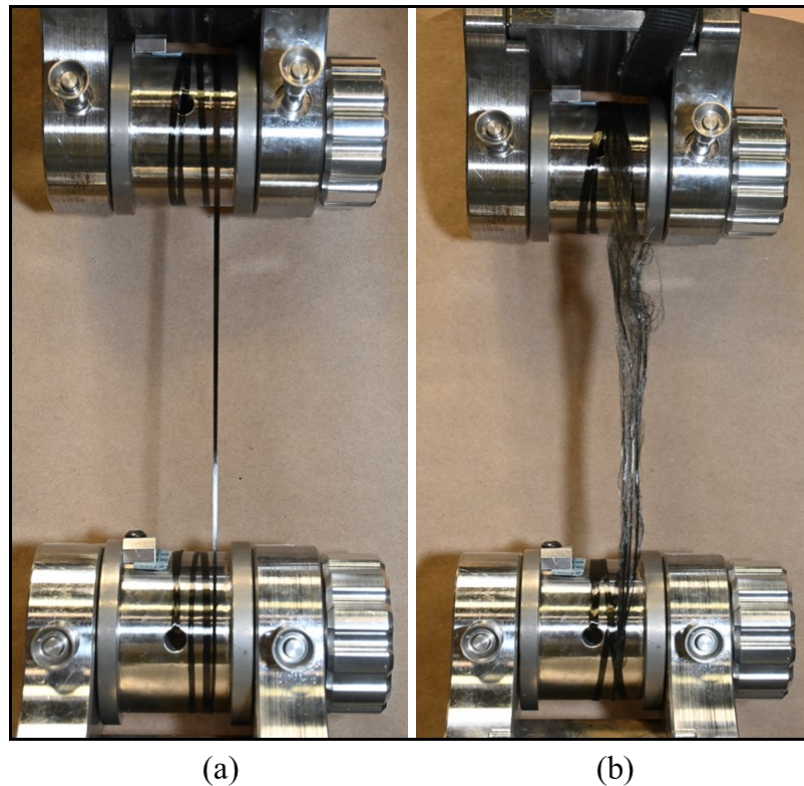


Figure 19. Mechanical testing using capstan grips for carbon fibers: (a) pretest and (b) post-failure.

4.4.2. Tabbing Method.

As mentioned earlier, BFs were found to typically fail during installation using the capstan grips, which motivated the selection of the tabbing method for the testing of BFs. Figure 20 shows a BF pre-test and post-failure using this method. The process in this case involves setting the gauge length and bonding the ends of the fibers using paper tabs, followed by mounting the ends into the grips of the testing machine.

This method was adopted from the standard ASTM C1557-20 [25]. A gauge length close to 250 mm and a stroke rate of 200.0 mm/min were applied for testing. It is interesting to note that in general the tabbing method yielded a more accurate depiction of modulus and elongation at break values for fibers, suggesting that this method is preferred as it controls gauge length and twist in the fibers more efficiently than using the capstan grips. Additionally, the tabbing method mitigates the slack or catenary effect between filaments, which results in a complete failure for the BFs as seen in Figure 20(b). However, if employed for high-strength fibers like CF, this method will result in slippage of sample from the grips.

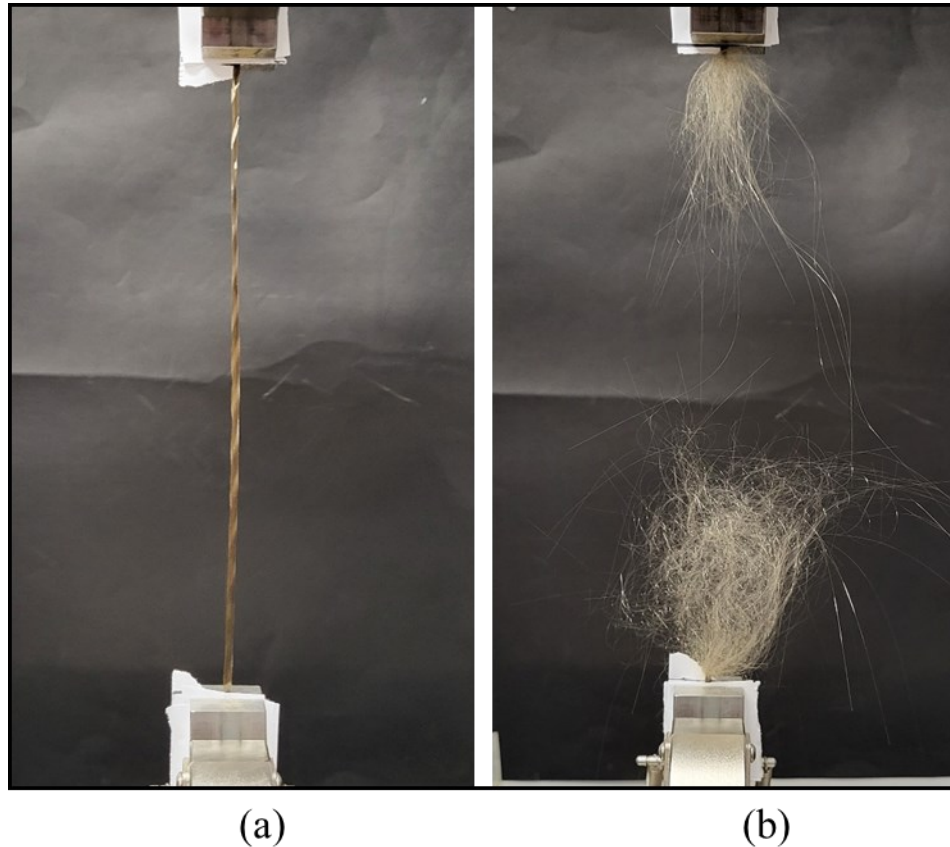


Figure 20. Mechanical testing of basalt fibers using paper tabs: (a) pretest and (b) post-failure.

4.5. Mass Spectroscopy

To investigate the type of elements leaching into the solution, mass dissolution tests were performed on BFs and CFs. Ten identical filaments were selected and placed in plastic tubes, as shown in Figure 21(a). 50 ml of deionized water was added to each tube, and the tubes were immersed in a water-filled glass jar and conditioned in the oven (Figure 21(b)). Accordingly, this method provides a uniform temperature distribution within the plastic tubes. Parallel experiments were performed at 60°C and 82° C for one week. Reference tubes without samples were also included along with the actual samples to account for any release of chemical species happening from the tubes themselves. The concentration of leached ions in water for

BFs was measured using a iCAP6300 Duo analyzer inductively coupled with a ICP-OES plasma-optical emission spectrometer (Thermo Fisher Scientific, Waltham, MA, USA). For CFs, the concentration of C and N ions released into the solution was analyzed using a Total Organic Carbon analyzer (TOC-L) with an ASI-L autosampler and a TNM-L total nitrogen unit (both Shimadzu Corporation, Kyoto, Japan).

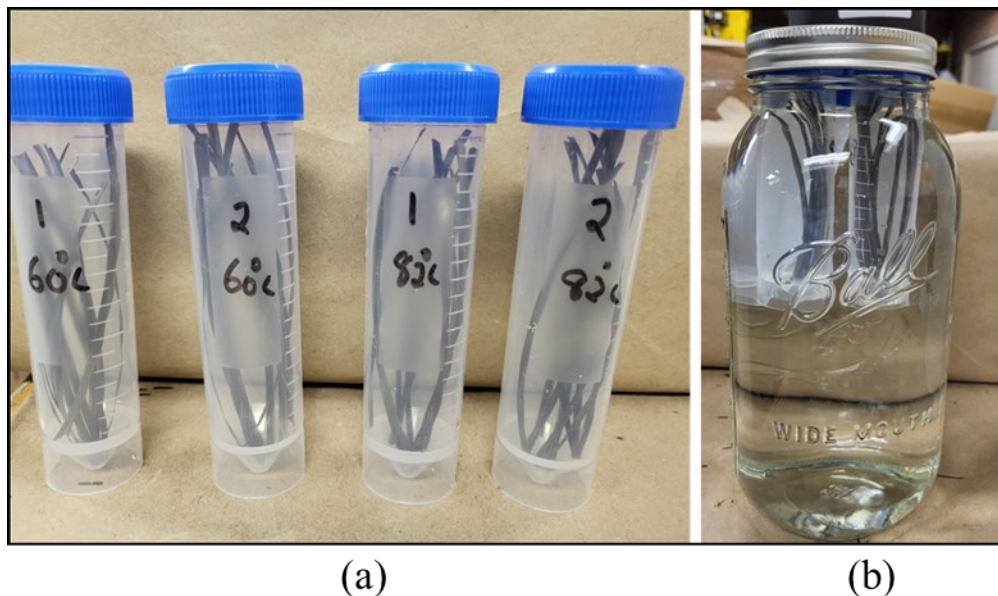


Figure 21. (a) Samples inside plastic tubes, (b) jars used for conditioning fibers.

4.6. Fourier Transform Infrared Spectroscopy

FTIR spectroscopy of the aged and unaged fibers was performed using a Nicolet Is50 FTIR spectrometer (Thermo Fisher Scientific). The creation of an infrared spectrum results from electromagnetic radiation absorption at frequencies corresponding to the vibration of groups of chemical bonds within a molecule. The samples were analyzed using attenuated total reflectance (ATR) mode with a diamond detector, in the range of 400-4000 cm^{-1} with a resolution of 4 $\text{cm}^{-1}/\text{min}$.

4.7. Scanning Electron Microscopy

The surface morphology hydrothermally aged and unaged fibers was compared using SEM (model S-4800, Hitachi, Tokyo, Japan). Before imaging, the samples were gold coated utilizing Denton sputter gold coating equipment (Moorestown, NJ, USA). An acceleration voltage of 5 kV and an emission current of 10 μA were used.

4.8. Result and Discussion

4.8.1. Variations in Fiber Strength

The variation in fiber strength can be described using breaking tenacity, which is the breaking load divided by linear density, or tensile strength, which is the breaking load divided by the sample's original

cross-section area. Here, strength variation is presented in terms of retention or reduction in strength values after aging; therefore, tenacity or tensile strength yield equivalent data. No noticeable variation in strength was observed for BFs tested for quantifying handling damages. On the other hand, CFs exhibited a slight reduction in strength due to handling, and corresponding values were considered in the strength calculation for various test configuration to ensure a conservative approach.

4.8.1.1. Strength Variations for Basalt Fibers

Figure 22 depicts the variations in strength retention values for BFs aged at 60°C, 71°C and 82°C for various test durations, for both, ‘wet’ testing and after drying for 24 hours. The error bars represent one standard deviation from the mean values. Distinct differences in strength retention values were observed between ‘wet’ and ‘dry’ samples, that is, the ‘wet’ samples exhibited lower mechanical strengths compared to the ‘dry’ samples. It is assumed that the water between the filaments acts like a lubricant when fibers are tested wet, which largely negates any load sharing between filaments. When tested dry, friction between fibers promotes load sharing between filaments and thus greater fiber strength, which is similar to filaments being embedded in a polymer matrix, but to a much lesser extent. The highest strength reduction occurred for BFs aged at 82°C (Figure 22 (c)) for 28 days, with a reduction in strength by 82% and 84 % when tested in ‘wet’ conditions and after drying. Strength values of samples aged for 7 days at 60°C, 71°C, and 82°C and tested after drying decreased by 9%, 17%, and 47%, respectively. Therefore, strength values dropped consistently as aging temperatures and durations were increased. Aging at 82°C was the most severe case for BFs as the strength dropped by 37% (tested dry) after exposure to water for just 3 days.

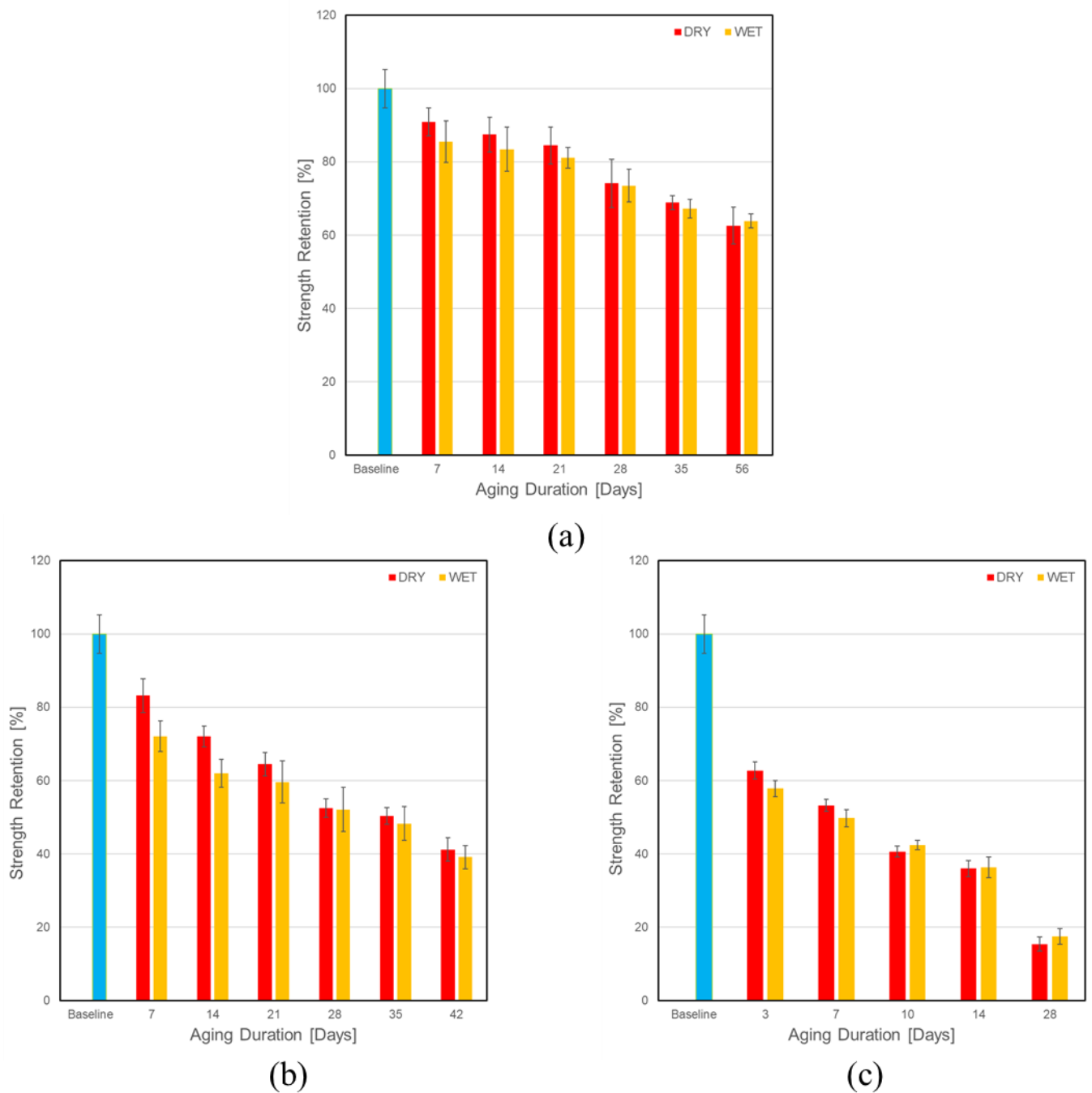


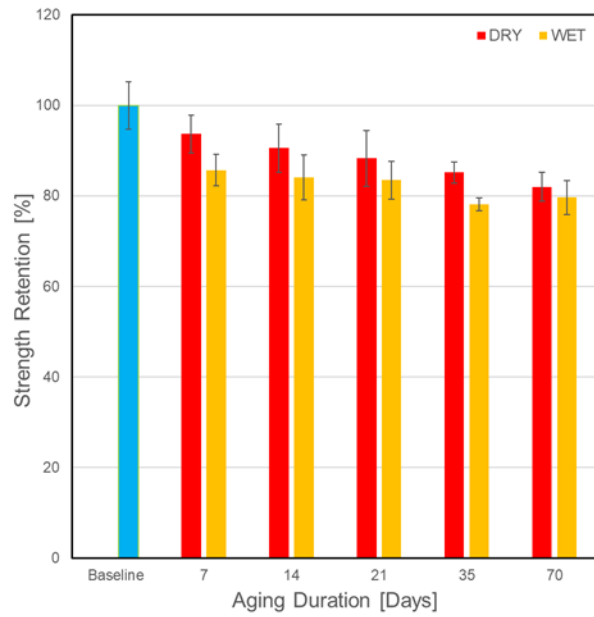
Figure 22. Variations in tensile strength for BF's aged at (a) 60°C, (b) 71°C, (c) 82°C.

4.8.1.2. Strength Variations for Carbon Fibers

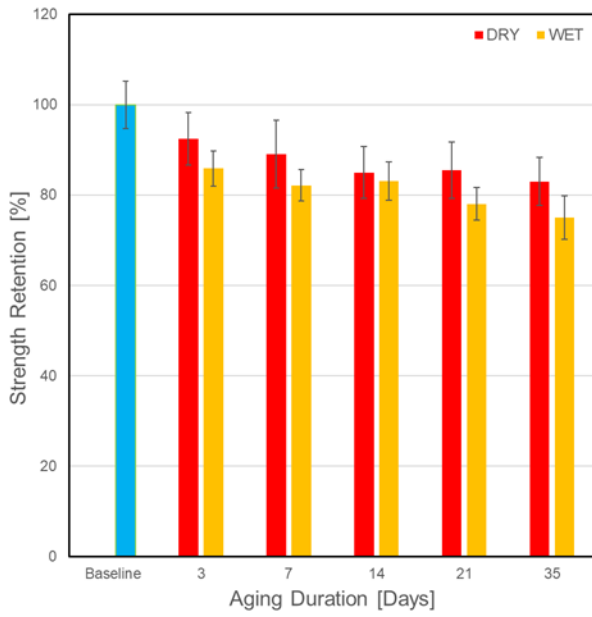
Figures 23 shows the variations in tensile strength for CFs aged at 60°C, 71°C and 82°C for different durations, again for 'wet' and 'dry' testing conditions. The error bars represent one standard deviation from

the mean values. CFs only exhibited a slight variations in strength retention values between ‘wet’ and ‘dry’ samples, that is, wet samples had slightly lower mechanical strengths than dried samples. This difference, albeit smaller than for BFs, was attributed again to reduced friction and load sharing effects between filaments when tested in a wet state.

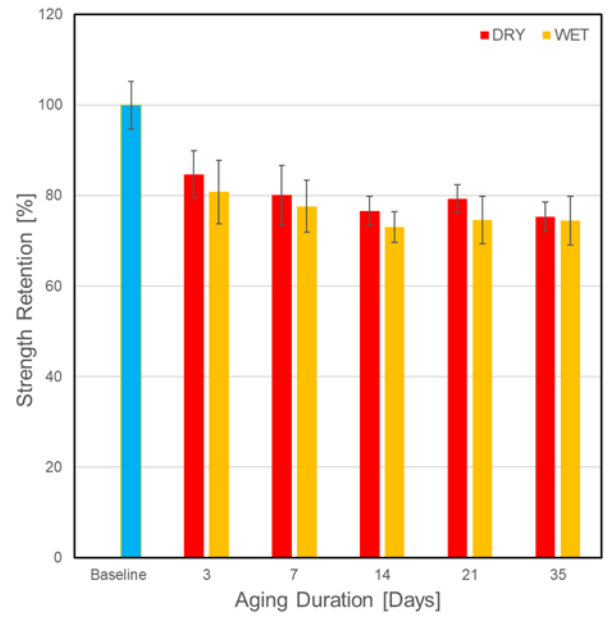
In contrast to BFs, the mechanical performance of CFs was found to be far superior for all three aging temperatures. The highest strength reduction occurred for CFs aged at 82°C (Figure 23(c)) for 35 days, with a reduction in strength by 26% and 25% when tested in wet conditions and after drying, respectively. The percentage reduction was at least double compared to BFs. Similarly, strength values of samples aged for 7 days at 60°C, 71°C, and 82°C and tested after drying decreased by 6%, 11%, and 20%, respectively. There was a notable initial decrease in strength after aging for 7 days, after which strength reduction occurred at a reduced rate. Strength values showed higher reductions with an increase in aging temperatures. The strength values showed a consistent reduction with respect to the increase in aging durations, except for samples aged for 21 days at 71°C and 82°C, which showed a slight increase in strength values with respect to the former aging durations. A similar observation was reported earlier in another work, where CFs aged at 60°C exhibited an increase in strength with an increase in aging durations [20]. This observation was explained by an increase in the number of twists in the fiber samples along the fiber length. As with the current testing methodology, careful attention was paid to eliminate any fiber twist after aging and drying of specimens. To ensure trustable results, some of the tests were repeated, and consistent results were obtained. Aging at 82°C was the most severe case for CFs as the strength dropped by 15% (tested dry) after exposure to water for just 3 days.



(a)



(b)



(c)

Figure 23. Variations in tensile strength for CF aged at (a) 60°C, (b) 71°C, (c) 82°C.

4.9. Prediction of Tensile Strength

4.9.1. Basalt Fibers

The basis of the prediction methodology is the standard Arrhenius relation (see Chapter 2, Section 2.4.1). The data for fibers tested in ‘dry’ condition was used for the analysis. The Arrhenius method is also called the predetermined life approach, where the first step involves the representation of the strength retention values by a fitted curve. Equation (3) describes the link in this model between performance retention and degradation time. This model is commonly used to represent the retention values at different temperatures for composite materials exposed to hydrothermal aging conditions [23].

$$Y = A_1 \exp\left(-\frac{t}{\tau}\right) + Y_0 \quad (3)$$

where Y represents the retention in mechanical properties, t is the exposure time, and τ , A_1 and Y_0 are regression fitting parameters. The values for the regression coefficients are given in Table 3, and the tensile strength retention is shown in Figure 24 as a function of time for the different aging temperatures. It can be observed that the different regression curves exhibit R^2 values of at least 0.94.

The general form of the Arrhenius model is given by:

$$k = A \cdot \exp\left(-\frac{E_a}{RT}\right), \text{ or } \ln k = -\frac{E_a}{RT} + \ln A \quad (1)$$

where k is the reaction rate constant or degradation rate constant, A is a constant related to the material and aging environment, E_a is the activation energy, \bar{R} is the universal gas constant, and T is the absolute temperature. The reaction rate k in the Arrhenius equation is frequently taken to be the time it takes for the material to attain a particular strength loss value [26]. The next step in the analysis involves plotting the logarithm of time to reach the retention values against $1000/T$, where T represents temperature in Kelvin. Strength retention levels of 70%, 80% and 90% were used for this study. The Arrhenius plots for different retention values are displayed in Figure 25. It can be noted that values for 82°C come to lie significantly below the linear trends that the 60°C and 71°C data would delineate. Recalling the tensile test results depicted in Figure 23, BFs aged as 82°C lost almost 50% of their strength after aging for only 7 days. It is assumed that there was a change in the degradation mechanisms at 82°C, which violates the fundamental assumption of the Arrhenius model. With such a deficient model, when extrapolate for lower temperatures, lifetimes would be significantly overpredicted. Hence, as seen in Figure 26, the data points for the 82°C aging conditions were omitted. In this manner, corrected lifetime prediction plots for the 70%, 80%, and 90% retention values were obtained. Fitted straight lines for the different retention levels are practically parallel, which supports the validity of the accelerated degradation tests and the applicability of the model to forecast the loss of BF tensile strength. The activation energy, 70 kJ, was calculated from the slope of

the plot. For example, when interpolating the plot to a temperature of 30°C, the time to reach retention levels of 70%, 80%, and 90% were predicted from the model as 455 days, 270 days, and 120 days, respectively.

To improve the present analysis, a third temperature lower than 60°C may be included to better calibrate the model, which may also help delineate and explain deviations from Arrhenius behavior for temperatures near 82°C and above. However, a test temperature lower than would come at the expense of greater test durations. Also, the observed material behavior makes it difficult to employ a time-temperature superposition approach for creating a master curve at a designated reference temperature (e.g., at 60°C). These findings indicate the challenges and risks of employing the Arrhenius model for service life predictions of composites and materials in general. In general, it is vital to carefully set test conditions and define upper and lower limits for the modelling range.

Table 3. Regression coefficients for strength retention curves for BFs.

Aging Temperature [°C]	A_1 [N]	τ [hour]	Y_0 [N]	E_a/\bar{R} [K]
60	58.65	1268.73	41.26	8410
71	81.11	837.48	18.16	8410
82	77.20	190.92	17.25	8410

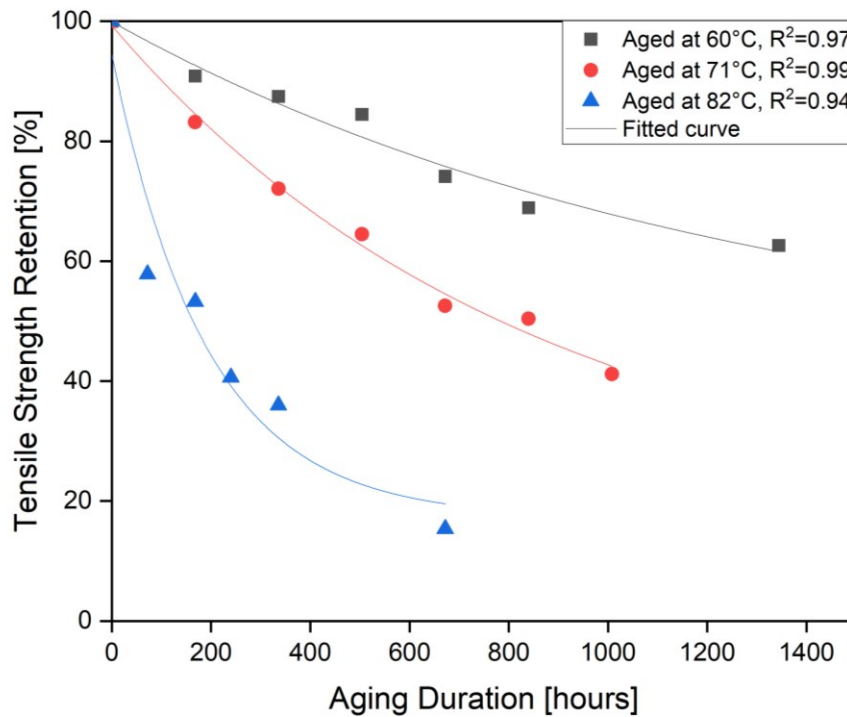


Figure 24. Plot for strength retention with fitted curves for BFs.

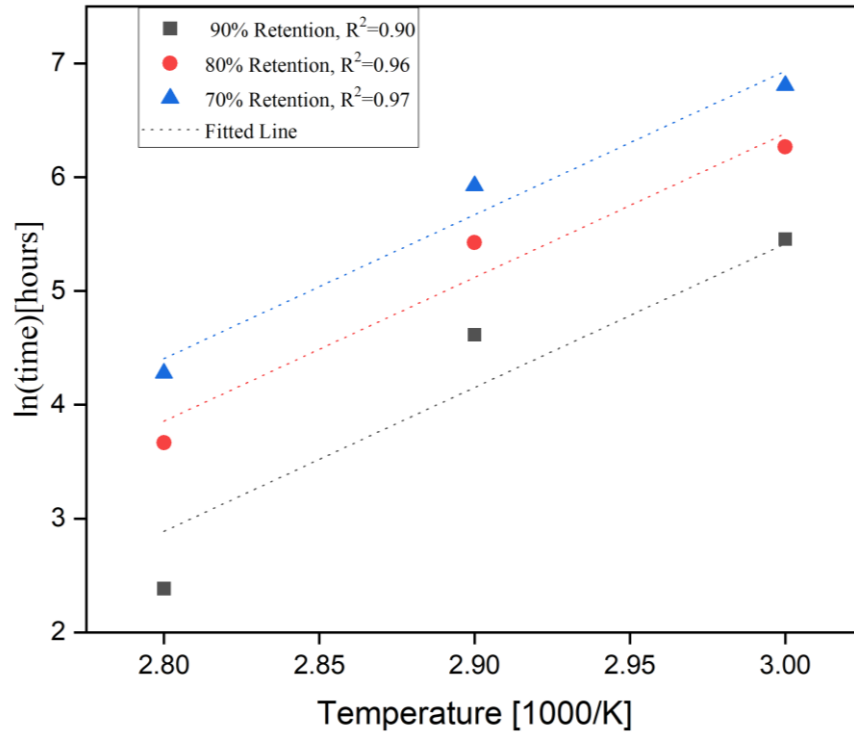


Figure 25. Arrhenius plot for different strength retention levels of BF.

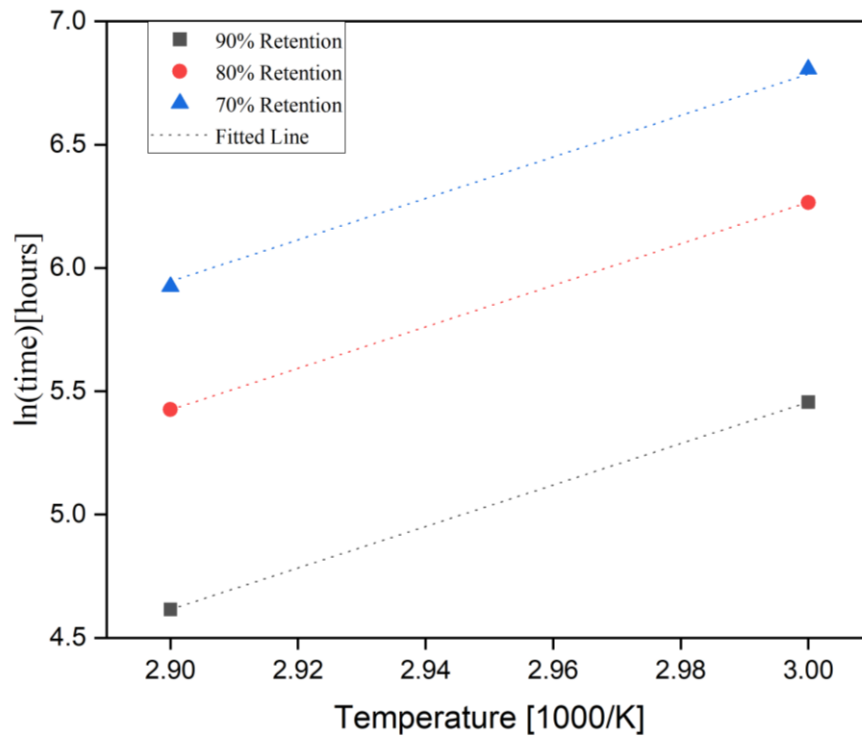


Figure 26. Corrected Arrhenius plot with different strength retention levels for BF.

4.9.2. Carbon Fibers

The underlying assumption for the Arrhenius model is that there is a single dominating degradation mechanism that does not change throughout exposure and that the degradation rate accelerates as exposure temperature increases [23, 27]. The analysis steps described in the previous section were followed for CFs and the same modelling approach were used to represent the retention values at different temperatures. The values for regression coefficients are given in Table 4, and the tensile strength retention data are shown in Figure 27 as a function of time for the different temperatures. Retention values for samples aged for 21 days at 71°C and 82°C were omitted, as an increase in retention values was observed at those aging periods compared with the former aging periods. Similar to the previous analysis involving BFs, this behavior is considered a violation of the Arrhenius model, as properties are expected to decrease with an increase in aging time. Strength retention levels of 85% and 90% were used for CFs, as these were the levels within the experimentally obtained data for all three temperatures. Retention levels beyond the experimental data are commonly not used for prediction as these could increase the error values associated with the prediction [26]. The Arrhenius plots for different retention values are displayed in Figure 28. The activation energy, 91 KJ, was calculated from the slope of the plot. Interestingly, when interpolating the plot to a temperature of 30°C, the time to reach a retention level of 90% was predicted from the model as 410 days, more than three times that predicted for BFs. This is a clear indication of a significantly better hydrothermal resistance of CFs over BFs.

Table 4. Regression coefficients for strength retention curves for CFs.

Aging Temperature [°C]	A_1 [N]	τ [hour]	Y_0 [N]	E_a/\bar{R} [K]
60	17.89	477.18	81.76	10940
71	16.51	146.75	83.18	10940
82	23.72	78.36	76.11	10940

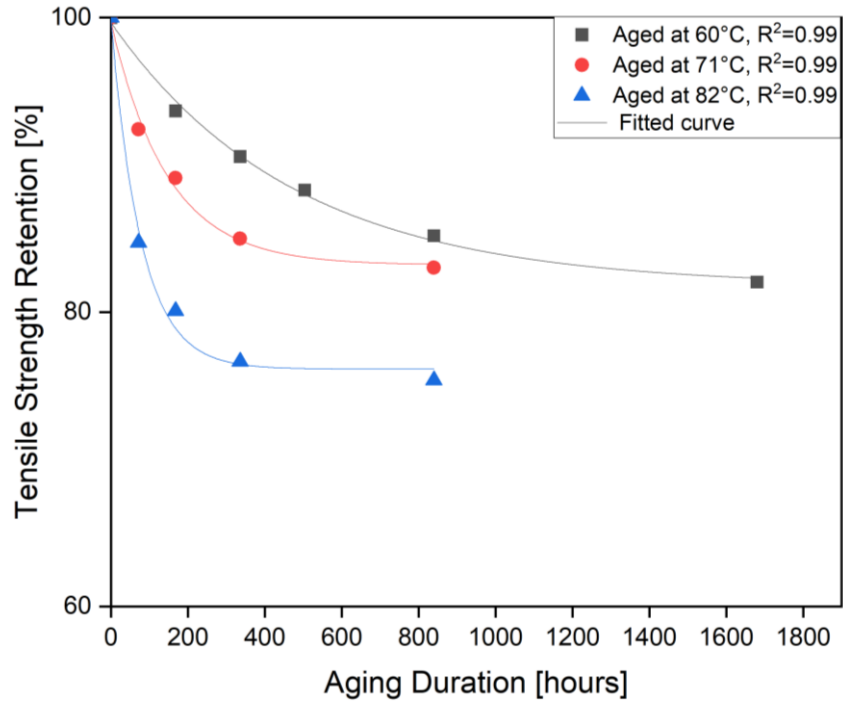


Figure 27. Plot for strength retention with fitted curves for CFs.

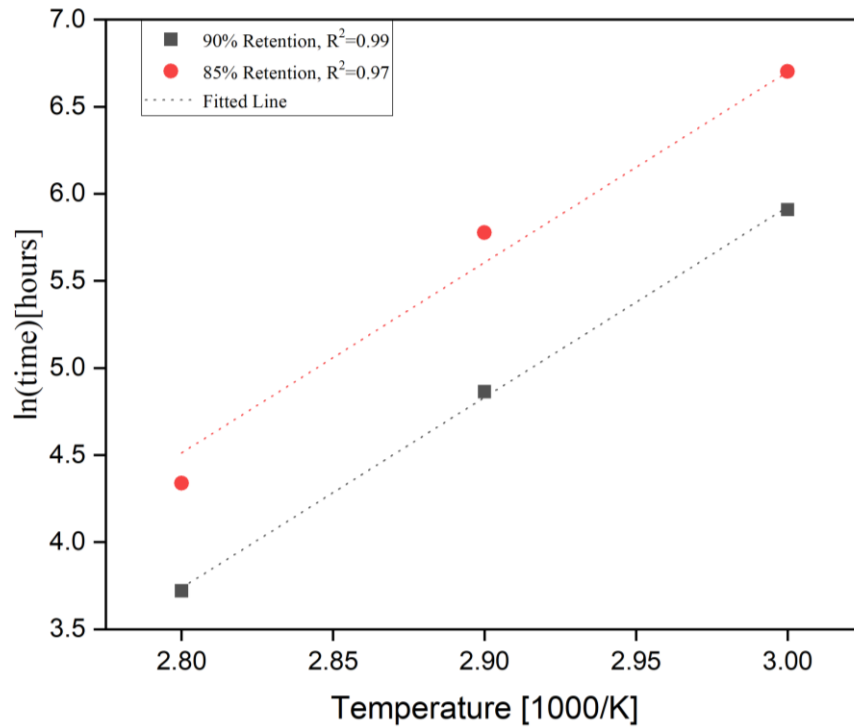


Figure 28. Arrhenius plot with different strength retention levels for CFs.

4.9.3. Variation in Tensile Strength After Exposure to Humidity

Figure 29 shows the variations in strength retention values for BFs and CFs aged at 90°C and 90% humidity. The fibers were tested immediately after removal from the environmental chamber. The error bars represent one standard deviation from the mean values. CFs exhibited a slight reduction in strength, by 5.5%, after aging for 28 days. In contrast, BFs exhibited an increase in strength by 9% after 28 days of exposure. This signifies that BFs are unaffected by the high temperature and humidity conditions, whereas CFs seems to have experienced a slight loss in strength. The reason for this reduction in strength is unknown. There is the possibility of fatigue damage induced to the fibers due to continuous air circulation and agitation of the fibers inside the oven. Also, in humidity aging, the whole length of fibers was exposed, instead of exposing only the gauge length portion as done in hydrothermal aging. Thus, it is possible that the entire fiber was weakened, leading to premature damage when mounting the samples for testing in capstan grips. Nevertheless, as one may have expected, the loss in strength is much lower when compared with that exhibited by the same fibers under hydrothermal aging conditions. This confirms the previous assumptions that hydrolysis of the fibers under hydrothermal conditions leads to significant strength reductions.

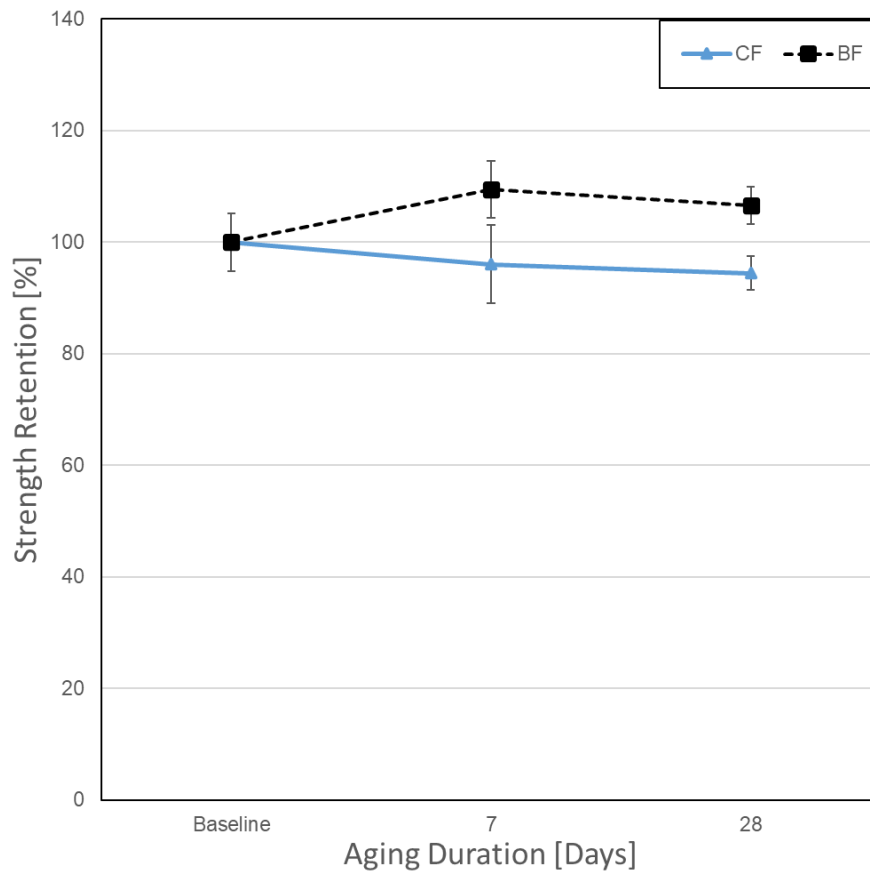


Figure 29. Variations in tensile strength for fibers exposed to 90°C and 90% humidity.

4.10. Leaching of Ions

4.10.1. Basalt Fibers

The following ions were released from the BFs: Si, Al, Ca, Na, Mg, K, Fe, and Mn, arranged in the order of decreasing concentration in the solution. The elemental analysis showed an increasing trend in concentration with an increase in temperature, as shown in Table 5. Noticeably, the amount of Si released after conditioning the fibers for 7 days at 82°C was almost three times higher than that at 60°C for the same duration. All the other elements showed the same trend with respect to the lower and higher aging temperatures. This significant difference is likely correlated with the strength reductions, i.e., strength of BFs aged for 7 days at 60°C and 82°C reduced by 9% and 47 %, respectively. All released ions were present in the chemical composition of BFs. The hydrolysis of the Si-O-Si framework in BFs, as indicated by Eqs.(4-10) in Chapter 3, is seen as the primary reason for the observed ion release, especially Si ions [28]. From these results, it was concluded that the damage occurred to the Si-O-Si framework of BFs due to hydrothermal aging, resulting in the significant release of Si ions and other elements. This finding therefore explains observed strength reductions, which will further be corroborated by FTIR and SEM studies.

Table 5. Mass of elements released from basalt fibers aged in water at 60°C and 82°C for 7 days.

Element	Si	Ca	Al	Na	Mg	K	Fe
Concentration at 60° C [mg/L]	3.15	0.38	0.7	0.51	0.23	0.21	0.01
Concentration at 82° C [mg/L]	12.49	1.54	4.12	1.36	1.16	0.67	0.02

4.10.2. Carbon Fibers

Table 6 shows the concentration of C and N released into the solution after aging the CFs for 7 days at 60°C and 82°C. Carbon fibers mainly comprise carbon above 90%, and nitrogen, in concentrations ranging from 3% to 7% [29]. Thus, the focus for this analysis was on C and N, as these elements constitute the backbone of carbon fibers. Differences in the release of these elements may explain strength variations under the given exposure conditions. After conditioning for 7 days at 82°C, the concentrations of C and N in the solution increased by 14% and 53% when compared with the respective concentrations at 60°C. It is postulated that the elemental release is due to hydrolysis of the polyacrylonitrile (PAN) network in CFs. However, it is interesting to note that changes in ion concentrations are much less pronounced as compared to BFs, which indicates a higher resistance of CF to water compared to BF.

Table 6. Mass of elements released from carbons fiber samples aged in water at 60°C and 82°C for 168 hours (1 week).

Element	C	N
Concentration at 60° C [mg/L]	30.52	0.27
Concentration at 82° C [mg/L]	34.79	0.42

4.11. FTIR Results

To further investigate the effects of exposure to tap water and the attack on fibers and their sizing, FTIR tests were performed on samples after drying. The FTIR spectrum of basalt fiber is depicted in Figure 30, which mimics the spectrum of glass fibers, confirming that the chemical bonds constituting the backbones of basalt and glass fibers are similar [30]. The tests were performed on the samples aged at 60°C and 82°C with the shortest and longest aging durations. In this manner the effects of increased temperatures and aging durations can be explored. For the BFs, the peaks at wavenumbers around 685 cm^{-1} and 900 cm^{-1} are attributed to the Si-O bending and Si-O-Si stretching vibrations, respectively [31]. A decrease in peak intensities can be observed as temperature and aging duration increase. Higher transmittance values imply a reduction in peak intensity and absorbance values. For BFs, the peak intensities decreased with an increase in aging duration and temperatures, and fibers aged for 28 days at 82°C showed the greatest reduction in peak intensity. Similarly, samples aged for 56 days at 60°C had decreased intensity values, compared with those aged for 7 days at 60°C and the unaged samples. The reduction in peak intensities corresponds well with the observed strength reductions at these temperatures, where samples aged 28 days at 82°C had a higher loss in strength when compared to samples aged for 56 days at 60°C and showed the same behavior with different aging durations within the same temperature. Damage occurring to the Si-O-Si framework by the hydrolysis reactions, as depicted by Eq.(2) in Chapter 3, explains the reduction in intensity as seen in the FTIR spectrum.

Figure 31 shows the variation in transmittance values corresponding to the Si-O-Si peaks occurring at a wavenumber of around 900 cm^{-1} . There is a steady increase in the transmittance values as temperature and aging duration increase, with higher transmittance implying a reduction in peak intensity and absorbance values. Peak intensity or peak height could be attributed to species concentration within the specimen, according to the Beer Lambert Law [32]. Samples aged for 28 days at 82°C have the highest increase in their transmittance values (19%), i.e., with the highest peak intensity reduction compared to pristine BFs. Similarly, samples aged for 7 days at 82°C and 60°C showed an increase in their transmittance values by 14% and 4%, respectively, indicating a variation in intensity values with increased aging temperatures. This reduction in intensity values is in good agreement with the difference in strength values with increased aging durations and temperatures. Here, the emphasis is given to the reduction across aging durations and within aging temperatures rather than pointing out the absolute values of variation, which may not be true in all cases. The observed intensity reductions confirm the hydrothermal attack on the Si-O-Si framework, which is the backbone of BFs, either weakening the bond or breaking the bonds leading to the release of ions by the reactions highlighted in the previous section leading to the ion release. This damage caused by the hydrothermal aging on the Si-O-Si framework can be considered to explain the reduction in tensile strength with increased aging temperatures and durations.

In contrast to BFs, no distinct peaks were observed in the FTIR spectra of CFs, because carbon absorbs IR waves in a wide range of frequencies. Therefore, FTIR data was inconclusive for explaining possible chemical reactions leading to strength losses in CFs. Other analysis methods, such as Raman spectroscopy or X-Ray photon spectroscopy, may shed further light on the actual degradation mechanism during hydrothermal aging of CFs.

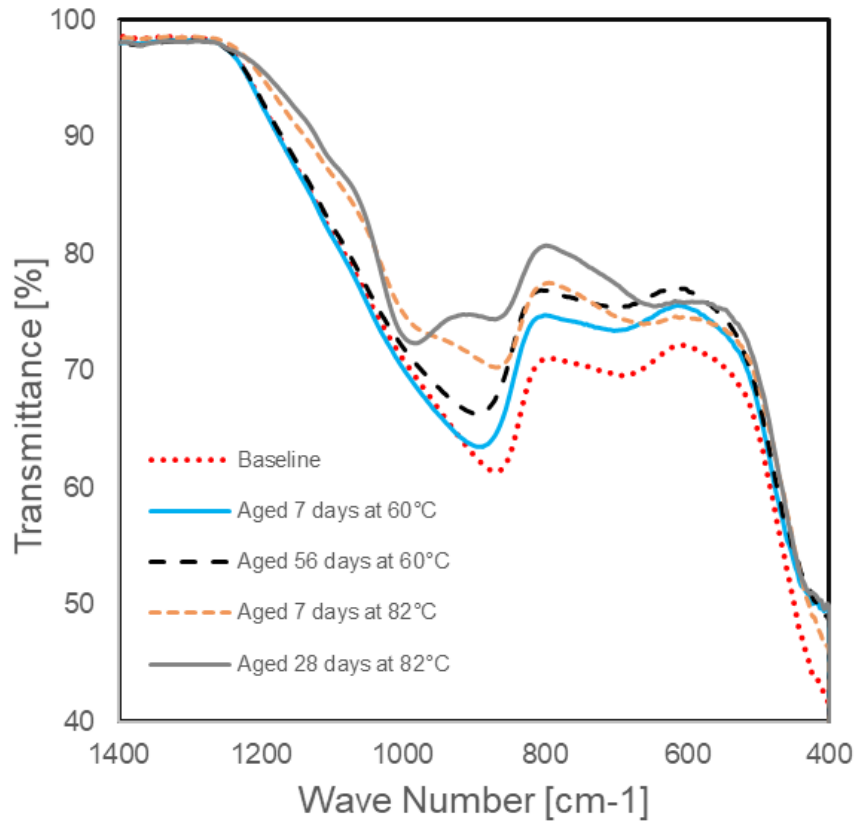


Figure 30. FTIR spectra of aged and unaged fibers.

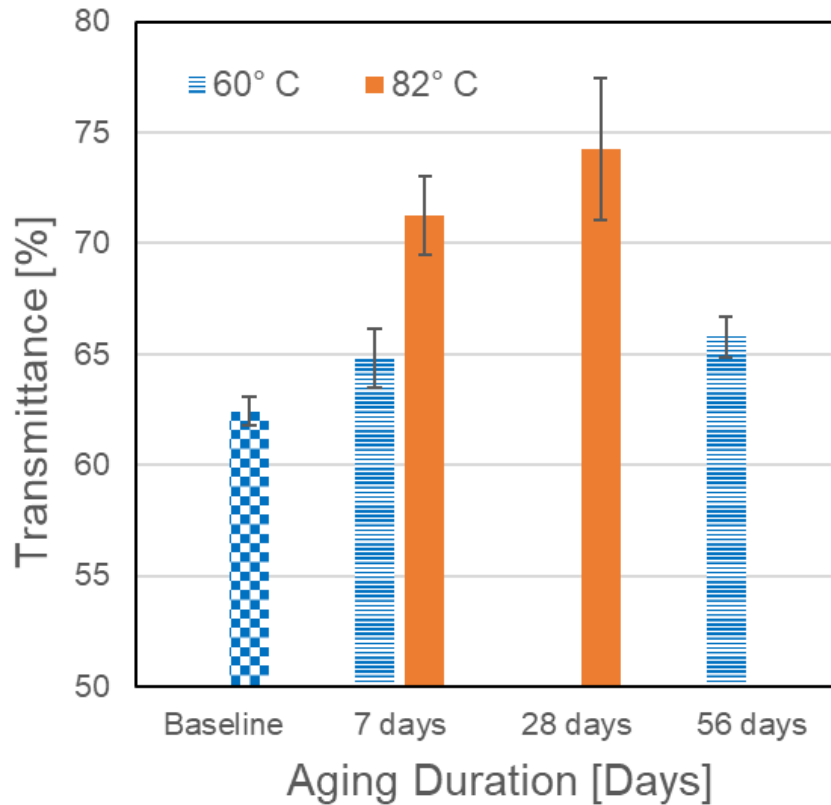


Figure 31. Variation in transmittance values for aged and unaged fibers.

4.12. Morphological Changes

SEM images of a BF sample are shown in Figure 32, where the top row shows the surface of a pristine filament, the middle row the surface of filaments aged at 60°C and 82°C for 7 days (1 week)), and the bottom row the surfaces of samples aged for 56 days (8 weeks) at 60°C (left) and 28 days (4 weeks) at 82°C (right). An increase in deterioration of the filament surface is evident for increasing aging temperatures and durations. The surfaces of filaments aged at 60°C seem to have a comparatively lower extent of damage when compared to the 82°C condition. For all the filaments, in addition to surface roughening, deposits can be observed to have formed on the surfaces, as seen especially for the 82°C aging conditions. These deposits are assumed to have developed because of sizing dissolution in tap water or other chemical reactions related to the sizing degradation of the fibers. For the 82°C condition, patches of material appear to become detached from the filaments, which suggests increased brittleness of the filament surface. The extensive damage occurring to the surface of BF filament could result from the reactions mentioned in the previous section, and most importantly, substantial damage to sizing on the surface. Overall, the observations made by SEM agree with the significant strength reduction for BFs observed at 82°C, compared with 60°C.

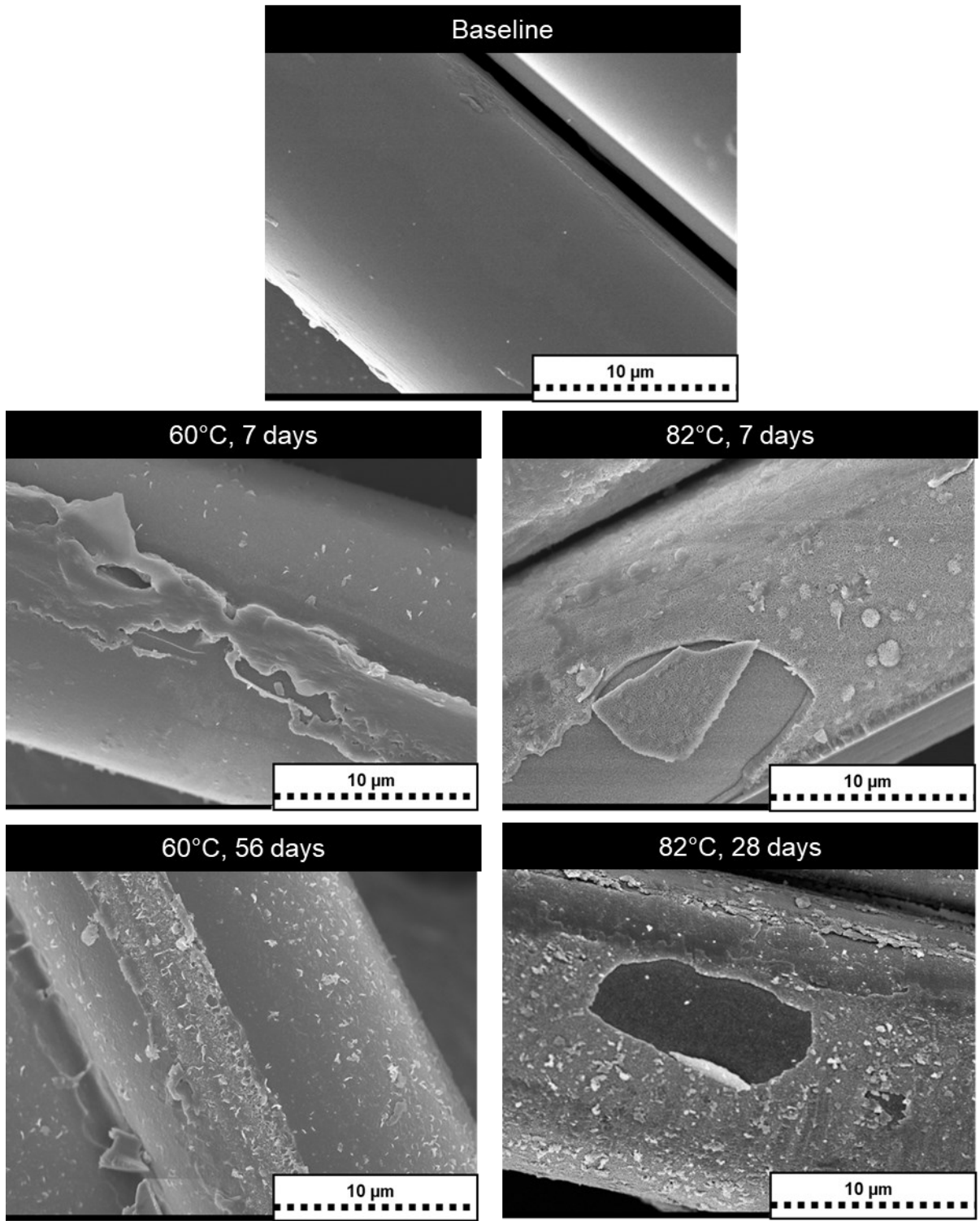


Figure 32. SEM images showing basalt fiber surfaces before and after aging. Baseline of pristine fiber (top row); aged at 60°C and 82°C for 7 days (middle row); and for 56 days (8 weeks) at 60°C and 28 days (4 weeks) at 82°C (bottom row).

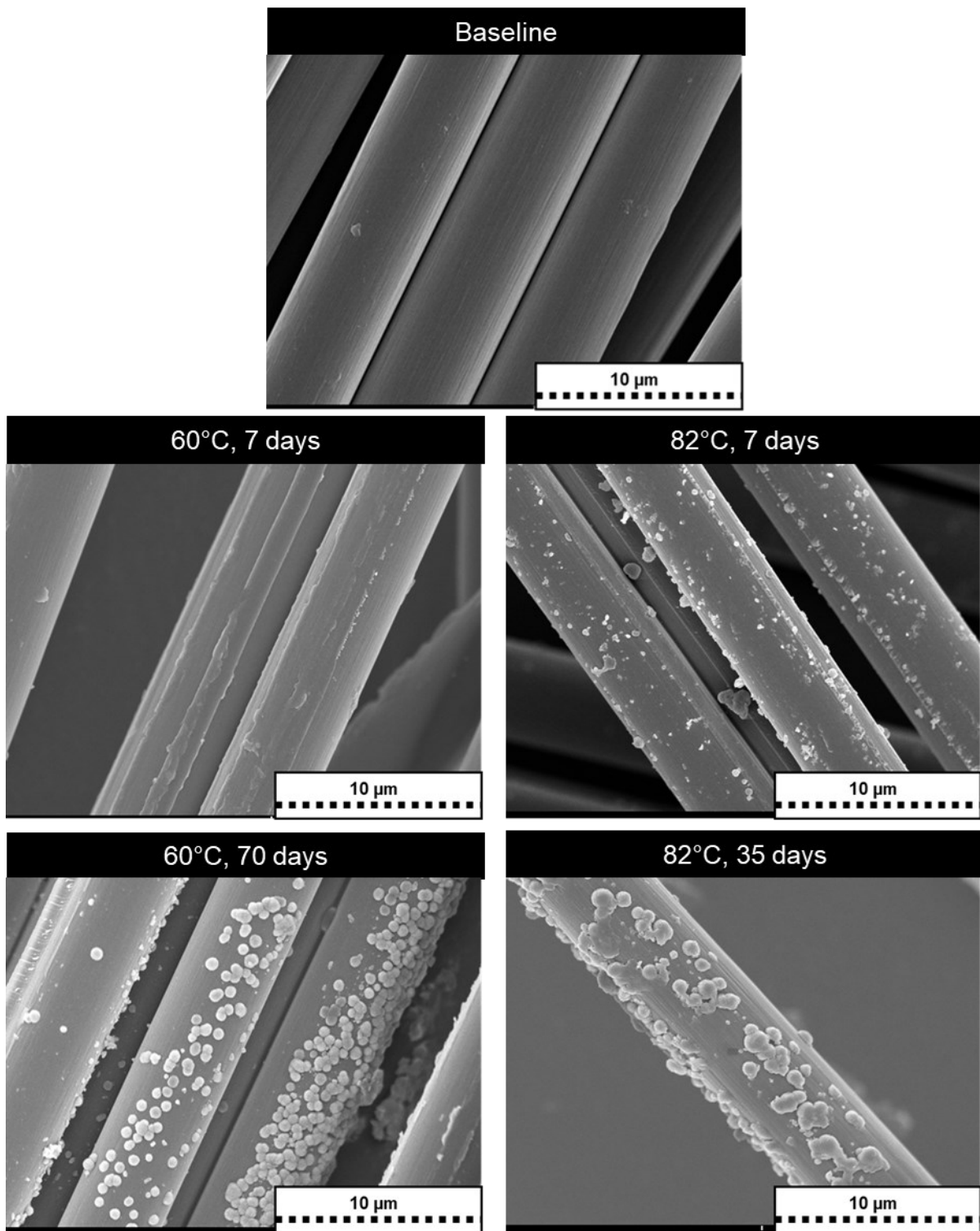


Figure 33. SEM images showing carbon fiber surfaces before and after aging. Baseline of pristine fiber (top row); aged at 60°C and 82°C for 7 days (middle row); and for 70 days (10 weeks) at 60°C and 35 days (5 weeks) at 82°C (bottom row).

SEM images of CF are shown in Figure 33, where the top row shows the surface of a pristine filament, the middle row the surface of filaments aged at 60°C and 82°C for 7 days (1 week), and in the bottom row the surfaces of samples aged for 70 days (10 weeks) at 60°C (left) and 35 days (5 weeks) at 82°C (right). Notably, fibers aged 35 days at 82°C exhibit significant deterioration compared to all other cases. As seen in the images, there is an increase in damage with increased aging temperatures and durations. Compared with BFs, the surfaces of carbon fibers exhibit more depositions, especially for the samples aged for longer durations at both 60°C and 82°C. These deposits are assumed to have formed because of sizing dissolution in tap water or other chemical reactions related to the sizing degradation of the fibers, or alternatively, due to a deposition of leached elements back on the filament surface.

In general, SEM images revealed a more severe degree of damage in BFs compared to CFs. Recalling the pronounced loss in mechanical properties after aging of BFs compared to CFs, it is postulated that a significant portion of the BF materials was subject to chemical degradation. In contrast, CFs appears to have experienced degradation only on the immediate filament surface and sizing. The postulate of fiber material degradation corresponds with the FTIR findings which indicate a loss of material and sizing, especially for BFs, by various reactions, resulting in a reduced strength after hydrothermal exposure.

4.13. Conclusions

After hydrothermal aging, BFs and CFs exhibited a noticeable loss in strength, with samples tested wet showing the highest reductions. Among the reinforcements, CF was most durable, with a maximum drop in the strength of 26 % for samples aged 35 days at 82°C. The percentage reduction was at least double for BF. For 90% humidity exposure, BF did not experience any loss in strength at 90°C, whereas CF experienced a reduction in strength by 5.5 % after 28 days of exposure. Changes in concentration values of ions released during hydrothermal aging for both CF and BF explained the higher reductions in strength occurring at higher aging temperatures. The intensity reductions in FTIR spectra for BF support the conclusion that chemical reactions led to substantial strength loss in BF. The mass dissolution and FTIR results indicate an attack by water on the chemical structure of the fibers, coupled with a loss of sizing, caused a reduction in tensile strength when exposed to hydrothermal conditions. SEM imaging revealed surface damage to the filament and their sizing. This supports the claim that the tested fiber materials are vulnerable to degradation when exposed to water at elevated temperatures.

Another notable finding is that changes in fiber strengths were observed to follow Arrhenius-based degradation behavior, within limits, as there is a corresponding increase in strength loss occurring with an increase in temperature and aging durations. Strength retention plots were established for both fibers. For BF, omitting data points associated with 82°C yielded a suitable fit to the Arrhenius model. These findings

suggests the need for additional temperatures below 60°C for calibrating the Arrhenius model while also exposing the limitation of the modeling approach for BF at the high temperature condition. For CF the strength retention values agreed with the Arrhenius model. Activation energies calculated using the Arrhenius model were 91 kJ and 70 kJ for CF and BF, respectively. Employing the developed models, the predicted times for a 90% retention level at 30°C are 120 and 410 days for BF and CF, respectively. The general modelling strategy may serve as a step toward developing a composite aging multiscale modeling paradigm involving reinforcement properties. Such an approach would be valuable to translate reductions in reinforcement strength to an actual composite structure, which could result in a significant decrease in cost and lead time required for these durability studies.

4.14. References

- [1] A.E. Krauklis, "Modular Paradigm for Composites: Modeling Hydrothermal Degradation of Glass Fibers.," *Fibers*, vol. 9, no. 12, p. 83, 2021.
- [2] A.E. Krauklis, Environmental Aging of Constituent Materials in Fiber Reinforced Polymer Composites. Ph.D. Thesis,, Trondheim, Norway: NTNU, 2019.
- [3] S. Feih, J. Wei, P. Kingshott and B. Sorensen, "The influence of fibre sizing on the strength and fracture toughness of glass fibre composites.," *Composites Part A: Applied Science and Manufacturing*, vol. 36, no. 2, pp. 245-255, 2005.
- [4] P. Cousin, M. Hassan, P. Vijay, M. Robert and B. Benmokrane, "Chemical resistance of carbon, basalt, and glass fibers used in FRP reinforcing bars.," *Journal of Composite materials*, vol. 53, no. 26-27, pp. 3651-3670, 2019.
- [5] B. Wei, H. Cao and S. Song, "Tensile behavior contrast of basalt and glass fibers after chemical treatment.," *Materials & Design*, vol. 31, no. 9, pp. 4244-4250, 2010.
- [6] J. Sim and C. Park, "Characteristics of basalt fiber as a strengthening material for concrete structures.," *Composites Part B: Engineering*, vol. 36, no. 6-7, pp. 504-512, 2005.
- [7] I. Grabovac and D. Whittaker, " Application of bonded composites in the repair of ships structures—A 15-year service experience.," *Composites Part A: Applied Science and Manufacturing*, vol. 40, no. 9, pp. 1381-1398, 2009.
- [8] M. Robert, R. Roy and B. Benmokrane, "Environmental effects on glass fiber reinforced polypropylene thermoplastic composite laminate for structural applications.," *Polymer composites*, vol. 31, no. 4, pp. 604-611, 2010.

- [9] E. Kuram, " Thermal and water ageing effect on mechanical, rheological and morphological properties of glass-fibre-reinforced poly (oxymethylene) composite.," *Proceedings of the Institution of Mechanical Engineers, Part E: Journal of Process Mechanical Engineering*, vol. 233, no. 2, pp. 211-224, 2019.
- [10] C. Borges, A. Akhavan-Safar, E. Marques, R. Carbas, C. Ueffing, P. Weißgraeber and L. da Silva, "Effect of water ingress on the mechanical and chemical properties of polybutylene terephthalate reinforced with glass fibers.," *Materials*, vol. 14, no. 5, p. 1261, 2021.
- [11] A. Messina, A. Airale, A. Ferraris, L. Sisca and M. Carello, "Correlation between thermo-mechanical properties and chemical composition of aged thermoplastic and thermosetting fiber reinforced plastic materials:," *Materialwissenschaft und Werkstofftechnik*, vol. 48, no. 5, pp. 447-455, 2017.
- [12] M. Silva, B. da Fonseca and H. Biscaia, " On estimates of durability of FRP based on accelerated tests.," *Composite Structures*, vol. 116, pp. 377-387, 2014.
- [13] A.E. Krauklis, A. Ggani and A. Echtermeyer, " Long-term hydrolytic degradation of the sizing-rich composite interphase.," *Coatings*, vol. 9, no. 4, p. 263, 2019.
- [14] A.E. Krauklis, C. Karl, A. Gagani and J. Jørgensen, "Composite material recycling technology— State-of-the-art and sustainable development for the 2020s," *Journal of Composites Science*, vol. 5, no. 1, p. 28, 2021.
- [15] A. Kasper, "Recycling composites: FAQs.," *Reinforced Plastics*, vol. 52, no. 2, p. 39, 2008.
- [16] M. Fang, N. Zhang, M. Huang, B. Lu, K. Lamnawar, C. Liu and C. Shen, "Effects of hydrothermal aging of carbon fiber reinforced polycarbonate composites on mechanical performance and sand erosion resistance.," *Polymers*, vol. 12, no. 11, p. 2453, 2020.
- [17] S. Dong, P. Zhou, R. Guo, C. Li and G. Xian, "Durability study of glass fiber reinforced polypropylene sheet under simulated seawater sea sand concrete environment.," *Journal of Materials Research and Technology*, vol. 20, pp. 1079-1092, 2022.
- [18] A.E. Krauklis, A. Gagani, K. Vegere, I. Kalnina, M. Klavins and A. Echtermeyer, "Dissolution Kinetics of R-Glass Fibers: Influence of Water Acidity, Temperature, and Stress Corrosion.," *Fibers*, vol. 7, no. 3, p. 22, 2019.
- [19] J. Davalos, Y. Chen and I. Ray, "Long-term durability prediction models for GFRP bars in concrete environment.," *Journal of Composite materials*, vol. 46, no. 16, pp. 1899-1914, 2012.

- [20] A. Echtermeyer, A. Krauklis, A. Gagani and E. Sæter, "Zero Stress Aging of Glass and Carbon Fibers in Water and Oil—Strength Reduction Explained by Dissolution Kinetics.," *Fibers*, vol. 7, no. 12, p. 107, 2019.
- [21] "Hexcel Carbon fiber technical datasheet," Hexcel, [Online]. Available: https://www.hexcel.com/user_area/content_media/raw/IM2A_HexTow_. [Accessed 5 September 2022].
- [22] "Basalt fiber technical data sheet," Mafic, [Online]. Available: <https://www.mafic.com/product-lines>. [Accessed 5 september 2022].
- [23] J. Zhu, Y. Deng, P. Chen, G. Wang, H. Min and W. Fang, "Prediction of long-term tensile properties of glass fiber reinforced composites under acid-base and salt environments.," *Polymers*, vol. 14, no. 15, p. 3031, 2022.
- [24] ASTM, D2256M-10, Standard testmethod for tensile properies of yarns by the single starnd method, 2015.
- [25] A. D2343-17, Standard Test Method for Tensile Properties of, 2009.
- [26] I. 11346, Rubber, vulcanized or thermoplastic-Estimation of life-time and maximum temperature of use., ISO, 2014.
- [27] O. Starkova, A. Gagani, C. Karl, I. Rocha, J. Burlakovs and A. Krauklis, "Modelling of environmental ageing of polymers and polymer composites- durability prediction methodhs," *Polymers*, vol. 14, no. 5, p. 907, 2022.
- [28] A.E. Krauklis and A. Echtermeyer, "Long-term dissolution of glass fibers in water described by dissolving cylinder zero-order kinetic model: Mass loss and radius reduction.," *Open Chemistry*, vol. 16, no. 1, pp. 1189-1199, 2018.
- [29] J. Pusch and B. Wohlmann, "Carbon fibers," in *Inorganic and Composite Fibers*, Elsevier, 2018, pp. 31-51.
- [30] J. Liu, M. Chen, J. Yang and Z. Wu, "Study on mechanical properties of basalt fibers superior to E-glass fibers.," *Journal of Natural Fibers*, vol. 19, no. 3, pp. 882-894, 2022.
- [31] M. Rani, P. Choudhary, V. Krishnan and S. Zafar, "Development of sustainable microwave-based approach to recover glass fibers for wind turbine blades composite waste.," *Resources, Conservation and Recycling*, vol. 179, p. 106107, 2022.
- [32] N. Abidi, FTIR Microspectroscopy, Springer International Publishing., 2021.

Chapter 5 : Hydrothermal Aging of Glass Fiber Reinforced Thermoplastic Composites

Aspects of the material discussed in this chapter have been submitted for publication in the proceedings of the American Society of Composites 38th Technical Conference, Boston, USA, September 17 - 20, 2023.

5.1. Introduction

Continuous fiber-reinforced polymer composites (FRPC) are increasingly used in structural applications, which can be attributed to their distinctive qualities, e.g., excellent corrosion resistance and high strength-to-weight ratio, compared to conventional metallic engineering materials [1]. FRPC typically comprise three basic constituents: the fibrous reinforcement phase, the polymer matrix, and a fiber surface coating known as sizing that promotes fiber-matrix adhesion. The synergistic interaction between these components results in the high mechanical performance of FRPC. FRPC are commonly made with a thermoset polymer matrix; however, thermoplastic matrix materials are increasingly employed as an effective substitute in recent years. Some key benefits of thermoplastic matrix materials over their thermoset counterparts are a practically infinite shelf life, the ability to recycle thermoplastic polymers, and potential reductions in manufacturing costs. The latter can be achieved using rapid and continuous fabrication processes [2,3]. In composite structures, the fibers chiefly carry the applied loads while the matrix distributes stresses to and between the fibers and shields them from damaging external forces and environmental factors. FRPCs used in structural applications are often exposed to water and humid environments. Both thermoset and thermoplastic matrices offer considerable resistance to water ingress, yet moisture may significantly affect material performance during long-term exposure. [4,5]. Since glass fibers (GFs) are hygroscopic, it is crucial to comprehend and quantify the water-induced aging effects of glass fiber-reinforced composites [6]. Given that high strength and stiffness of composite materials can be impaired by the unpredictability of the material's interaction with the environment and loading conditions, environmental durability is one of the concerns that restrict the greater use of these materials in a variety of structural applications. Adding to that, with the inclusion of temperature, the aging process becomes accelerated [7,8]. Moreover, the composite constituents are impacted by environmental aging in different ways [9]. To ensure the composite's environmental durability, it is crucial to understand the causes and kinetics of environmental aging of each component.

Over the past few decades, extensive research has been performed on the relationship between environmental exposure and thermomechanical performance of fiber-reinforced thermosetting-matrix composites used in the fields of aerospace, automotive, marine, and oil/gas (e.g., GF, carbon fiber (CF), basalt fiber (BF), aramid, and hybrid fibers) under various aging conditions [10-13]. Only lately has the aging of thermoplastic-matrix composites received greater attention, focusing on the effects of sample

preparation techniques and fiber surface treatments to make fibers compatible with the matrix [14,15]. There have been very few attempts to investigate the influence of environmental conditions on continuous fiber-reinforced thermoplastics. Elmar et al. [16] studied the influence of hydrothermal aging on glass fiber reinforced polyamide-6 (PA6) and polypropylene (PP) composites. They stated that the fiber-matrix interaction is negatively impacted by the effects of water at higher temperatures. PA6 and PP-based specimens experienced this effect due to the capillary effect along micro-fissures between the fibers and the polymer. This well-known effect explains why the fiber-matrix adhesion was deteriorating, which in turn caused a reduction in mechanical properties. Robert et al. [17] examined the effect of the aging behavior of GF-reinforced PP laminates by exposing them to tap water at 23°C, 50°C and 70°C and to a salt solution with 3% NaCl. It was found that immersion in the salt solution caused a higher reduction in flexural strength than immersion in tap water. The findings show that the NaCl solution amplifies the degradation of the fiber-matrix interphase and thus the composite mechanical properties. The decrease in flexural properties was caused by moisture absorption and by the exchange of Na⁺ and Cl⁻ ions at the interphase between GF and PP. In a similar study, Aziz [18] studied the effect of hydrothermal aging on the thermomechanical behavior of CF and GF reinforced polyetherimide (PET) composites by subjecting samples to thermal cycling between a temperature range of -40°C and 80°C. They stated that compared to hydrothermally aged GF reinforced composites, the loss modulus was larger for CF reinforced composites. This was attributed to the lower thermal expansion coefficient of CF, resulting in a greater thermal expansion mismatch between matrix and fibers. Hence, the fiber-matrix interface of CF composites was affected more than the composites reinforced with GF. It was concluded that interfacial loading, and deformations at the interface, were the reason for reduction in mechanical properties and morphological changes. Recently, Shaoce et al. [19] investigated the durability of GF-polypropylene (GF-PP) unidirectional sheets by exposing them to distilled water and a combination of seawater, sea sand, and concrete for up to 6 months at 25°C and 60°C. The authors then evaluated changes in mechanical properties. The findings showed that the GF-PP sheets are vulnerable to sea water immersion at elevated temperatures, resulting in an abnormally increased water uptake of 3.4% at 60°C. The longitudinal tensile strength retention after a six-month immersion in 25°C and 60°C in sea water was 22.7% and 3.3%, respectively. When submerged in water, GF-PP sheets retained their properties to a much greater extent; for example, at 60°C for 6 months of aging, the longitudinal and transverse tensile strength retention was 79.3% and 84.0%, respectively. The saturated water uptake of GF-PP sheets in water at 60°C was 0.69%. The decreased mechanical properties of the GF-PP sheet was attributed to a poor fiber-matrix interface, the relatively thin sheet thickness, and a weak resistance of GF to seawater.

The reviewed technical literature confirms that damage occurring to the fiber-matrix interphase or the fibers themselves are primary reasons for the reduction in mechanical properties under hydrothermal

conditions. Improving the adhesion at the fiber-matrix interphase using fiber sizing can improve the property retention under aging conditions [20]. Hence, a focus should be placed on the fiber-matrix interphase properties and the fibers themselves to understand the reactions and changes that occur to these composite constituents when exposed to water at elevated temperatures. The long-term hydrothermal aging-related behavior of continuous fiber-reinforced thermoplastics is only discussed in a relatively small number of papers, with a focus on applications in the automotive and aviation industries. Nonetheless, accurate knowledge of long-term behavior of thermoplastic based FRPC is crucial for their usage in safety-related applications. To broaden the application spectrum for these materials, it is necessary to perform durability tests and expand the research data set. In addition to understanding how continuous fiber-reinforced thermoplastics degrade, it is critical to derive lifetime prediction models that can be used to extrapolate property values under various scenarios. Thermoplastic composites, particularly GF-PP and GF reinforced high-density polyethylene (GF-HDPE), are attractive for high-volume applications such as in the oil and gas industry. Yet, data on long-term durability is limited compared to FRPC with thermoset matrices. Therefore, the present study is seen as an early contribution investigating the durability of unidirectional GF-PP and GF-HDPE composite tapes by conditioning them in deionized water for up to 70 days at 60°C and 28 days at 95°C, measuring the water absorption behavior and tensile strength. The focus of this study is on understanding the damage effects on the fiber-matrix interphase and the fibers, as these components dictate the performance of the composite. Mechanical testing was performed on dried material samples after aging. The chemical elements leached into the aging fluid during conditioning were analyzed. Fiber degradation mechanisms by environmental aging were investigated by characterizing the chemical composition and morphology of fiber surfaces before and after aging.

5.2. Materials and Methods

5.2.1. Unidirectional Composite Tapes

Commercially available GF-HDPE tape (CFRT, Shenggang, Taizhou, ZJ, China) and GF-PP Tape (GPP62-750, Jiangsu Qiyi Technology, China) were selected for this study. These thermoplastic tapes were chosen for the experiments due to their comparatively low thickness which implies shorter aging times for water absorption tests. As per the manufacturer specifications, the GF-HDPE and GF-PP tapes had a thickness and width of 0.5 mm and 50 mm, and 0.33 mm and 49 mm, respectively. The fiber weight fractions of the tapes were verified by fiber burnout tests and was found to be within manufacturer specifications of 60 ± 2 %.

5.2.2. Sample Conditioning

Samples were slit to the desired size using a paper cutter, as shown in Figure 34(A). Specimens were then placed into glass jars filled with deionized water and immersed inside an aging cell, see Figure 34(B),

with a heater set to maintain a specified temperature inside the jars. The selected aging temperatures were at 60°C and 95°C, with aging durations of 14 and 70 days at 60°C and 14 and 28 days at 95°C.

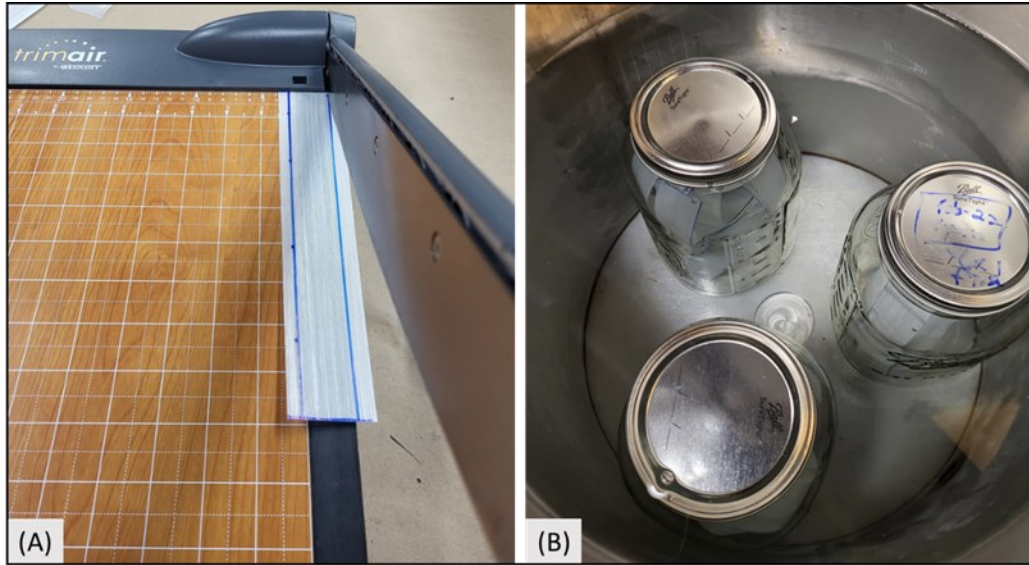


Figure 34. (A) Slitting of tapes, and (B) samples inside jars placed inside aging cell.

5.2.3. Water absorption testing

Water absorption tests of GF-PP and GF-HDPE sheets were conducted according to ASTM D5229 [21]. A balance with accuracy of 0.001 g was used for weight gain measurement. Specimens with a size of 75 mm by 30 mm were tested for each aging conditions and type of tape. Before aging, specimens were dried inside an oven. After certain intervals during aging, specimens were taken from the aging fluid, dried with tissue paper, and weighed. The weight gain due to water absorption was calculated using Eq. (11).

$$W = \frac{w_t - w_i}{w_i} \quad (11)$$

where W is the water uptake percent, w_i and w_t is the weight of specimens before immersion and after a specified aging duration.

5.2.4. Mass Dissolution Testing

To assess which elements were released during the aging process, mass dissolution studies were performed on GF-PP and GF-HDPE tapes exposed for a duration of 14 days at 60°C and 95°C. Samples of equal mass were selected for both sets of tapes and were immersed in plastic tubes with 50 ml of deionized water. Reference solutions without the samples were also simultaneously placed in the water bath at the same conditions to recognize any elements that may be released from the plastic tubes. The concentration of dissolved ions in water was measured using an inductively coupled plasma-optical emission spectrometer (iCAP6300 Duo / ICP-OES, Thermo Fisher Scientific, Waltham, MA, USA).

5.2.5. Tensile Testing

The longitudinal tensile strength of GF-PP and GF-HDPE tape specimens was tested according to ASTM D3039 [22]. Six specimens with length of 250 mm and nominal cross-section were prepared for each material and specified aging time. The stroke rate for the tests was 5 mm/min, using the universal testing machine (type 810, MTS Systems, Eden Prairie, MN, USA). Prior to testing at room temperature, aged samples were dried for 24 hours. Sandpaper, tabs, and aluminum tapes were placed at the specimen extremities and constant gripping pressure was applied to prevent damaging the specimens at the grips, thus ensuring that failure occurred inside the specimen gauge length.

5.2.6. Fourier Transform Infrared Spectroscopy

Fourier Transform Infrared Spectroscopy (FTIR) of the pristine and aged samples was performed using a Nicolet Is50 FTIR spectrometer (Thermo Fisher Scientific). The creation of an infrared spectrum results from electromagnetic radiation absorption at frequencies corresponding to the vibration of groups of chemical bonds within a molecule. The samples were analyzed using attenuated total reflectance with a diamond detector, in the range of 400 cm^{-1} to 4000 cm^{-1} with a resolution of $4\text{ cm}^{-1}/\text{min}$.

5.2.7. Scanning Electron Microscopy

The surface morphology of pristine and hydrothermally aged fibers was compared using scanning electron microscopy (SEM) (model S-4800, Hitachi, Tokyo, Japan). An acceleration voltage of 5 kV and an emission current of $10\text{ }\mu\text{A}$ were used. Before imaging, the samples were gold-coated using gold coating equipment (Denton Sputter, Moorestown, NJ, USA).

5.3. Results and Discussion

5.3.1. Water absorption results

Figures 35 and 36 show the water absorption behavior of GF-HDPE and GF-PP composite tapes. For the GF-HDPE tape, the weight gain at 95°C was almost double that observed at 60°C . At both aging temperatures, the specimens exhibited saturation with a weight gain of 0.41% and 0.25% after exposure for 14 days at 95°C and 60°C , respectively. Similar behavior was displayed by the GF-PP tapes, with 1.38% and 1.07% increase in weight after exposure for a period of 14 days at 95°C and 60°C , correspondingly, with water uptake approaching saturation after 14 days. For the same immersion durations, GF-PP tapes absorbed significantly more water compared to GF-HDPE composite tapes. It is postulated that the HDPE matrix offered higher protection from the aging environment to the reinforcements than the PP matrix. There are two primary ways moisture can enter the composite materials: (1) through capillary transport along fissures at the fiber-matrix interfaces, as well as wicking of water along dry fiber bundles, and (2) permeation through the matrix and transport through matrix microcracks created during material processing [17].

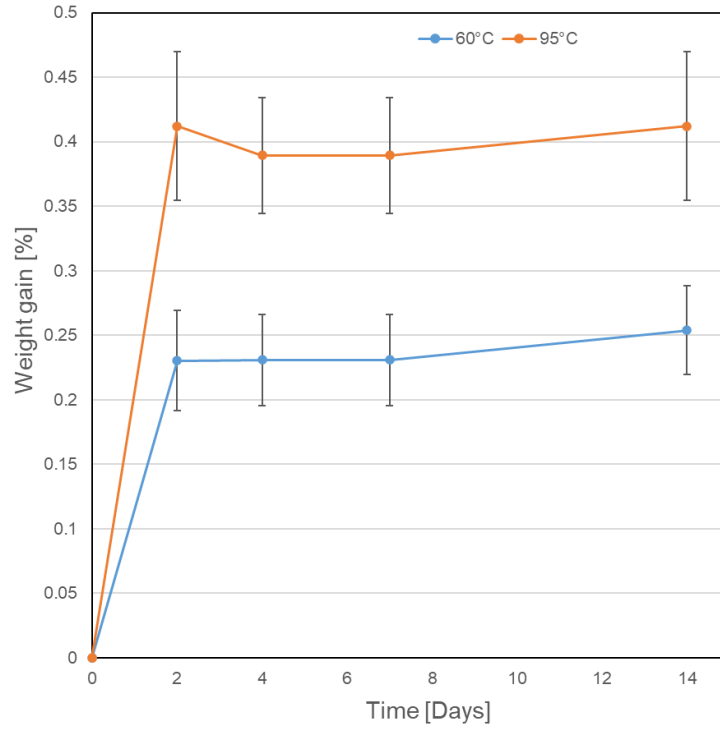


Figure 35. Weight gain versus time plot for GF-HDPE composites.

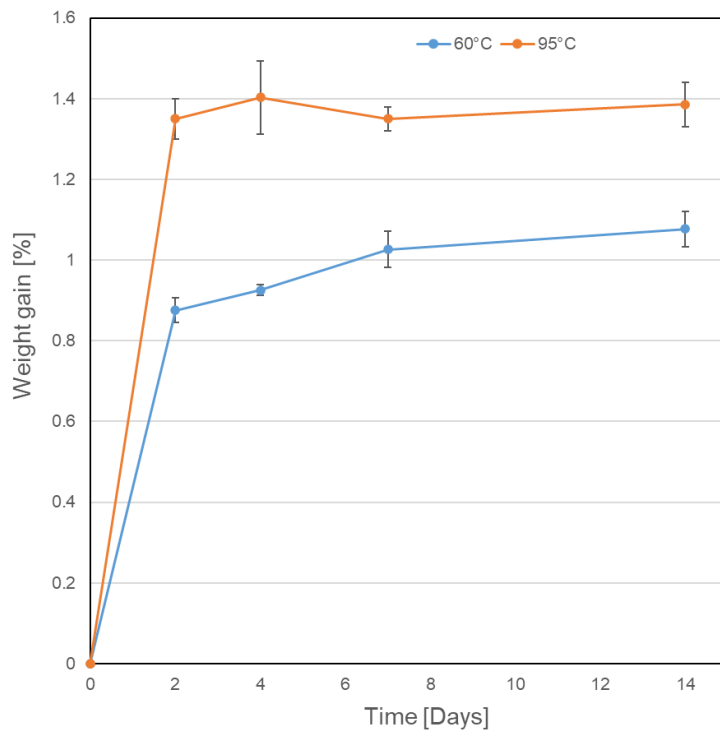


Figure 36. Weight gain versus time plot for GF-PP composites.

5.3.2. Strength Changes After Aging

The variations in longitudinal tensile strength of GF-PP and GF-HDPE composite tapes aged at 95°C and 60°C are depicted in Figures 37 and 38. Error bars represent one standard deviation from the mean. As the primary interest is in understanding the damage occurring to the reinforcements, the focus is given on tensile strength in this study. For GF-PP samples aged at 95°C (Figure 37), the strength dropped by almost 51% after aging for 14 days. Correspondingly, 34% reductions in strength were observed for GF-HDPE samples aged at 95°C for 14 days. These reductions increased with aging duration, and after 28 days at 95°C, GF-PP and GF-HDPE specimens showed reductions in strength by 59% and 45%, respectively. The reductions were significantly lower for samples aged at 60°C, with both GF-HDPE and GF-PP specimens exhibiting a loss of about 9% after exposure for 14 days. However, GF-HDPE specimens showed a significant reduction in strength by 33% after exposure for 70 days at 60°C; in contrast, GF-PP specimens showed better performance with a strength reduction of 20%. The strength reduction values of GF-PP specimens aged at 60°C agree with those reported in the technical literature for GF-PP composites [19]. Higher strength reductions were observed when the aging temperature and durations increased for GF-PP and GF-HDPE composites. Also, it is essential to point out the higher reductions in strength observed for GF-HDPE composites exposed to water at 60°C for extended durations. There is only limited research on the behavior of GF-HDPE composites exposed to water at elevated temperatures. Hence, it is inconclusive if GF-HDPE is more water-resistant than GF-PP composites at 60°C. On the other hand, present testing provides evidence that at 95°C, GF-HDPE specimens have better water resistance compared to GF-PP composites.

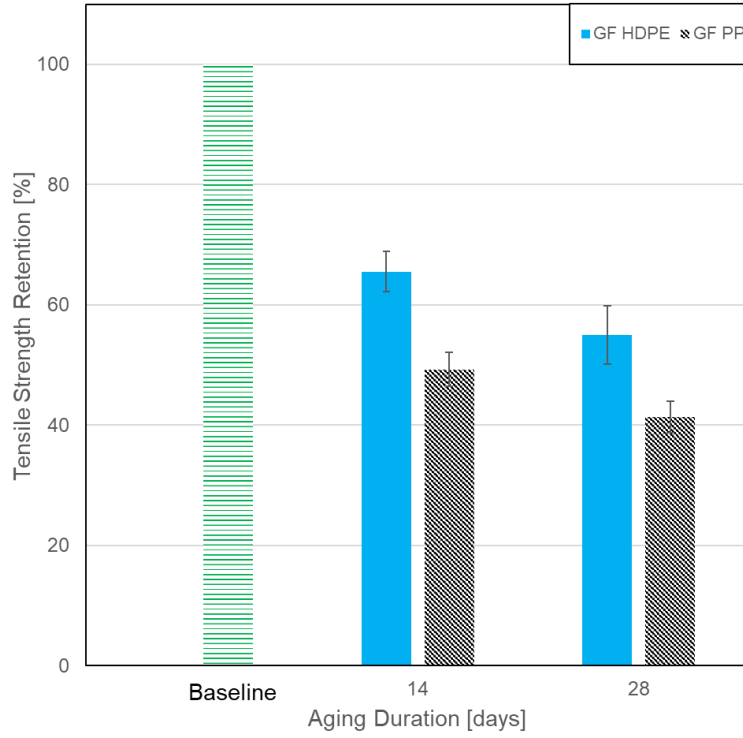


Figure 37. Variation in tensile strength at 95°C.

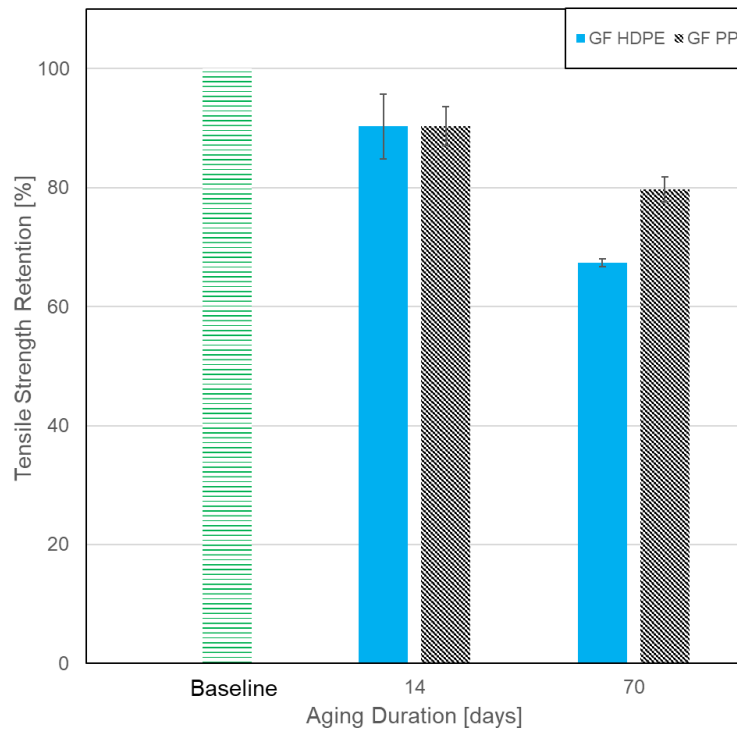


Figure 38. Variation in tensile strength at 60°C.

5.3.3. Concentration of Elements Released During Aging

Tables 7 and 8 represent the elements leached from the GF-PP and GF-HDPE specimens aged for 14 days at 60°C and 95°C, respectively. The elements taken into consideration were Al, Ca, Fe, K, Mg, Na and Si, which constitute the basic composition of GF [9]. Therefore, changes in the concentration of these elements in the aging fluid at the studied aging temperatures is considered indicative of underlying mechanism leading to composite strength loss.

Table 7. Concentration of elements leached into solution for GF-PP.

Element	Concentration at 60° C [mg/L]	Concentration at 95° C [mg/L]
Al	0.008	3.493
Ca	0.148	9.440
Fe	0	0.002
K	0.082	0.234
Mg	0	0.457
Na	0	0.222
Si	0.215	28.063

Table 8. Concentration of elements leached into solution for GF-HDPE.

Element	Concentration at 60° C [mg/L]	Concentration at 95° C [mg/L]
Al	0.016	3.445
Ca	0.116	7.390
Fe	0	0.004
K	0.080	0.266
Mg	0	0.261
Na	0	0.261
Si	0.034	30.330

As shown in Tables 7 and 8, for both GF-PP and GF-HDPE composites, there is a significant increase in the concentration of the elements released at 95°C compared to that of samples aged at 60°C for 14 days. This finding gives strong indication of damage to the GFs and possibly the fiber matrix interphase due to hydrothermal aging. Noticeably, Si had the highest concentration in the aged solution for both GF-PP and GF-HDPE samples. The critical damage mechanism associated with these results is the hydrolysis of Si-O-Si bonds which constitute the backbone of GF. It is well established that hydrolysis of Si-O-Si bonds in GF exposed to water significantly reduces fiber tensile strength [1]. These findings are in corroboration with the comparatively higher reduction in tensile strength observed for both the samples aged at 95°C. The low thickness of the composite tapes likely contributed to the substantial GF degradation. On the other

hand, given the low concentration of elements released at 60°C for both types of composites, it is possible that water molecules infiltrating the matrix and propagating along GFs and the fiber-matrix interface reduced the efficiency of load sharing between fibers inside the composites leading to the loss of tensile properties. The distinction between the composite degradation mechanisms at 60°C and 95°C water exposure is that, in addition to damage to fibers and fiber-matrix interface, the composite matrix also absorbs water to a greater extent at the higher aging temperature, which was demonstrated in the water absorption results. Hydrolysis of the matrix may even be the primary cause for tensile strength reductions at 60°C, especially for extended aging durations. Lastly, the present findings confirm a limited water resistance of the GF-HDPE and GF-PP thermoplastic composites and justifies the need for a more extensive testing campaign to understand the durability of thermoplastic composites, especially for UD composite tapes.

5.3.4. FTIR Results

5.3.4.1. GF-PP Specimens

FTIR spectra of GF-PP specimens before and after conditioning in water at 95°C are shown in Figure 39. Three carbon atoms are present in one unit of the PP molecule chain, each in a distinct group: $-\text{CH}_2$ (2915 cm^{-1} : asymmetrical stretching, 2837 cm^{-1} : symmetrical stretching, 841 cm^{-1} and 809 cm^{-1} : rocking vibration), $-\text{CH}-$ (1356 cm^{-1} : wagging vibration wagging vibration, and 1166 cm^{-1} : asymmetrical stretching asymmetrical rocking wagging vibration), and $-\text{CH}_3$ (2950 cm^{-1} : asymmetrical stretching, 2860 cm^{-1} : symmetrical stretching, 1457 cm^{-1} : asymmetrical bending; 1376 cm^{-1} : symmetrical bending, and 998 cm^{-1} : asymmetrical rocking) [23,24]. The signal at around 900 cm^{-1} can be attributed to Si-O stretching vibrations in GFs, however, no prominent peak is observed due to the coating of fibers with the PP matrix. No new peaks were observed after exposure to DI water for 28 days at 95°C, however, there was a slight reduction in intensity for the $-\text{CH}_3$ and $-\text{CH}_2$ peaks when compared with the unaged samples. These intensity reductions may be attributed to chain scissions occurring in the PP polymer chains, indicating that degradation occurred by hydrolysis and that chemical bonds formed that hold water [24].

5.3.4.2. GF-HDPE Specimens

Figure 40 depicts the FTIR spectra of GF-HDPE specimens before and after conditioning in water at 95°C. Strongest peaks are associated with the matrix, i.e., to CH_2 asymmetric and asymmetric stretching at 2920 cm^{-1} and at 2964 cm^{-1} , respectively. Similarly, peaks around 1460 cm^{-1} and 720 cm^{-1} are assigned to the bending and rocking mode of CH_2 group [23-26]. The key peak of interest is the broad peak at around 900 cm^{-1} which is indicative to Si-O-Si bending vibrations [27]. All other PE peaks exhibit nearly unchanged intensities, and no new peaks were observed. Therefore, the intensity difference of peaks around 900 cm^{-1} may indicate damage occurring to the GF due to hydrolysis reactions leading to the release of Si, which is supported by the mass dissolution results discussed earlier.

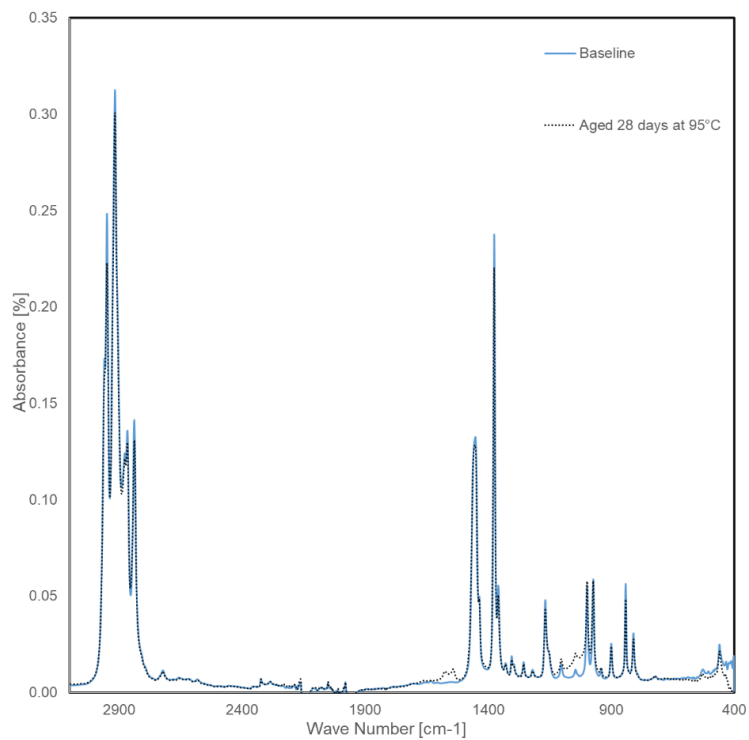


Figure 39. FTIR spectra of GF-PP samples before and after aging.

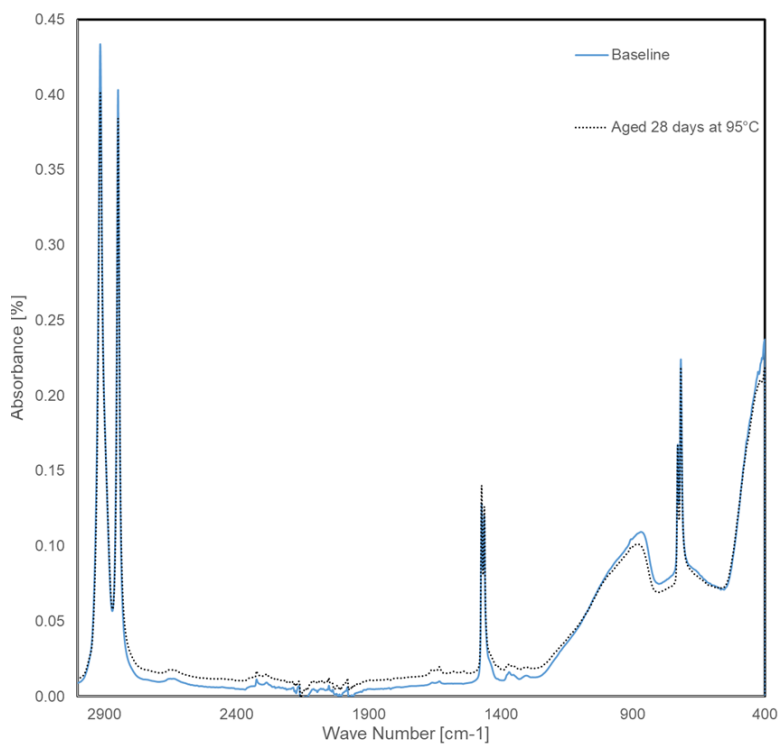


Figure 40. FTIR spectra of GF-HDPE samples before and after aging.

5.3.5. Changes in Surface Morphology

SEM analysis is a popular technique for examining the morphological changes occurring in composites subjected to aging environments. After tensile tests, fractured GF-PP sheet were removed and examined. Images in Figure 41 (a) and (c) present fracture surfaces of GF-PP and GF-HDPE specimens before aging. Figure 41 (b) and (d) show the surfaces for GF-PP and GF-HDPE specimens after aging for 28 days at 95°C. Notably, no apparent fiber damage was observed after aging for both the GF-PP and GF-HDPE specimens. However, exposed fibers observed in Figure 41 (b) and (d) indicate a weakening of fiber matrix interphase as fibers appear devoid any adhering matrix. This observation suggests that fiber-matrix debonding occurred. As water interacted with fiber-matrix interphase a reduction in transmission and sharing of loads between fibers and matrix likely ensued, thus reducing the bulk strength of the composite. Moreover, resulting presence of water at the fiber surface may also cause fiber degradation, which would play a significant role in composite strength reduction. Yet, clear evidence for substantial fiber damage could not be observed.

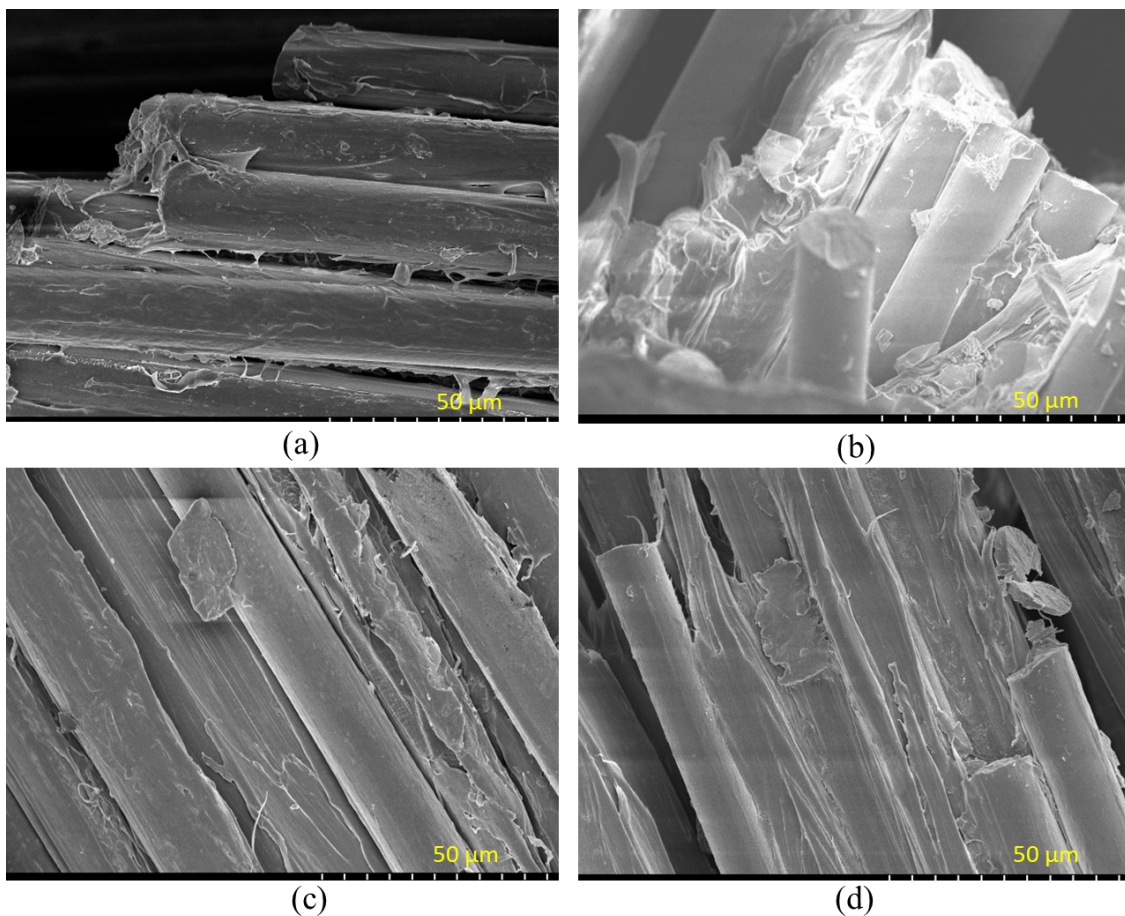


Figure 41. SEM images of fracture surfaces. GF-PP unaged (a) and after aging for 28 days at 95°C (b), and GF-HDPE unaged (c) and after aging for 28 days at 95°C (d).

5.4. Conclusions

The present study investigated the durability of unidirectional GF-PP and GF-HDPE thermoplastic composites exposed to water at 60°C and 95°C. GF-PP composites exhibited a higher water uptake behavior when compared with that of GF-HDPE composites, and both composites showed significantly higher weight gain at 95°C. After hydrothermal aging, GF-PP and GF-HDPE specimens exhibited a noticeable loss in tensile strength, with samples aged at 95°C showing the highest reductions. GF-PP samples lost almost 51% of their tensile strength after exposure to water at 95°C for 14 days. GF-HDPE composites exhibited a loss of 34% under the same conditions. Strength reductions increased with increased aging temperatures and durations for both composites. Reductions in strength of these composites are attributed to damage occurring to the fibers and a weakening of fiber-matrix interphase. The presence of fiber damage was established from mass dissolution tests. Significantly higher concentrations of Si and other elements associated with the fiber chemistry were observed in the solution used for conditioning samples at 95°C, when compared with that of at 60°C. This release of elements provides evidence for damage occurring to the fibers by hydrolysis of Si–O–Si bonds. FTIR results indicated that damage also occurred to the matrix, which likely played a role for reduced strengths as well. The findings of this work give context for understanding how hydrothermal aging affects the thermomechanical behavior of GF based thermoplastic composite materials. Also, it emphasizes the importance of understanding the aging behavior of bare fibers (i.e., without being embedded in matrix), given the rather poor resistance of thermoplastic matrices to water ingress. The present findings confirm that elevated temperature-induced accelerated hydrothermal aging testing is a useful technique to expediently identify causes of composite degradation. Still, additional work is needed to fully grasp the underlying aging mechanisms, which is a prerequisite for forecasting a composite's long-term behavior.

5.5. References

- [1] A. E. Krauklis, . Environmental Aging of Constituent Materials in Fiber-, Trondheim, Norway: NTNU, 2019.
- [2] A. E. Krauklis, C. Karl, A. Gagani and J. K. Jorgensen, "Composite material recycling technology—State-of-the-art and sustainable development for the 2020s.," *Journal of Composites Science*, vol. 5, no. 1, p. 28, 2021.
- [3] A. Kasper , "Recycling composites: FAQs.," *Reinforced Plastics*, vol. 52, no. 2, p. 39, 2008.
- [4] Y. Weitsman and M. Elahi, "Effects of fluids on the deformation, strength and durability of polymeric composites—An overview," *Mechanics of Time dependend materials*, vol. 4, pp. 107-126, 2000.

- [5] K. Pochiraju, G. Tandon and G. Schoeppner, Long-term durability of polymeric matrix composites., Springer Science & Business Media, 2011.
- [6] A. DiBenedetto, "Tailoring of interfaces in glass fiber reinforced polymer composites: a review.," *Materials Science and Engineering: A*, vol. 302, no. 1, pp. 74-82, 2001.
- [7] J. Davalos, Y. Chen and I. Ray, "Long-term durability prediction models for GFRP bars in concrete environment.," *Journal of Composite materials*, vol. 46, no. 16, pp. 1899-1914, 2012.
- [8] M. Silva, B. da Fonseca and H. Biscaia, "On estimates of durability of FRP based on accelerated tests.," *Composite Structures*, vol. 116, pp. 377-387, 2014.
- [9] A. E. Krauklis, A. I. Gagani and A. T. Echtermeyer, "Long-term hydrolytic degradation of the sizing-rich composite interphase.," *Coatings*, vol. 9, no. 4, p. 263, 2019.
- [10] K. Zulueta, A. Burgoa and I. Martinez, "Effects of hygrothermal aging on the thermomechanical properties of a carbon fiber reinforced epoxy sheet molding compound: An experimental research.," *Journal of Applied Polymer Science*, vol. 138, no. 11, p. 50009, 2021.
- [11] M. Heshmati, R. Haghani and M. Al-Emrani, "Durability of CFRP/steel joints under cyclic wet-dry and freeze-thaw conditions.," *Composites Part B: Engineering*, vol. 126, pp. 211-216, 2017.
- [12] E. Guzman, J. Cugnoni and T. Gmur, "Multi-factorial models of a carbon fibre/epoxy composite subjected to accelerated environmental ageing.," *Composite Structures*, vol. 111, pp. 179-192, 2014.
- [13] E. Poodts, G. Minak and A. Zucchelli, "Impact of sea-water on the quasi static and fatigue flexural properties of GFRP.," *Composite Structures*, vol. 97, pp. 222-230, 2013.
- [14] C. Unterweger, J. Duchoslav, D. Stifter and C. Furst, "Thermo-oxidative degradation of carbon fiber sizings and its impact on the mechanical performance of carbon fiber reinforced polypropylene composites," in *Proceedings 17th European Conference for Composite Materials*, 2017.
- [15] S. Yao, F. Jin, K. Rhee, D. Hui and S. Park, "Recent advances in carbon-fiber-reinforced thermoplastic composites: A review.," *Composites Part B: Engineering*, vol. 142, pp. 241-250, 2018.
- [16] E. Moritzer, M. Hüttner and J. Wächter, "The influence of environmental aging on the material properties of back-molded composite sheets.," in *AIP conference proceedings (Vol. 2065, No. 1, p. 030024)*, 2019.

- [17] M. Robert, R. Roy and B. Benmokrane, "Environmental effects on glass fiber reinforced polypropylene thermoplastic composite laminate for structural applications.," *Polymer composites*, vol. 31, no. 4, pp. 604-611, 2010.
- [18] A. Arici, "Effect of hygrothermal aging on polyetherimide composites," *Journal of reinforced plastics and composites*, vol. 26, no. 18, pp. 1937-1942, 2007.
- [19] S. Dong, P. Zhou, R. Guo, C. Li and G. Xian, "Durability study of glass fiber reinforced polypropylene sheet under simulated seawater sea sand concrete environment.," *Journal of Materials Research and Technology*, vol. 20, pp. 1079-1092, 2022.
- [20] D. Lariviere, P. Krawczak, C. Tiberi and P. Lucas, "Hydrothermal ageing of GF/PP composites: When glass/polymer adhesion favours water entrapment.," *Polymers and Polymer Composites*, vol. 13, no. 1, pp. 27-35, 2005.
- [21] ASTM, ASTM D5229/D5229-12 standard test method for moisture absorption properties and equilibrium conditioning of polymer matrix composite materials., 2012.
- [22] ASTM, ASTM D3039-standard test method for tensile properties of polymer matrix composite materials, 2017.
- [23] R. Caban, " FTIR-ATR spectroscopic, thermal and microstructural studies on polypropylene-glass fiber composites.," *Journal of Molecular Structure*, vol. 1264, p. 133181, 2022.
- [24] P. Zhou, C. Li, Y. Bai, S. Dong, G. Xian, A. Vedernikov, I. Akhatov, A. Safonov and Q. Yue, "Durability study on the interlaminar shear behavior of glass-fiber reinforced polypropylene (GFRPP) bars for marine applications.," *Construction and Building Materials*, vol. 349, p. 128694, 2022.
- [25] S. Y. Krimm, C. Y. Liang and G. B. Sutherland, "Infrared spectra of high polymers. II. Polyethylene.," *The journal of chemical physics*, vol. 25, no. 3, pp. 549-562, 1956.
- [26] C. Rameshkumarr, A. Anderson and S. Ravichandran , "UV, FIRT and surface properties of fiber reinforced low-density polyethylene laminated composites.," *Materials Today: Proceedings*, vol. 45, pp. 6216-6233, 2021.
- [27] M. Rani, P. Choudhary, V. Krishnan and S. Zafar, "Development of sustainable microwave-based approach to recover glass fibers for wind turbine blades composite waste.," *Resources, Conservation and Recycling*, vol. 179, p. 106107, 2022.

Chapter 6 : Conclusions and Future Work

6.1. Conclusions

Glass, carbon, and basalt fibers were the primary focus of this thesis, with the aim to understand the effect of hydrothermal aging on the performance of these fibers and the underlying mechanism leading to the variation in mechanical properties. In the first stage of this study, a tensile testing methodology was established for the various materials. Notably, different personnel performed similar testing on different fibers, confirming the repeatability of the developed methodologies. The critical parameters affecting the tensile strength of fibers were gauge length, twist in the fibers, and test speed. After developing a repeatable tensile testing process, a hydrothermal aging setup was created using glass beakers and ovens to determine the material's behavior under hydrothermal aging conditions.

After aging in tap water, the glass fiber generally exhibited a loss in breaking strength, with fibers tested when wet exhibiting the most significant decline in strength. Tensile strength declined as immersion time and aging temperature increased, yet the rate of decline slowed with time. Results from mass dissolution and FTIR measurements indicate that hydrothermal exposure caused an attack on the Si-O-Si framework in the glass material, which, coupled with the loss of sizing, caused substantial reductions in tensile strength. This conclusion was further supported by the SEM imaging, which showed significant damage occurring to the filament surface and material loss. An analytical model based on the Arrhenius theory was adopted to predict the tensile strength retention of glass fibers upon aging. The Arrhenius model was validated using experimental data, proving its broad applicability. The activation energy calculated using the Arrhenius model was 56.6 KJ, which agrees with values found in the technical literature.

After hydrothermal aging, basalt and carbon fiber exhibited a noticeable loss in strength. Basalt fiber tested when wet exhibited the highest reductions. In contrast, there was no significant difference in the strength of carbon fibers when tested dry and wet. Among the three reinforcements, carbon fiber was the most durable, with a maximum drop in strength of 26 % for samples aged 35 days at 82°C. The percentage reduction was at least double for the glass and basalt fibers. However, after exposure 90% humidity at 90°C, basalt fiber did not experience any loss in strength, whereas carbon fiber experienced a slight reduction in strength by 5.5 % after 28 days of exposure. The changes in concentration values of ions released for both carbon and basalt fiber explained the higher reductions in strength happening at higher aging temperatures under hydrothermal aging. The intensity reductions in FTIR spectra for BF support the conclusion that chemical reactions lead to substantial strength loss in BF, similar to that observed for glass fibers, as both fibers have SiO₂ as their backbone. The mass dissolution and FTIR results indicate that the water attack on the chemical structure of fibers, coupled with a loss of sizing, caused a reduction in tensile strength when exposed to hydrothermal conditions. Imaging with a scanning electron microscope revealed

surface damage to the fibers and their sizing. This supports the claim that the tested fiber materials are vulnerable to degradation when exposed to water at elevated temperatures. Another notable finding is that changes in fiber strength follow Arrhenius-based degradation behavior, as a corresponding increase in strength loss occurs with an increase in temperature and aging durations. Strength retention plots were established by establishing a suitable model and modeling limits for both fibers. For basalt fibers, omitting data points associated with 82°C provided a appropriate fit to the Arrhenius model. The analyses suggest the need for at least one additional temperature below 60°C for the Arrhenius model, while also indicating the limitation in the usage of basalt fiber for high temp applications. The strength retention values for carbon fiber agreed with the Arrhenius model. The activation energy calculated using the Arrhenius model was 91 kJ and 70 kJ for carbon and basalt fiber, respectively.

In composite tapes, after hydrothermal aging, GF-PP and GF-HDPE specimens exhibited a noticeable loss in tensile strength, with samples aged at 95°C showing the highest reductions. GF-PP samples lost almost 51% of their tensile strength after exposure to water at 95°C for 14 days. GF-HDPE composites exhibited a loss of 34% under the same conditions. Strength reductions increased with increased aging temperatures and durations for both composites. Reductions in the strength of these composites are attributed to damage occurring to the fibers and a weakening of the fiber-matrix interphase. The presence of fiber damage was established from mass dissolution tests. Significant concentrations of Si and other elements associated with the fiber chemistry were observed in the solution used for mass dissolution studies at 95°C, compared with that of at 60°C. This release of elements provides evidence for damage occurring to the fibers by hydrolysis of Si–O–Si bonds. FTIR results indicated that damage also occurred to the matrix, which likely played a role in reduced strengths. The findings of this work give context for understanding how hydrothermal aging affects the thermomechanical behavior of GF-based thermoplastic composite materials. Also, it emphasizes the importance of understanding the aging behavior of bare fibers (i.e., without being embedded in the matrix), given the relatively poor resistance of thermoplastic matrices to water ingress. The present findings confirm that elevated temperature-induced accelerated hydrothermal aging testing is a valuable technique to expediently identify causes of composite degradation

The thesis provides a better understanding of the environmental aging mechanisms of the constituents in fiber-reinforced thermoplastic composites and their effect on the mechanical properties of such materials. Based on environmental aging experiments, analytical models were proposed and developed to predict changes in the properties of the composite microconstituents due to exposure to such environments. These practical tools, i.e., models and methods, were provided for the quantitative prediction of water-induced changes in the microconstituent materials and composites. The tools assist in partially substituting the rigorous physical testing procedures that are state-of-the-art. Prediction of long-term properties of

composites should significantly reduce costs associated with extensive testing and allow a partial transition toward the multiscale modeling approach.

Although only glass, carbon, and basalt fibers were the focus of the current testing campaign and modeling effort, the general strategy is thought to hold for all types of fibers, like aramid, hybrid fibers, towpregs, etc. These findings offer novel insights regarding the significant decline in the mechanical performance of fibers when subjected to a combination of water and temperature. Upon completing additional studies into the aging of technical fibers, the created tools may form a basis to forecast and track the long-term performance of fibers in engineering applications. Also, it is of interest to explore if findings from this study can form the foundation for a multiscale approach for predicting the performance of fiber-reinforced polymer matrix composites, which may involve examining the performance of fibers, matrix, and their interface condition independently and then extrapolating attributes of the composite material from the constituents' behavior. Lastly, the present study aids in building a strong foundation for future students to continue thermoplastic composite research at the Advanced Composite Materials and Engineering Group.

6.2. Scope for Future Work.

The effects of hydrothermal aging on fiber reinforcements are addressed in this thesis. However, there are a few associated issues and study areas that can more thoroughly be explored. Several factors would be of great relevance to industry and academic research:

- Development of a multiscale methodology where separate short-term exposure tests on reinforcements and polymers can be used to predict a thermoplastic composite's service life. Such methodology can result in considerable reductions in cost and time required for the long-term durability studies of composites.
- The methodology of using the Arrhenius model can be used to predict the life of reinforcements if exposed to humidity or thermal aging, as this would be very valuable to industries, especially relating to determining the shelf-life of reinforcements.
- The results of this work could be used as valuable input to help in decision-making processes for selecting suitable reinforcements for high-temperature applications in thermoplastic composite piping.
- Expanding the investigation to fibers from multiple vendors and adding aramid fibers or similar candidates based on the application.
- Expanding the hydrothermal aging to composites and employing acoustic emission based damage detection techniques to understand the damage mechanisms after hydrothermal exposure.

- Modifying reinforcements with a suitable thermoplastic coating (i.e., towpregs) or sizing and evaluating the hygrothermal resistance.
- Performing fatigue tests in addition to the tensile tests.
- Developing a methodology based on an optical extensometer or digital image correlation to measure the reinforcements' elongation at break and modulus values.
- Formulation of an improved data reduction technique to model the statistical variation in the strength of different fibers.
- Repeating hydrothermal aging with fibers in a 'stressed' condition, i.e., aging of fibers with an applied mechanical load, as such a setup is a closer representation of the actual loading in composite structures.
- Performing short term hydrothermal aging with durations between 1 and 7 days to further calibrate the strength retention versus aging duration plots.
- Performing thermal aging for extended durations to facilitate separating thermal effects from hydrothermal effects.

Bibliography

- [1] A. E. Krauklis, A. Gagani and A. Echtermeyer, "Long-term hydrolytic degradation of the sizing-rich composite interphase," *Coatings*, vol. 9, no. 4, p. 263, 2019.
- [2] X. Gabrion, V. Placet, F. Trivaudey and L. Boubakar, "About the thermomechanical behaviour of a carbon fiber reinforced high-temperature thermoplastic composite," *Composites Part B: Engineering*, vol. 95, pp. 386-394, 2016.
- [3] S. Yao, F. Jin, K. Rhee, D. Hui and S. Park, "Recent advances in carbon-fiber-reinforced thermoplastic composites: A review," *Composites Part B: Engineering*, vol. 142, pp. 241-250, 2018.
- [4] M. A. Silva, B. da Fonseca and H. Biscaia, "On estimates of durability of FRP based on accelerated tests.," *Composite Structures*, vol. 116, pp. 377-387, 2014.
- [5] A. Idrisi, A. Mourad, B. Abdel -Magid and B. Shivamurthy, "Investigation on the durability of E-Glass/Epoxy composite exposed to seawater at elevated temperature.," *Polymers*, vol. 13, no. 13, p. 2182, 2021.
- [6] N. Guerhazi, A. Tarjem, I. Ksouri and H. Ayedi, "On the durability of FRP composites for aircraft structures in hygrothermal conditioning.," *Composites Part B: Engineering*, vol. 85, pp. 294-304, 2016.
- [7] M. Robert, R. Roy and B. Benmokrane, "Environmental effects on glass fiber reinforced polypropylene thermoplastic composite laminate for structural applications.," *Polymer composites*, vol. 31, no. 4, pp. 604-611, 2010.
- [8] E. Kuram, "Thermal and water ageing effect on mechanical, rheological and morphological properties of glass-fiber-reinforced poly (oxymethylene) composite," *Proceedings of the Institution of Mechanical Engineers, Part E: Journal of Process Mechanical Engineering*, vol. 233, no. 2, pp. 211-224, 2019.
- [9] C. Borges, A. Akhavan-Safar, E. Marques, R. Carbas, C. Ueffing, P. Weißgraeber and L. Silva, "Effect of water ingress on the mechanical and chemical properties of polybutylene terephthalate reinforced with glass fibers," *Materials*, vol. 14, no. 5, p. 1261, 2021.
- [10] M. Fang, N. Zhang, M. Huang, B. Lu, K. Laamnawar, C. Liu and C. Shen, "Effects of hydrothermal aging of carbon fiber reinforced polycarbonate composites on mechanical performance and sand erosion resistance.," *Polymers*, vol. 12, no. 11, p. 2453, 2020.
- [11] A. E. Krauklis, "Environmental Aging of Constituent Materials in Fiber-Reinforced Polymer Composites.," 2019.

- [12] A. E. Krauklis, A. Gagani, K. Vegere, I. Kalnina, M. Klavins and A. Echtermeyer, "Dissolution Kinetics of R-Glass Fibers: Influence of Water Acidity, Temperature, and Stress Corrosion.," *Fibers*, vol. 7, no. 3, p. 22, 2019.
- [13] B. Wei, H. Cao and S. Song, "Tensile behavior contrast of basalt and glass fibers after chemical treatment.," *Materials & Design*, vol. 31, no. 9, pp. 4244-4250, 2010.
- [14] Shawcor, "Composite linepipe," [Online]. Available: <https://www.shawcor.com/composite-systems/composite-linepipe..> [Accessed 23 October 2022].
- [15] R. Jones and J. Stewart, "The kinetics of corrosion of e-glass fibers in sulphuric acid.," *Journal of non-crystalline solids*, vol. 356, no. 44-49, pp. 2433-2436, 2010.
- [16] A. Baharlou and K. Nasouri, "A new comprehensive evaluation of the corrosion mechanism of E-type glass fibers in sulfuric acid solutions," *Construction and Building Materials*, vol. 268, p. 121213, 2021.
- [17] S. Feih, K. Manatpon, Z. Mathys, A. Gibson and A. Mouritz, "Strength degradation of glass fibers at high temperatures," *Journal of materials science*, vol. 44, pp. 392-400, 2009.
- [18] A. E. Krauklis and A. Echtermeyer, "Long-term dissolution of glass fibers in water described by dissolving cylinder zero-order kinetic model: Mass loss and radius reduction.," *Open Chemistry*, vol. 16, no. 1, pp. 1189-1199, 2018.
- [19] B. Wei, H. Cao and S. Song, "Tensile behavior contrast of basalt and glass fibers after chemical treatment.," *Materials & Design*, vol. 31, no. 9, pp. 4244-4250, 2010.
- [20] H. Kliger and E. Barker, "A comparative study of the corrosion resistance of carbon and glass fibers.," *Polymer-Plastics Technology and Engineering*, vol. 24, no. 1, pp. 85-108, 1985.
- [21] A. Echtermeyer, A. Krauklis, A. Gagani and E. Saeter, "Zero Stress Aging of Glass and Carbon Fibers in Water and Oil—Strength Reduction Explained by Dissolution Kinetics.," *Fibers*, vol. 7, no. 12, p. 107, 2019.
- [22] R. Gorowara, W. Kosik, S. Mcknight and R. Mccullough, "Molecular characterization of glass fiber surface coatings for thermosetting polymer matrix/glass fiber composites," *Composites Part A: Applied Science and Manufacturing*, vol. 32, no. 3-4, pp. 323-329, 2001.
- [23] J. Thomason, "Glass fiber sizing: A review of size formulation patents.," *Create Space Independent Publishing Platform.*, 2015.
- [24] J. Thomason, "Glass fiber sizing: A review.," *Composites Part A: Applied Science and Manufacturing*, vol. 127, p. 105619, 2019.

- [25] M. Bader, K. Kedward, Y. Sawada, A. Kelly and C. Zweben, *Comprehensive Composite Materials: Design Applications.*, Elsevier, 2000.
- [26] A. DiBenedetto, "Tailoring of interfaces in glass fiber reinforced polymer composites: a review.," *Materials Science and Engineering: A*, vol. 302, no. 1, pp. 74-82, 2001.
- [27] I. Rocha, S. Raijmaekers, R. Nijssen, F. Van der meer and L. Sluys, "Hygrothermal ageing behaviour of a glass/epoxy composite used in wind turbine blades.," *Composite Structures.*, vol. 174, pp. 110-122, 2017.
- [28] J. Kim, M. Sham and J. Wu, "Nanoscale characterisation of interphase in silane treated glass fiber composites.," *Composites Part A: applied science and manufacturing*, vol. 32, no. 5, pp. 607-618, 2001.
- [29] Y. Weitsman, "Coupled damage and moisture-transport in fiber-reinforced, polymeric composites.," *International Journal of Solids and Structures*, vol. 23, no. 7, pp. 1003-1025, 1987.
- [30] R. Plonka, E. Mader, S. Gao, C. Bellman, V. Dutschk and S. Zhandarov, "Adhesion of epoxy/glass fiber composites influenced by aging effects on sizings.," *Composites Part A: Applied science and manufacturing*, , vol. 35, no. 10, pp. 1207-1216, 2004.
- [31] L. Peters, "Influence of glass fiber sizing and storage conditions on composite properties.," *Durability of composites in a marine environment 2*, pp. 19-31, 2018.
- [32] D. Wang, F. Jones and P. Denison, "TOF SIMS and XPS study of the interaction of hydrolysed γ -aminopropyltriethoxysilane with E-glass surfaces.," *Journal of adhesion science and technology*, vol. 6, no. 1, pp. 79-98, 1992.
- [33] J. Davalos, Y. Chen and I. Ray, "Long-term durability prediction models for GFRP bars in concrete environment.," *Journal of composite materials*, vol. 46, no. 16, pp. 1899-1914, 2012.
- [34] O. Starkova, A. Gagani, C. Karl, I. Rocha, J. Burlakovs and A. Krauklis, "Modelling of environmental ageing of polymers and polymer composites- durability prediction methods," *Polymers*, vol. 14, no. 5, p. 907, 2022.
- [35] J. Zhou, X. Chen and S. Chen, "Durability and service life prediction of GFRP bars embedded in concrete under acid environment.," *Nuclear Engineering and Design*, vol. 241, no. 10, pp. 4095-4102, 2011.
- [36] I. 11346, Rubber, vulcanized or thermoplastic-Estimation of life-time and maximum temperature of use., ISO, 2014.
- [37] L. Bank, T. Gentry, B. Thomson and J. Russel, "Model specification for composites for civil engineering structures," *Transportation research record*, vol. 1814, no. 1, pp. 227-236, 2002.

- [38] J. Zhu, Y. Deng, P. Chen, G. Wang, H. Min and W. Fang, " Prediction of long-term tensile properties of glass fiber reinforced composites under acid-base and salt environments.," *Polymers*,, vol. 14, no. 15, p. 3031, 2022.
- [39] M. Hoque, A. Saha, H. Chung and P. Dolez, "Hydrothermal aging of fire-protective fabrics.," *Journal of Applied Polymer Science*, vol. 139, no. 30, p. e52666, 2022.
- [40] B. Mahltig and Y. Kyosev, *Inorganic and composite fibers: Production, properties, and applications*, Duxford, United Kingdom: Woodhead Publishing is an imprint of Elsevier, 2018.
- [41] J. Pusch and B. Wohlmann, "Chapter 2 - Carbon fibers," in *Inorganic and Composite Fibers*, Woodhead Publishing, 2018, pp. 31-51.
- [42] B. Mahltig, "Chapter 9 -Basalt fibers," in *Inorganic and Composite Fibers*, Woodhead Publishing, 2018, pp. 195-217.
- [43] ASTM, D2256M-10, Standard testmethod for tensile properies of yarns by the single starnd method, 2015.
- [44] ASTM, Standard test method for tensile properties of glass fiber stands, 2009.
- [45] ASTM, Standard Test Method for Tensile strength and Youngs modulus of fibers.
- [46] ISO, Textile glass — Yarns — Determination of, 2000.
- [47] A. Kelly and A. Tyson, "Tensile properties of fiber-reinforced metals: copper/tungsten and copper/molybdenum.," *Journal of the Mechanics and Physics of Solids*, vol. 13, no. 6, pp. 329-350, 1965.
- [48] ASTM, ASTM D3039-standard test method for tensile properties of polymer matrix composite materials, 2017.
- [49] ASTM, ASTM D5229/D5229-12 standard test method for moisture absorption properties and equilibrium conditioning of polymer matrix composite materials., 2012.
- [50] R. Caban, " FTIR-ATR spectroscopic, thermal and microstructural studies on polypropylene-glass fiber composites.," *Journal of Molecular Structure*, vol. 1264, p. 133181, 2022.
- [51] P. Cousin, M. Hassan, P. Vijay, M. Robert and B. Benmokrane, "Chemical resistance of carbon, basalt, and glass fibers used in FRP reinforcing bars.," *Journal of Composite materials*, vol. 53, no. 26-27, pp. 3651-3670, 2019.
- [52] J. De Kanter, L. C.G and A. Tubulars, "Thermoplastic composite pipe: analysis and testing of a novel pipe system for oil & gas.," *Proceedings of the 17th ICCM*, pp. 1-10, 2009.

- [53] S. Dong, P. Zhou, R. Guo, C. Li and G. Xian, "Durability study of glass fiber reinforced polypropylene sheet under simulated seawater sea sand concrete environment.," *Journal of Materials Research and Technology*, vol. 20, pp. 1079-1092, 2022.
- [54] E. Guzman, J. Cugnoli and T. Gmur, "Multi-factorial models of a carbon fiber/epoxy composite subjected to accelerated environmental ageing.," *Composite Structures*, vol. 111, pp. 179-192, 2014.
- [55] M. Heshmati, R. Haghani and M. Al-Emrani, "Durability of CFRP/steel joints under cyclic wet-dry and freeze-thaw conditions.," *Composites Part B: Engineering*, vol. 126, pp. 211-216, 2017.
- [56] Z. M. Ishak, . A. A and S. R, "Effects of hygrothermal aging and a silane coupling agent on the tensile properties of injection molded short glass fiber reinforced poly (butylene terephthalate) composites," *European polymer journal* , vol. 37, no. 8, p. 1635–1647, 2001.
- [57] A. Kasper, "Recycling composites: FAQs," *Reinforced Plastics*, vol. 52, no. 2, p. 39, 2008.
- [58] S. Y. Krimm, C. Y. Liang and G. B. Sutherland, "Infrared spectra of high polymers. II. Polyethylene.," *The journal of chemical physics*, vol. 25, no. 3, pp. 549-562, 1956.
- [59] D. Lariviere, P. Krawczak, C. Tiberi and P. Lucas, "Hydrothermal ageing of GF/PP composites: When glass/polymer adhesion favours water entrapment.," *Polymers and Polymer Composites*, vol. 13, no. 1, pp. 27-35, 2005.
- [60] J. Liu, M. Chen, J. Yang and Z. Wu, "Study on mechanical properties of basalt fibers superior to E-glass fibers.," *Journal of Natural Fibers*, vol. 19, no. 3, pp. 882-894, 2022.
- [61] E. Martynova and H. Cebulla, "Chapter 7- Glass fibers," in *Inorganic and Composite Fibers*, Duxford, Woodhead Publishing, 2018, pp. 131-163.
- [62] A. Messana, A. Airale, A. Ferraris, L. Sisca and M. Carello, "Correlation between thermo-mechanical properties and chemical composition of aged thermoplastic and thermosetting fiber reinforced plastic materials.," *Materialwissenschaft und Werkstofftechnik*, vol. 48, no. 5, pp. 447-455, 2017.
- [63] E. Moritzer, M. Hüttner and J. Wächter, "The influence of environmental aging on the material properties of back-molded composite sheets.," in *AIP conference proceedings (Vol. 2065, No. 1, p. 030024)*, 2019.
- [64] K. Pochiraju, G. Tandon and G. Schoeppner, *Long-term durability of polymeric matrix composites.*, Springer Science & Business Media, 2011.
- [65] E. Poodts, G. Minak and A. Zucchelli, "Impact of sea-water on the quasi static and fatigue flexural properties of GFRP.," *Composite Structures*, vol. 97, pp. 222-230, 2013.

- [66] C. Rameshkumarr, A. Anderson and S. Ravichandran , "UV, FIRT and surface properties of fiber reinforced low-density polyethylene laminated composites.," *Materials Today: Proceedings*, vol. 45, pp. 6216-6233, 2021.
- [67] M. Rani, P. Choudhary, V. Krishnan and S. Zafar, "Development of sustainable microwave-based approach to recover glass fibers for wind turbine blades composite waste.," *Resources, Conservation and Recycling*, vol. 179, p. 106107, 2022.
- [68] J. Sim and C. Park, "Characteristics of basalt fiber as a strengthening material for concrete structures," *Composites Part B: Engineering*, vol. 36, no. 6-7, pp. 504-512, 2005.
- [69] C. Unterweger, J. Duchoslav, D. Stifter and C. Furst, "Thermo-oxidative degradation of carbon fiber sizings and its impact on the mechanical performance of carbon fiber reinforced polypropylene composites," in *Proceedings 17th European Conference for Composite Materials*, 2017.
- [70] K. Zulueta, A. Burgoa and I. Martinez, "Effects of hygrothermal aging on the thermomechanical properties of a carbon fiber reinforced epoxy sheet molding compound: An experimental research.," *Journal of Applied Polymer Science*, vol. 138, no. 11, p. 50009, 2021.
- [71] A. E. Krauklis, C. Karl, A. Gagani and J. Jørgensen, "Composite material recycling technology— State-of-the-art and sustainable development for the 2020s," *Journal of Composites Science*, vol. 5, no. 1, p. 28, 2021.
- [72] A. E. Krauklis, "Modular Paradigm for Composites: Modeling Hydrothermal Degradation of Glass Fibers.," *Fibers*, vol. 9, no. 12, p. 83, 2021.
- [73] Y. Shao and S. Kouadio, "Durability of fiberglass composite sheet piles in water.," *Journal of composites for construction*, vol. 6, no. 4, pp. 280-287, 2002.
- [74] S. A. Grammatikos, M. Evernden, J. Mitchels, B. Zafari, J. T. Mottram and G. C. Papanicolaou, "On the response to hygrothermal aging of pultruded FRPs used in the civil engineering sector," *Materials & Design*, vol. 96, pp. 283-295, 2016.
- [75] P. Ghabezi and N. M. Harrison, "Hygrothermal deterioration in carbon/epoxy and glass/epoxy composite laminates aged in marine-based environment (degradation mechanism, mechanical and physicochemical properties).," *Journal of Materials Science*, vol. 57, no. 6, pp. 4239-4254, 2022.
- [76] R. Guo, G. Xian, F. Li, C. Li and B. Hong, "Hygrothermal resistance of pultruded carbon, glass and carbon/glass hybrid fiber reinforced epoxy composites.," *Construction and Building Materials*, vol. 315, p. 125710, 2022.

Appendices

Appendix A: Humidity Aging Results for Glass Fibers

Glass fibers were tested using tabbing method as described in Chapter 2. Figure 42 shows the variations in strength of fibers exposed to 90°C and 90% humidity for a duration of 7 and 28 days. As seen from the plots, no reduction in strength was observed for glass fibers, which was similar to what was observed for basalt fibers. These results confirm the absence of hydrolysis of the Si-O-Si network in glass and basalt fibers which was seen as a reason for the strength loss in hydrothermal aging.

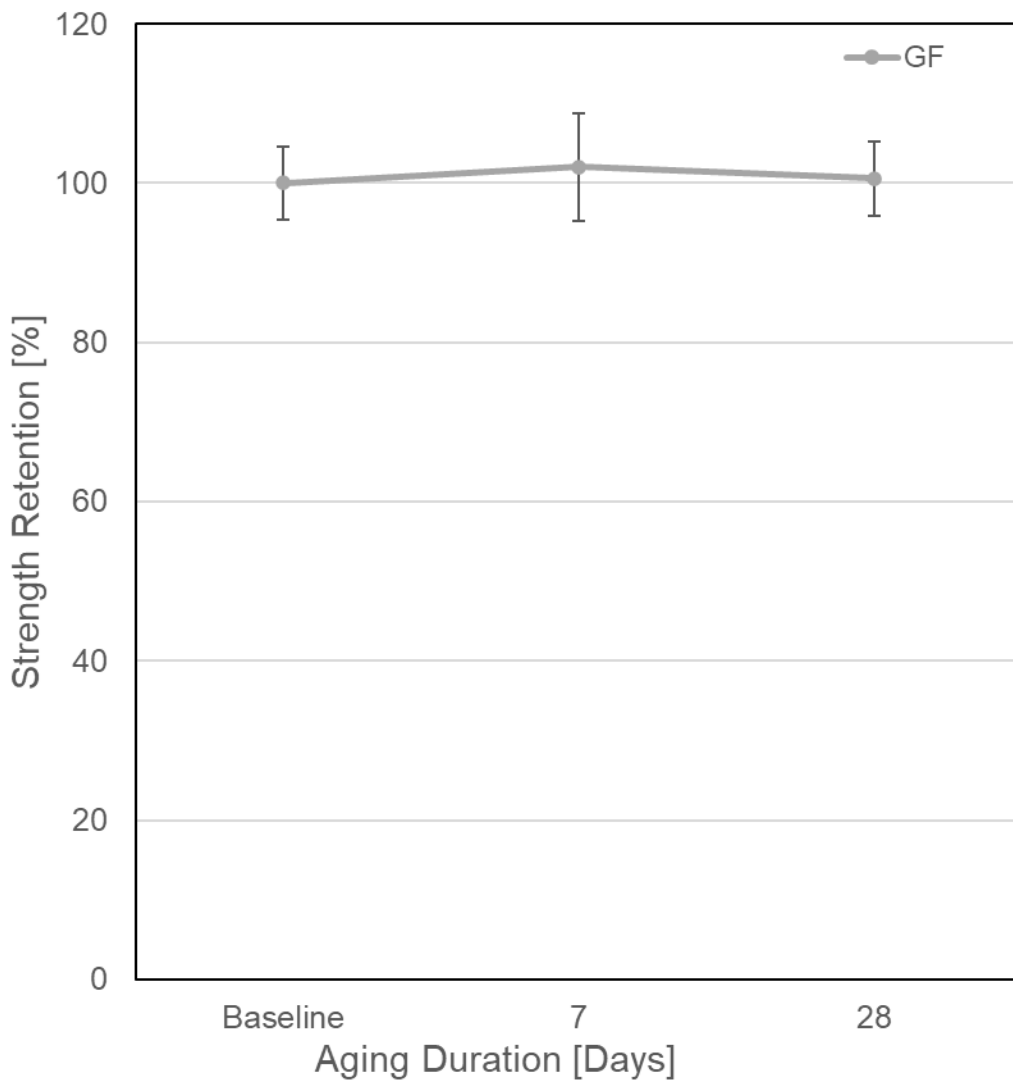


Figure 42. Variations in tensile strength for fibers exposed to 90°C and 90% humidity.

Appendix B: Investigation of strength variation of glass fibers across different batches

16 bobbins from two different batches of glass fibers were selected for this study. At least 10 samples were tested from each of the 32 bobbins. The main aim was to establish the statistical significance between different batches of fibers and to check for any bobbins with low strength values. Testing was performed using a protocol defined by the industrial partner, where preconditioning of the samples was done before testing by conditioning at 40°C for 3 hours. The tabbing method was used for the testing, and the stroke rate was 250 mm/min with a sample gauge length of 250 mm.

The variation in breaking load values for batch 1 and batch 2 is given by Figures 42 and 42. The average load for batch 1 was 499 N, whereas batch 2 showed a slightly higher breaking load value of 515 N. Statistical analysis were performed to prove that the strength values are statistically similar.

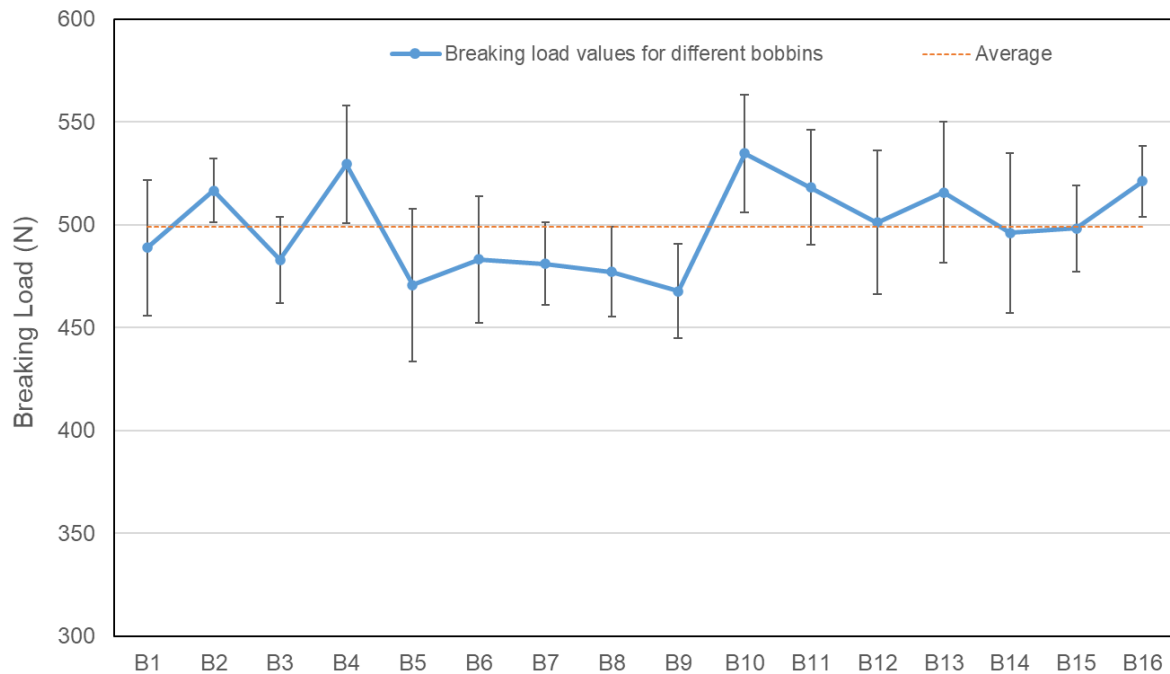


Figure 43. Breaking load variation across the bobbins for batch 1

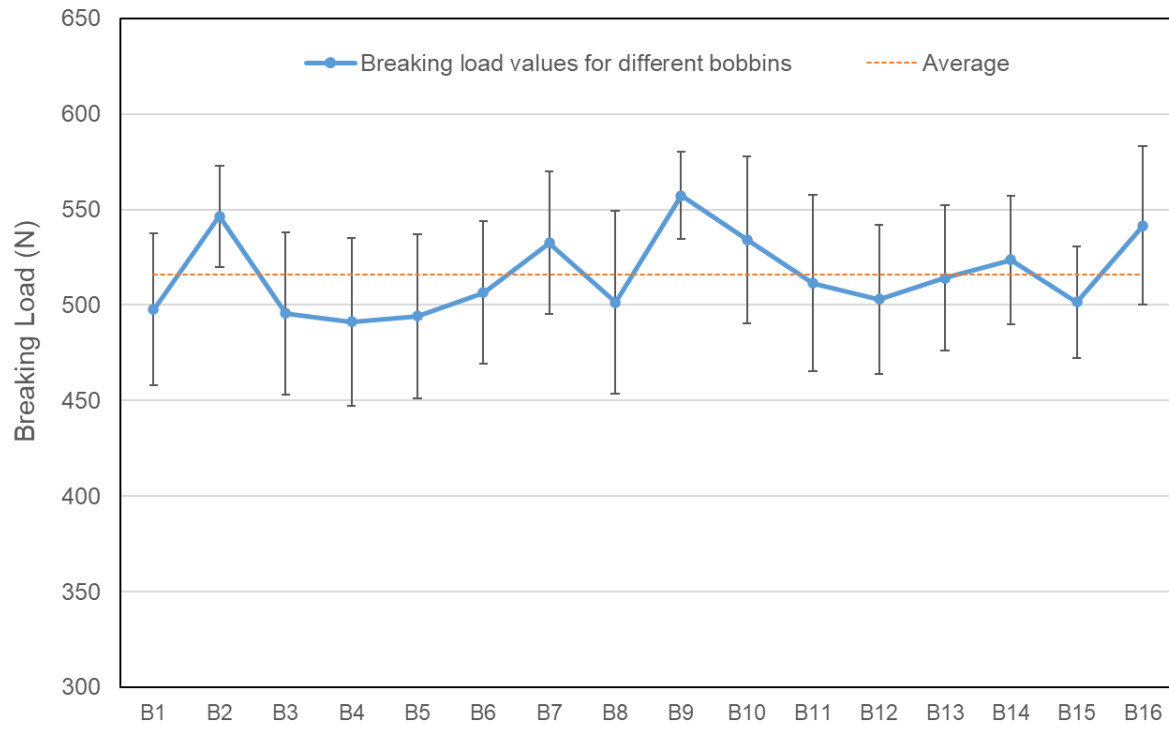


Figure 44. Breaking load variation across the bobbins for batch 2.